Controlled release and targeted drug delivery using polyelectrolyte microcapsules

By Devendra Inder Deo

Supervisors:

Professor Wen Wang

Professor Gleb Sukhorukov

Professor Shu Ye

Submitted for the Degree of Doctor of Philosophy

Institute of Bioengineering

Queen Mary University of London

2014

I, Devendra Inder Deo, confirm that the research included within this thesis is my own work or that where it has been carried out in collaboration with, or supported by others, that this is duly acknowledged below and my contribution indicated. Previously published material is also acknowledged below.

I attest that I have exercised reasonable care to ensure that the work is original, and does not to the best of my knowledge break any UK law, infringe any third party's copyright or other Intellectual Property Right, or contain any confidential material.

I accept that the College has the right to use plagiarism detection software to check the electronic version of the thesis.

I confirm that this thesis has not been previously submitted for the award of a degree by this or any other university.

Devendra Inder Deo

09/12/14

Publications

Devendra I. Deo , Julien E. Gautrot , Gleb B. Sukhorukov and Wen Wang. *Biofunctionalization of PEGylated microcapsules for exclusive binding to protein substrates*. Biomacromolecules, 2014, 15 (7), pp 2555–2562.

Abstract

Polyelectrolyte microcapsules were first established in 1998 as a potential drug delivery vehicle. Despite being well-established, microcapsules have not yet been thoroughly considered as a viable means of targeted drug delivery. This is largely due to the fact that microcapsules are inherently prone to unspecific binding to cells and proteins. Targeted delivery of drugs to specific diseased sites in the body is an area of research that has attracted many studies, particularly in drug deliveries that utilise microparticles. By achieving targeted delivery of a drug, one can increase the efficacy of the treatment, thus, reducing unwanted side effects. This thesis investigates methods which can modify these microcapsules in order to fine tune the release of the encapsulated drug as well as site-specific delivery of these vesicles i.e. obtain spatiotemporal control. To this end, biodegradable microcapsules of varying constituents are manufactured and their biodegradability is indirectly measured through quantification of the release of an encapsulated fluorescent protein (Rhodamine B-BSA). Fluorometry analysis of the supernatants of these microcapsule suspensions indicated that microcapsules synthesised from poly-L-arginine and poly-L-glutamic acid have the ability to encapsulate bovine serum albumin (BSA) with a high encapsulation efficiency (79.7%). Furthermore, they are able to produce a sustained release of BSA over a period of 5 Days.

To complement this controlled-release study, an investigation into self-degradable microcapsules was undertaken. To achieve this, proteinase was encapsulated in both biodegradable and non-biodegradable microcapsules of different thickness. Analysis of the protein release over a period of 24 hours revealed that the release profiles of these

microcapsules can be successfully controlled. Biodegradable microcapsules released 87% more protein than their non-biodegradable counterpart after 2 hours of incubation in deionised water. This provides conclusive evidence that the biodegradable microcapsules were, indeed, self-degradable.

The latter part of this thesis focuses on achieving specific and exclusive targeted delivery using polyelectrolyte microcapsules, with respect to protein substrates. This is accomplished by creating an antibody-functionalised poly(ethylene glycol) (PEG) assembly within the microcapsule structure. Site-specific adsorption of these microcapsules is tested using protein micropatterns. Results obtained from adsorption assays using anti-collagen type IV-functionalised microcapsules show a 600-fold increase in binding to collagen type IV islands, compared to control proteins (fibronectin and BSA). This proves that significant adsorption was achieved on the target protein, with unspecific adsorptions being heavily suppressed on control proteins. Furthermore, similar results were found when microcapsules were functionalised with anti-fibronectin and exposed to fibronectin, highlighting the versatility of this type of biofunctionalisation.

Acknowledgements

I would like to thank my three supervisors: Professor Wen Wang, Professor Gleb Sukhorukov and Professor Shu Ye, for their continuous support throughout the past 4 years. I am grateful for everything you have taught me. It was a privilege to have worked in Professor Sukhorukov's laboratory, surrounded by experts in biomaterials. In particular, I would like to thank Dr Weizhi Liu and Dr Anton Pavlov for teaching me how to synthesise polyelectrolyte microcapsules via the layer-by-layer method.

I would like to convey my gratitude to Dr Julien Gautrot. My project could not be completed without his advice and support. His expertise in biomaterial interactions has proved invaluable to this scientific contribution. He had generously gave his time to my project and was indeed, considered as a supervisor himself. He had also selflessly provided training in protein micro-patterning. His professionalism and kindness has been truly inspirational.

I would like to especially thank Mr Wei-Qi Li for his guidance during my cell culture studies and help with confocal microscopy. His help with image processing is also greatly appreciated.

Many thanks to Dr Yanhua Hu, Dr Zhongyi Zhang and Dr Lingfang Zeng at King's College London for generously providing me with *ex-vivo* samples and guiding me through the relevant protocols. I appreciate all of the valuable advice you have given for this aspect of my work.

I'd like to also express my gratitude towards Dr. Ruth Rose from the School of Biological and Chemical Sciences at Queen Mary University of London for giving me access to their surface plasmon resonance machine.

I would like to thank all current and previous members of Professor Wang's group, including: Dr Yankai Liu, Dr Ke Bai, Mr. Xiaotian Yu, Mrs. Lin Qiu, Mrs. Miao Lin, Mr Xia Chen, and Mr Zhengjun Lv. I have been fortunate enough to be part of Professor Gleb's pioneering biomaterials research group including: Mr Hao Ran, Dr Qiangying Yi, Dr Maria Antipina, Mr Li Zhao, Miss Hui Gao, Mr Dong Luo and Miss Iffat Patel. Your support with both academic and non-academic aspects during this period has provided me with knowledge and strength to complete this project.

Finally, I would like to thank the EPSRC and Queen Mary University of London for their financial support throughout my studies.

Table of Contents

List of Tables

List of Figures

1. Introduction

Drug delivery systems have been in use for decades with the first mechanisms including administration by simple intravenous injections or ingestion of white powder tablets. However, these methods may not always be applicable to a particular drug treatment e.g. structural changes of a chemical due to interaction with the gastro-intenstinal tract may occur, rendering the drug inactive. To a certain degree, capsules, usually made from gelatin, have circumvented this problem. However, the control of release of such capsules is challenging. Research in biomaterials has led to the production of microcapsules that have the ability to encapsulate materials with reasonable success. These microcapsules can then be held in a suspension which can be injected directly into the body, thus bypassing the harsh environment of the gastro-intestinal tract. The use of such microcapsules may indeed be a viable option for drug delivery, however, research into more specific diseases that are not systemic in nature, has increased the demand for smarter more advanced drug delivery mechanisms. Control over both the site-specific delivery and rate of release of a drug from microcapsules are therefore of paramount importance.

The work presented in this thesis aims to develop a novel method for targeted delivery and controlled release of therapeutic drugs using polyelectrolyte microcapsules, with the intention of treating diseases that are site-specific. An example of a site-specific disease is atherosclerosis, a leading cause of death in the western world (Phipps, 2000). The disease shall be briefly discussed, highlighting current surgical treatments available.

1.1 Atherosclerosis

Atherosclerosis is a cardiovascular disease by which macrophages and low density lipoprotein cholesterol infiltrate the endothelium and form an atherosclerotic plaque also known as an atheroma. This plaque is sealed via a fibrous cap which is formed by smooth muscle cells as shown in Figure 1.

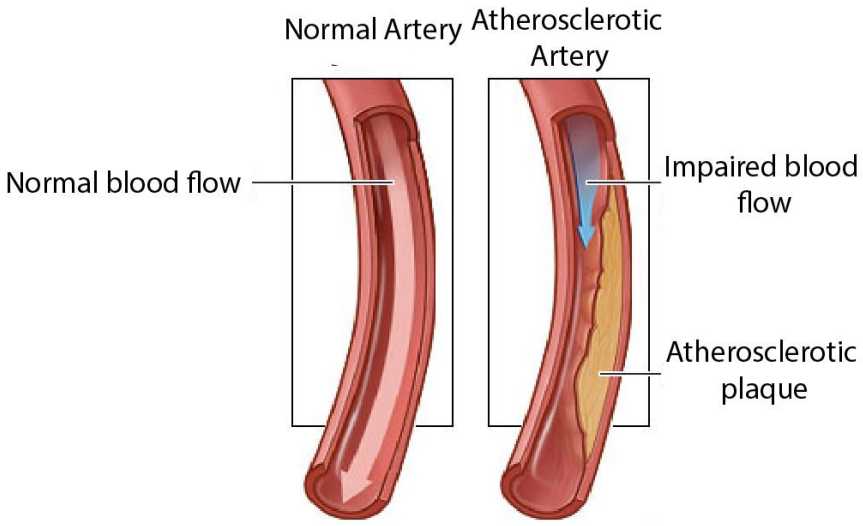

Figure 1. Atherosclerotic Artery. Adapted from (Thompson, 2008).

Over time, the plaque may either occlude the lumen or become unstable, releasing its thrombogenic contents which ultimately results in thrombus formation leading to total vessel occlusion. This may lead to the occurrence of a stroke or myocardial infarction depending on the location of the occlusion (Channon, 2002).

The normal inner wall of a blood vessel is made up of the endothelium and the underlying basement membrane. The endothelium lines the lumen of the vessel. It is made up of a monolayer of endothelial cells. These cells are in direct contact with the blood flow in the lumen. Endothelial cells are able to respond to physiological stimuli (e.g. shear stress) and do so by producing signalling molecules that have effects on the endothelium, blood cells and neighbouring smooth muscle cells.

A vital signalling molecule produced by endothelial cells is nitric oxide (NO). This is produced by endothelial nitric oxide synthase. When synthesised, NO diffuses into the lumen and the neighbouring smooth muscle cells in the media. This leads to an enzymatic reaction which leads to an increase in intracellular cyclic guanosine monophosphate (cGMP) which causes smooth muscle relaxation in smooth muscle cells. cGMP also has an inhibitory effect on platelets. This relaxation of the smooth muscle cells helps prevent atherosclerosis. This is known as endothelium-dependent relaxation. In atherosclerosis, oxidised low-density lipoprotein (ox- LDL) inhibits agonist stimulated endothelium dependent relaxation. Endothelial dysfunction is characterised by a loss in NO bioactivity resulting in predisposition to inflammatory cell adhesion and recruitment and thrombosis. A study had shown that upon introducing NOS inhibitors to an artery could lead to the acceleration of neointimal formation and consequently, acceleration of atherogenesis (Marek et al., 1995).

1.2 Current surgical treatments for Atherosclerosis

Angioplasty is a common surgical procedure used to remove atherosclerotic plaque. It is a mechanical treatment where the plaque is destroyed. Percutaneous transluminal angioplasty is generally carried out by using inflatable balloons, however, there is an increasing trend towards the use of expandable stents to remove plaque. Briefly, a catheter with a balloon attached at its tip, is inserted percutaneously into the affected artery as shown in Figure 2.

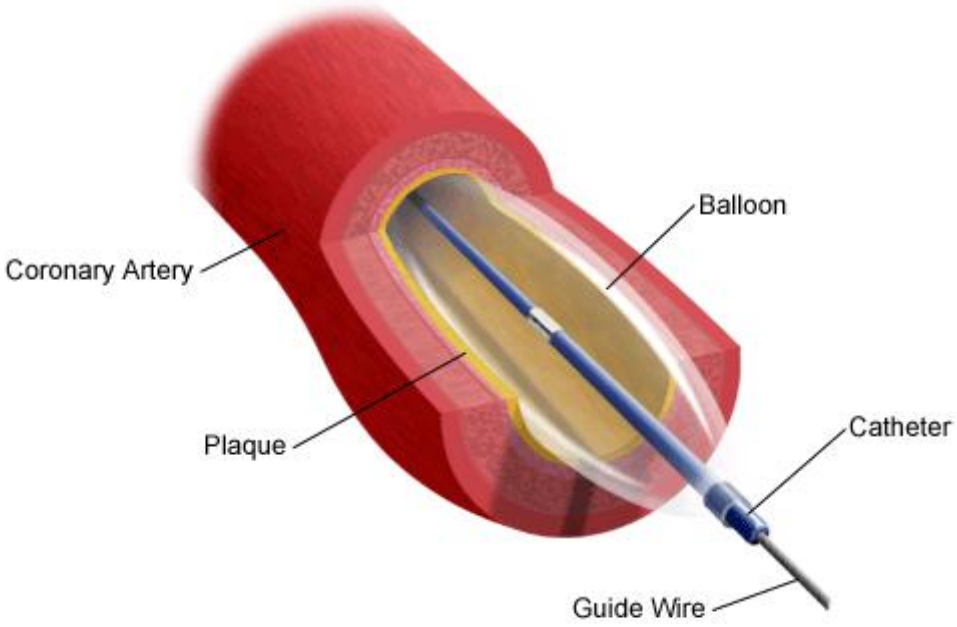

Figure 2. Inflation of balloon inside artery. Adapted from (Inflation of Balloon Inside a Coronary Artery, 2011).

Once at the site of the plaque, the balloon is inflated to break the plaque and increase the lumen area to improve blood flow. The procedure is done under fluoroscopy to visually aid the surgeon. This solution indeed offers short term relief, however, over time,

restenosis is likely to occur. Restenosis is where stiffening and intimal hyperplasia reoccurs after angioplasty. Its prevalence is reported to be as high as 50% in all cases worldwide (Horlitz et al., 2002). It is believed to take place in response to endothelium injury, where endothelial cells are removed from the inner lining of the artery, exposing the underlying thrombogenic basement membrane. Exposure of the basement membrane results in platelet adhesion which leads to the release of various growth factors that promote vascular smooth muscle cell migration and proliferation (Farb et al., 1999). In an attempt to maintain an adequate lumen cross-sectional area, expandable stents which are permanently installed in the atheromatous region, have been developed. Research suggests that patients are less likely to experience restenosis under stenotic treatment, however, patients are required to take anticoagulants on a regular basis to prevent thrombosis. It has been established that even a small thrombosis located on the endothelium has the ability to act as a scaffold for smooth muscle cell migration and consequential restenosis. This migration is stimulated by the release of various factors from activated platelets (Lowe et al., 2001). Furthermore, as can be seen in Figure 3, stent treatment still results in endothelium denudation where the stent is forced against the surface of the vessel, rendering intimal hyperplasia a possibility (Harnek et al., 1999).

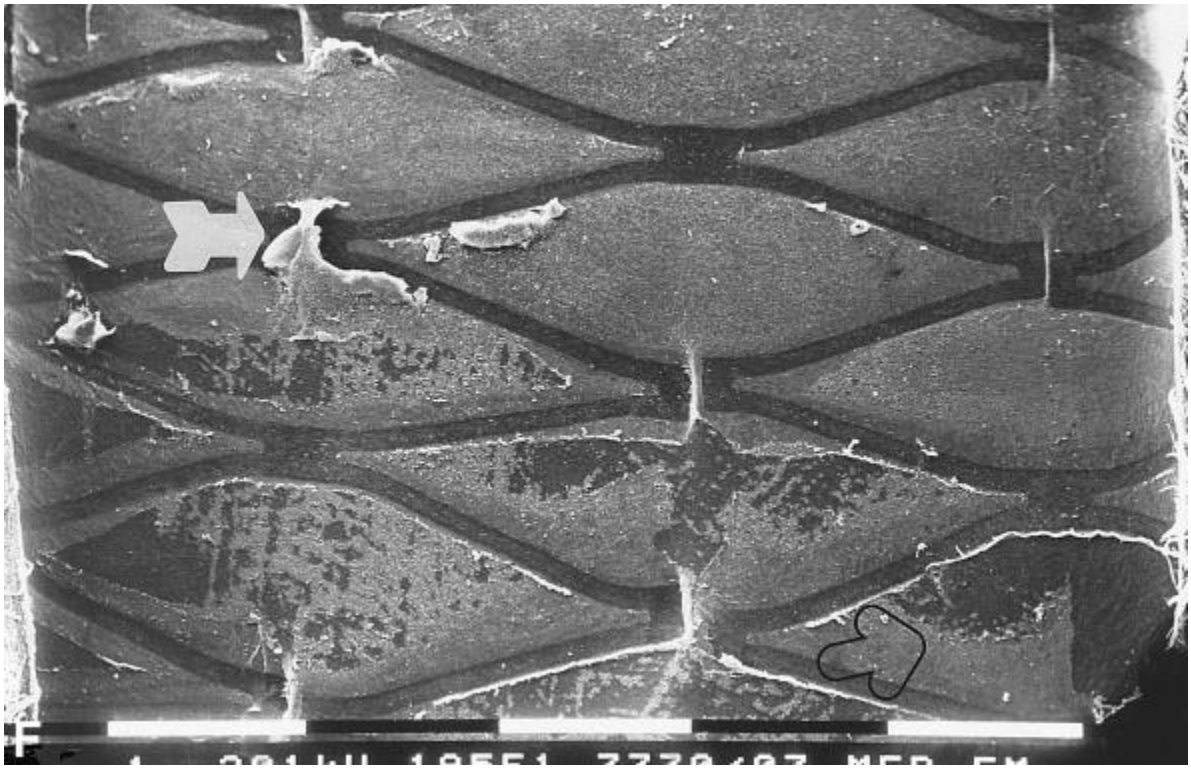

Figure 3. Scanning electron microscope image of stent-injured endothelium. Adapted from (Harnek et al, 1999).

In response to the aforementioned complications, drug eluting stents have been developed. Such stents release drugs to help restrict intimal hyperplasia. Typical drugs include paclitaxel (Kivela and Hartikainen, 2006) and sirolimus (Qian et al., 2009). More recently, a study assessed a dual drug eluting stent that eluted drugs to combat thrombosis as well as smooth muscle cell proliferation (Venkatraman et al., 2010). The cobalt-chromium stents were coated in a biodegradable polymer (PLGA) which would serve as a controlled release carrier. The polymer was preloaded with Sirolimus and Triflusal to control cell proliferation and thrombosis respectively. *In-vivo* results indicated a substantial decrease in platelet aggregation and smooth muscle proliferation. However, a long term *in-vivo* study has not been performed. This would help determine the viability of this concept as a long term treatment.

In patients with severe atherosclerosis, where the plaque has grown to an extent where occlusion of a blood vessel occurs, balloon angioplasty is often required. This is where a balloon is percutaneously inserted near the site of the disease and subsequently inflated and deflated until the plaque is sufficiently removed (Harnek et al., 1999). A common problem with this technique, as described earlier, is the occurrence of restenosis. This is where vascular endothelial injury post angioplasty exposes the thrombogenic subendothelium (basement membrane) results in platelet adhesion and results in the release of various growth factors that promote vascular smooth muscle cell migration and proliferation (Farb et al., 1999) . This ultimately results in excessive extracellular matrix production, known as neointimal hyperplasia. More recent developments using stent technology has reduced the prevalence of restenosis, however, it still occurs in approximately 15-20% of procedures within 6 months of the operation (Horlitz et al., 2002). By targeting the exposed membrane with microcapsules encapsulated with the aforementioned drugs, restenosis may be preventable. To determine the suitability of microcapsules for the treatment of this disease as well as other applications that require controlled and targeted drug delivery, polyelectrolyte microcapsules are henceforth discussed.

1.3 Microencapsulation

Encapsulation and release of drugs is an essential field of study in biomedical research. More specifically, research has suggested that encapsulation of pharmaceutical drugs using microcapsules, with a diameter of approximately 4μm, is a promising new mode of drug delivery. The fabrication of such capsules is usually achieved by applying the so-called layer-by-layer (LbL) technique. This method is based on the sequential deposition

of oppositely charged polyelectrolytes onto a colloidal core. Such cores are usually made from materials such as calcium carbonate, cross-linked melamine formaldehyde, polystyrene, magnesium carbonate and silicon dioxide (De Temmerman et al., 2011).

1.3.1 Synthesis

The layer-by-layer technique was first established in 1991 (Peyratout and Dähne, 2004). The technique was initially applied to planar substrates e.g. silica glass slides. By sequentially adsorbing cationic and anionic polymers onto the surface, thin polymer films are formed, with each individual layer being held by electrostatic attraction. This method of synthesising polymer films has proven to be popular in the field of materials science due to the ability to form bespoke films which can be functionalised with various functional groups. It is also a relatively inexpensive way of forming polymer films. Briefly, the substrate is submerged in a polyelectrolyte solution to allow the polyelectrolyte to electrostatically adsorb to the surface until the surface is saturated. After washing off excess polyelectrolyte that has not been adsorbed, the substrate is submerged into a counterpolyion solution, where the oppositely charged polyelectrolytes adsorb and saturate the surface. This self-assembly process is repeated until the desired film thickness has been reached. Each polyelectrolyte layer is approximately 2 nm in thickness (Mermut et al., 2003). However, this can be altered by changing the ionic strength/pH of the polyelectrolyte solutions. In deionised water, the charges along the polymer chain repel one another allowing the polymer chains to adopt a more linear conformation. When ions are present in the solution, these repulsion forces are shielded, hence the chains adopt a more globular conformation leading to the development of a thicker polymer layer (Ragnetti and Oberthür, 1986).

This layer-by-layer technique can be applied to micro-sized colloidal cores which serve as microscopic spherical templates. A crucial characteristic of cores used in this process is the ability to be dissolved. After layer-by-layer polymer adsorption and subsequent dissolution of the cores, hollow microcapsules are formed. The most commonly used template is calcium carbonate. This is easily synthesised by a co-precipitation technique whereby sodium carbonate is mixed with calcium chloride in a 1:1 molar ratio. After 30 seconds of vigorous stirring, colloidal cores are formed with a diameter ranging between 3 and 6 µm. It is important to realise that this step is crucial in producing a non-aggregated and monodisperse suspension of microcapsules. Calcium carbonate naturally forms into three distinct crystalline forms, the most common being calcite, as shown in Figure 4B. The other 2 crystal species are aragonite and vaterite (Figure 4A), the latter of which is the most ideal template for polyelectrolyte microcapsules.

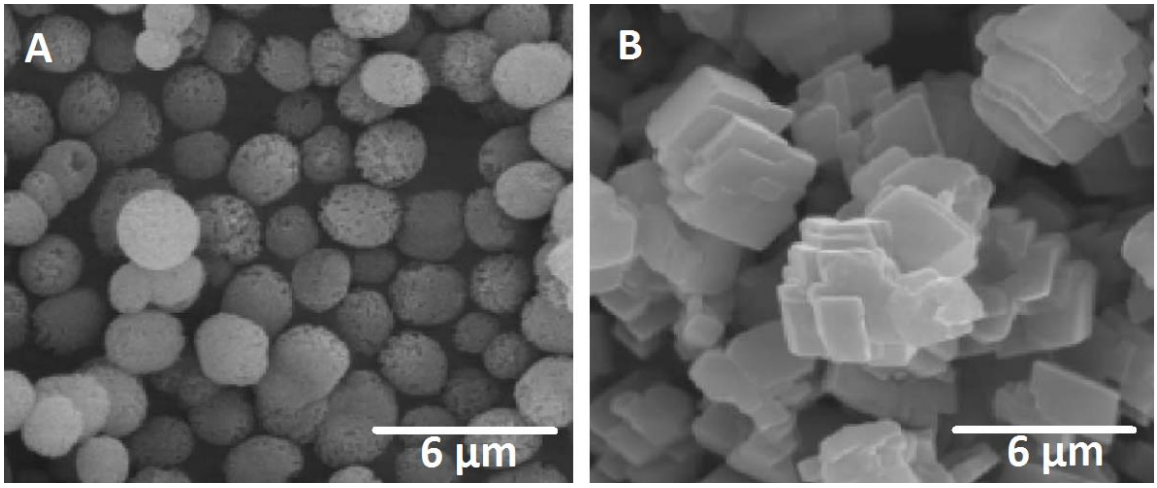

Figure 4 - SEM micrographs showing the vaterite (A) and calcite (B) crystals of calcium carbonate (Adapted from Tong et al., 2004)

This form is favourable since the cores are porous, thus facilitating the entrapment of molecules to be encapsulated in the so-called pre-loading technique. Furthermore, vaterite usually exists as spherical cores, which are ideal templates for microcapsules.

Thirdly, unlike calcite, large aggregates are not present, allowing individual microcapsules to be formed during the layer-by-layer process. A major disadvantage of using calcium chloride as a template is that the co-precipitation method usually results in a slightly aggregated sample that is not entirely monodisperse. Alternatively, where monodispersity is required, silica particles may be used. However, these cores are not porous and hence cannot be preloaded with molecules. When forming calcium carbonate from sodium carbonate and calcium chloride, the size and the crystal structure is influenced by many aspects of the methodology used including: time left to crystallise, temperature and the speed of stirring. More research must be conducted to fully understand how these aspects influence the core formation. In light of this, a study has shown that by forming calcium carbonate cores in the presence of aspartic acid, one can control the crystal structure and prevent the formation of calcite (Tong et al., 2004).

1.3.2 Morphology

The morphology of polyelectrolyte microcapsules can be visualised through SEM techniques. Typically, microcapsules formed on calcium carbonate or melamine formaldehyde colloidal cores exhibit a grainy surface topology. These nano-sized structures are believed to be manifested from segregated polyelectrolyte complexes and have been reported to be as large as 124 +/- 10 nm. In general, biodegradable microcapsules exhibit a rougher surface topology than non-biodegradable microcapsules, as depicted in Figure 5 (Gao et al., 2000).

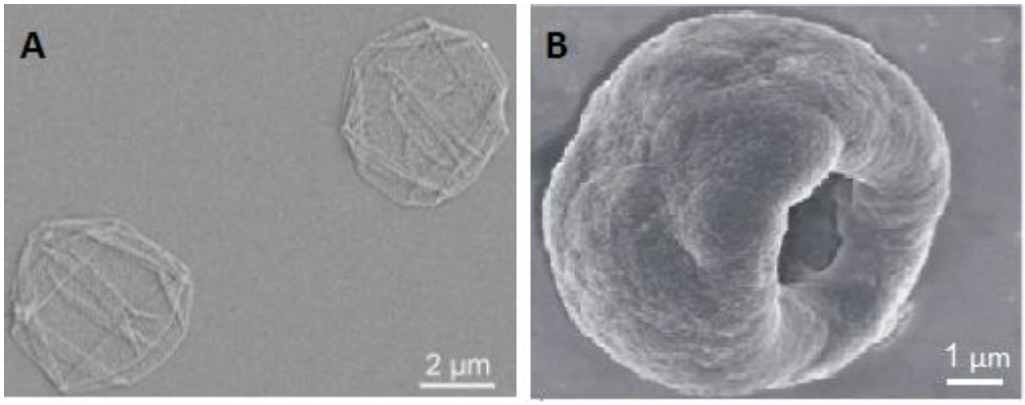

Figure 5. SEM images of non-biodegradable PAH/PSS microcapsules (A) and biodegradable protamine/dextran sulphate microcapsules (B). Adapted from (Köhler et al., 2004, Palamà et al., 2010).

The schematic shown in Figure 6 demonstrates the manufacturing process for polyelectrolyte microcapsules. The macromolecule is co-precipitated with calcium carbonate resulting in colloidal cores with embedded macromolecules (A). Then the LbL process proceeds with a cationic polymer layer (highlighted in red) electrostatically absorbed onto the calcium carbonate core followed by an anionic polymer layer (highlighted in blue) (B). When using calcium carbonate as the core, either polyanion or polycation can be adsorbed first since the core has regions of positive and negative charge. It is recommended to perform a zeta potential measurement to determine the net charge and hence initiate the process with an oppositely charged polymer. When the desired number of layers has been reached, the calcium carbonate core is dissolved using EDTA (C). The Ca^{2+} and CO_3^{2-} ions are able to pass through the porous capsule membrane, resulting in a microcapsule with encapsulated macromolecules.

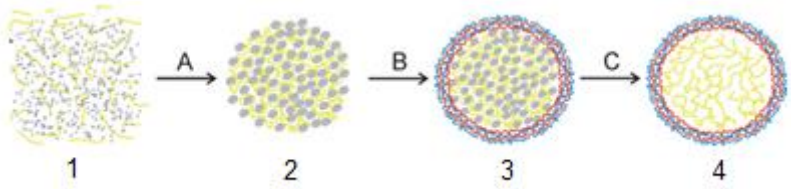

Figure 6. Schematic drawing of the fabrication of microcapsules using the LbL technique. Adapted from (De Geest et al., 2009b). Calcium chloride and Sodium carbonate are mixed with a protein solution (1). After co-precipitation (A), colloidal cores are formed with impregnated protein (2). Polyelectrolytes of alternating charge are then sequentially deposited on the cores (B) resulting in an encapsulated core (3). Cores are finally dissolved using EDTA (C) resulting in a microcapsule with encapsulated protein (4).

In between the polyelectrolyte deposition steps, the microcapsules must be separated from the solution to allow for washing of the sample. This is usually carried out by centrifugation, typically at 1500 rpm for polyelectrolyte-coated cores, and 5000 rpm for hollow microcapsules. This action often results in loss of particles, particularly if they are small. The high force of centrifugation can lead to damage of the microcapsules, ultimately resulting in shell rupture. Instead of subjecting the microcapsules to centrifugal force, the washing steps may be entirely eliminated by adding the exact amount of polymer required to coat the particles in the suspension, then adding the second polymer in a similar fashion. A major limitation of this method is the inevitable production of free polyelectrolyte complexes in the solution as polymers of opposite charges electrostatically bind. This is likely to result in unwanted aggregation. This problem can be bypassed by filtration using a filter with pores smaller than the microcapsules themselves. In addition to providing less stress to the microcapsules, this technique can be up-scaled to an industrial production level (Peyratout and Dähne, 2004).

1.3.3 Materials for fabrication

The most popular polyelectrolyte combination for microcapsule fabrication is polyallylamine hydrochloride and polystyrene sulfonate. This combination is favoured for its high reproducibility and lack of capsule aggregation during and after synthesis (De Geest et al., 2007). Although biocompatible, these synthetic polymers are not biodegradable. Biodegradable polymers used in microcapsule fabrication include polysaccharides such as dextran sulphate and polypeptides such as poly-L-arginine. Such microcapsules offer more complex drug release rate profiles that are dependent on enzyme concentration of the environment. A study by Sah et al. (1995) showed that a sustained release could be achieved over a period of 24 days using biodegradable poly-D,L-lactide-co-glycolide/ poly-D,L-lactic acid microcapsules. This was reflected in a more recent study which highlighted a similar drug release profile study which used chitosan/alginate microcapsules (Wang et al., 2007b). The release profile generated from this study can be seen in Figure 7. Over a period of 200 hours, the ibuprofen-loaded capsules had released most of their contents, with over 50% of the total amount expelled within the first 24 hours. This initial burst is a common characteristic of all capsules including synthetic non-biodegradable variants.

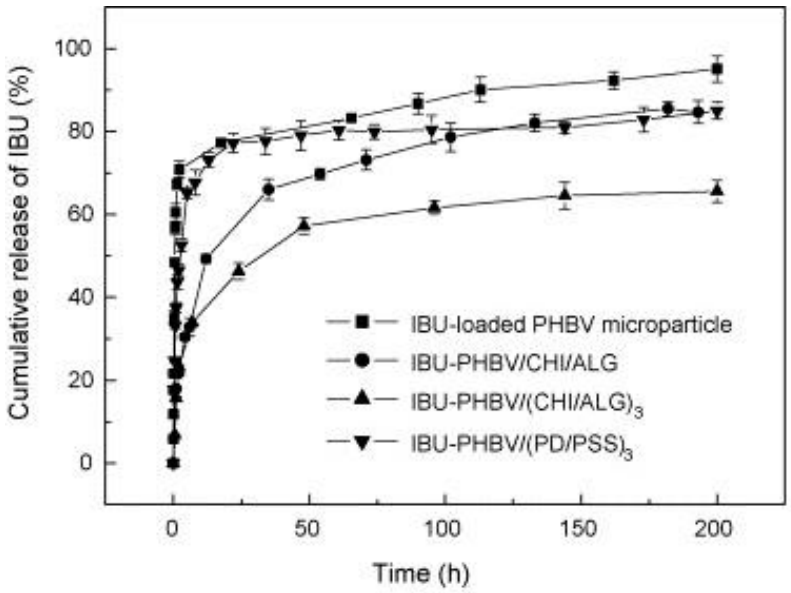

Figure 7. IBU (Ibuprofen) release profile of poly(3-hydroxybutyrate-co-3-hydroxyvalerate (PHBV) microparticles coated with various polymer coatings including: chitosan (CHI) sodium alginate (ALG), poly(diallyldimethylammonium chloride) (PD) and sodium (polystyrene sulfonate) (PSS). Adapted from (Wang et al., 2007b).

A problem with enzyme-sensitive microcapsules is that enzymes are ubiquitous *in-vivo* and prolonged exposure to these enzymes may result in unwanted liberation of the encapsulated drug, hence unwanted side effects are likely to be experienced. To overcome this, the microcapsules may be adapted to specifically adhere to regions of the disease. This may be achieved by functionalising the capsule membrane with specific ligands (Toublan et al., 2006). Chemotherapy is a well-established technique for the treatment of cancer, however, due to a lack of specific targeting, many side effects are experienced. Toublan et al (2006) exploit the fact that integrin receptors are more heavily expressed on tumours and hence decided to functionalise microcapsules with integrin-receptor specific peptide ligands. Ligands consisted of short polylysine units with an RGB (arginine-glycine-aspartic acid) motif incorporated into different regions of the polylysine chain. The RGB motif has a strong affinity to integrin-receptors. These ligands were conjugated to the membrane of the microcapsules via electrostatic attraction

between the cationic polylysine chain and the anionic bovine serum albumin outer surface of the microcapsules. The adhesive microcapsules were preloaded with Nile red dye and incubated with colon tumour cells. After washing, it was noticed that the microcapsules were successfully retained on the surface of the cells.

1.3.4 Permeability of microcapsules

The microcapsules fabricated using the LbL technique are moderately porous. As a result it is recommended that the size of the molecule to be encapsulated should be greater than 5kDa in order for successful retention. Smaller molecules will simply transverse the porous capsule membrane (Sukhorukov et al., 1999). The ionic strength of the dispersant increases the permeability of the polyelectrolyte shells due to competition with salt ions. As salt ions neutralise the charges of the polyelectrolytes, the electrostatic attraction between adjacent layers diminishes resulting in instability within the shell. Furthermore, by varying the pH of the dispersant, the permeability/stability of polyelectrolyte microcapsules can be altered. For example, in acidic conditions, the H^+ ions decreases the charge per unit length on polyanions, thus leading to repulsion between cationic layers within the layer-by-layer structure, ultimately resulting in shell disintegration (Haynie et al., 2005). The general mechanism responsible for the change in porosity associated with weakly charged biodegradable microcapsules is based on the premise that the charge of a polymer/protein is dependent on the pH of the solution they are dissolved in. It is therefore dependent on the isoelectric point of the polymer. The isoelectric point (pI) can be described as the pH at which the electrostatic charge of the polyelectrolyte is zero. At a pH above this isoelectric point, the polymer will carry a net negative charge and at a pH below this isoelectric point, the polymer will carry a net positive charge. As changes in

the pH strengthen/weaken the electrostatic charges of the polyelectrolytes, the shell loses integrity and the porosity subsequently alters (Zhao and Li, 2008).

This characteristic of polyelectrolyte microcapsules aids in the post-loading mechanism of encapsulating molecules. One can alter the ionic strength or pH of the solution to increase the porosity of the polyelectrolyte shell, thus allowing molecules to enter the interior of the capsules. Once loaded, the ionic strength or pH may be reversed to reduce the porosity of the shell and hence lock in the contents. This is rarely performed however, since preloading typically yields higher encapsulation efficiencies (Vergaro et al., 2011).

1.4 State-of-the-art polyelectrolyte microcapsules

Current literature highlights various types of microcapsules that utilise different technologies in order to react to different external stimuli. These numerous techniques prove the versatility of microcapsules as a means of drug delivery that is capable of releasing their payload with precise control. The state-of-the-art polyelectrolyte microcapsules are extensively reviewed henceforth.

1.4.1 Triggered release of encapsulated contents from polyelectrolyte microcapsules

Infrared radiation is well established as a sufficient method of triggering the release of encapsulated drug. One can exploit its ability to penetrate through soft tissues, hence microcapsules *in-vivo* can be externally triggered with high efficiency. Sensitivity to infrared radiation can be achieved by incorporating gold nanoparticles in the shell. Gold nanoparticles can be easily trapped between the layers of the layer-by-layer-constructed

shell. As the infrared is pulsed onto the capsules (short pulses of less than 10 ns), these gold nanoparticles absorb the energy and transform it into heat, which damages the shell of the capsules (Angelatos et al., 2005, Radt et al., 2004, Skirtach et al., 2005). Depending on the extent of the damage, the capsule porosity will increase or the capsule shell may rupture, thus releasing the encapsulated contents. However, when release is desired in a deeper region *in vivo*, the infrared may be adsorbed before it reaches the microcapsules, hence the release cannot be triggered. A recent study has shown that a similar kind of release mechanism can be obtained without the use of infrared (Carregal-Romero et al., 2015). The authors successfully show that local heating and subsequent rupture of the microcapsule shells can be achieved through magnetism, more specifically, application of an alternating magnetic field. The absorption of this field by soft tissue is negligible, thus circumventing the problems associated with infrared. Briefly, iron oxide nanoparticles of diameter of 18 nm were integrated within the layer-by-layer structure of the microcapsules. Upon application of an alternating magnetic field, the microcapsules were seen to heat up and rupture, ultimately releasing the encapsulated cascade blue-dextran within.

1.4.2 Encapsulation of low molecular weight molecules

Ordinarily, microcapsules are unable to retain drugs/molecules with sub-kilodalton molecular weights, due to their relatively large shell pore size of approximately 10 nm (Song et al., 2009b). Molecules with a lower molecular weight will diffuse through most microcapsules. Recent studies have addressed this problem in order to retain therapeutic drugs, which typically have a molecular weight of less than 1 kDa. Conversely, a more recent study has successfully demonstrated that low molecular molecules (<1kDa) can be well retained within microcapsules made from conventional polystyrene sulfonate and

polyethylene imine (Manju and Sreenivasan, 2011). In this study, curcumin (MW 368.38) was effectively encapsulated and well retained with a curcumin release of just 2.77% of the total release, within one week. This is an extremely slow initial release of capsular content, considering the low molecular weight of the substance. The authors suggest that this slow release may have arisen due to build-up of curcumin on the inner surface of the membrane leading to pore occlusion. A slow rate of release may have also arisen as a result of the large number of polyelectrolyte layers used to construct the microcapsules. The authors used 12 layers in total, which is larger than typical polyelectrolyte microcapsules which are generally made from between 4 and 8 layers. The outcome of this study was confirmed by a small total release in comparison to the initial encapsulated amount. This may be disadvantageous since the total release of the drug may be inadequate in producing a significant therapeutic effect.

A more recent study by Yi and Sukhorukov (2013) showed that upon ultraviolet (UV) irradiation of microcapsules fabricated from diazonium and sulfonate groups, the electrostatic interactions between the layers were replaced by covalent bonds. This led to the generation of a hydrophobic shell and consequently a stable microcapsule capable of retaining Rhodamine B, a low molecular weight dye with a molar mass of 479 g mol^{-1} (Yi and Sukhorukov, 2013). UV irradiation has also been utilised for triggered release of encapsulated contents in polyelectrolyte microcapsules. These so-called photo-cleavable microcapsules have the ability to rupture on exposure to UV irradiation. Triggered release by light can be achieved by incorporating light absorbing nanoparticles e.g. gold or silver nanoparticles within the microcapsule shell. By utilising chemical groups such as azobenzenes, which change shape upon irradiation, UV irradiation can consequently lead to rupture of the capsule shell. A more recent study has demonstrated that

microcapsules synthesised from polyurea, can also produce a similar response upon UV irradiation (Dispinar et al., 2013).

Further research has demonstrated that cross-linking between the layers in a layer-by-layer fabricated microcapsule can be achieved without the use of UV irradiation. The research group exploited the reaction between azlactone groups and amine groups in order to crosslink polymers with both constituents. Upon dissolution of the calcium carbonate core, the fabricated microcapsules were able to retain FITC-dextran. More significantly, the FITC-dextran was retained despite the capsules being subjected to harsh pH values and ionic strengths. Remarkably, the microcapsules were able to withstand both basic and acidic environments (5M sodium hydroxide and 5M hydrochloric acid) for at least 22 hours (Saurer et al., 2011).

Research has shown that microcapsules synthesised from polypeptides can also been cross-linked via disulphide bridges. Interestingly, the inspiration for this method was taken from the well-known stabilisation of hormones e.g. insulin, by disulphide bridges (Haynie et al., 2005). This biomimetic solution is achieved by incorporating the sulphur-rich peptide, cysteine within the polyelectrolyte layers. 12 bilayers were formed using peptides containing glutamic acid, tyrosine, lysine, valine and glycine, in addition to the aforementioned cysteine. Disulphide bond formation was achieved by immersing the capsules in diemethyl sulfoxide (DMSO), an oxidising agent. For control purposes, a sample was left to incubate without the addition of DMSO. Experiments were carried out in acidic conditions (pH 1.6) i.e. in an environment which favours microcapsules disintegration, as explained earlier. After 30 days, the majority of the capsules in the

control sample were degraded, leaving only 10% of the original quantity intact. Remarkably, this figure was increased by three-fold once the disulphide bonds were formed, effectively proving that by cross-linking layers with disulphide bonds, a greater level of stability is achieved. These studies conclusively demonstrate that the drawback of instability of microcapsules due to changes in pH and ionic strength can be circumvented.

1.4.3 Cellular uptake of polyelectrolyte microcapsules

Due to their microscopic dimensions, microcapsules also possess the ability to be internalised by cells via phagocytosis. Research has demonstrated that capsule uptake by cells is dependent on the surface properties of the microcapsules. Internalisation is favoured by microcapsules terminated with a positively charged polyelectrolyte, in order to allow for electrostatic interactions between the microcapsule and the negatively charged cellular surface. Atomic force microscopy (AFM) analysis of PAH-terminated microcapsules on human epithelial cells revealed that only 44% of the cells had not ingested microcapsules after 1 hour of incubation. In contrast, for the anionic PSS-terminated microcapsules, 82% of the cells failed to ingest microcapsules. Phagocytic cells e.g. cancer and immune cells are able to uptake microcapsules more readily, as demonstrated by a study that revealed that breast cancer cells can uptake approximately 30 PAH/PSS microcapsules with a diameter of 5 μm (Sukhorukov et al., 2005). Recent research has shown that microcapsules can be internalised by non-phagocytic cells such as Human Umbilical Vein Endothelial cells (HUVECs). This has been achieved by encapsulating neuraminidase within polystyrene sulfonate/polyallylamine hydrochloride microcapsules and allowing the neuraminidase to passively diffuse and subsequently

cleave the glycocalyx. Once cleaved, the microcapsules are free to enter the HUVECs (Liu et al., 2014).

1.4.4 Biodegradable polyelectrolyte microcapsules

As previously explained, biodegradable microcapsules can be synthesised simply by incorporating biodegradable polyelectrolytes within the layer-by-layer assembly. The disintegration of these microcapsules are regulated entirely by enzymatic degredation of the polymers. Further research has led to the development of microcapsules that can be degraded without enzymatic intervention. So-called charge shifting polymers are able to achieve this feat, by alternating their charge and consequently leading to repulsion and ultimate destruction of the layer-by-layer constructed shell. An example of such polymer is Poly(HPMA-DMAE), which consists of amine groups bound to the polymer backbone by carbonate ester bonds. When in the presence of a physiological buffer at 37 °C, the ester bonds are hydrolysed causing the cationic amine groups to dissociate, thus creating a neutral polymer (De Geest et al., 2006).

1.4.5 Polyelectrolyte microcapsules in bio-sensing

As described earlier, the properties of the polymer shells which make up microcapsules are heavily influenced by the external environment. To this end, microcapsules can be employed as biosensors for various applications. Polyelectrolytes constructed of weak polyelectrolytes will ultimately suffer swelling and decomposition as the pH of the surrounding solution passes the pKa of at least one of the polyelectrolytes used, due to the decrease in electrostatic attraction between the polymers in the capsule shells (Sato et al., 2011). Such capsules may be loaded with a fluorescent dye which would be released

as a consequence of the destruction of the microcapsule shell. Although, responsive to pH, these microcapsules maintain their structure to a certain degree and may not respond when the environment changes from basic to acidic or vice versa. This limitation has been circumvented by a study that encapsulated seminaphtharhodafluor (SNARF) in polyelectrolyte microcapsules. SNARF is a pH-sensitive fluorescent molecule which emits red and green fluorescence when in the presence of basic and acidic environments, respectively. This proved particularly useful when determining whether microcapsules had been internalised by cells which are slightly acidic due to the endosomal environment (Kreft et al., 2007).

1.4.6 Polyelectrolyte microcapsules in cancer therapy

A number of investigations have been conducted to test the potential of microcapsules as a drug delivery mechanism in cancer therapy. To discuss the potential, it is vital to understand the interaction between polyelectrolyte microcapsules and cancer cells. As demonstrated by Sukhorukov et al, breast cancer cells readily uptake polyelectrolyte microcapsules via phagocytosis (Sukhorukov et al., 2007). By conducting *in-vitro* experiments, with the nuclei stained with DAPI, De Geest et al. has shown that the microcapsules refrain from penetrating the nucleus itself. In fact, the study proves that upon internalisation, the microcapsules are contained within acidic vesicles, as indicated by fluorescent lysosomal staining (De Geest et al., 2006). This was confirmed by a study which utilised the biosensing capabilities of microcapsules as described earlier. SNARF was encapsulated within the microcapsules confirmed that the microcapsules were in an acidic endosomal/lysosomal environment (Kreft et al., 2007). With respect to drug encapsulation, polyelectrolyte microcapsules are an ideal form of encapsulation, particularly when the drug is non-soluble.

When drugs are kept in a non-soluble state, layer-by-layer assemblies can be applied to the crystals directly. This is particularly advantageous when sensitive drugs must be protected from harsh *in-vivo* environments in order to remain functional. Several drugs have been encapsulated using this principle, including ibuprofen and furosemide (Vergaro et al., 2011). To kick-start the layer-by-layer process, drug crystals are often treated with surfactants in order to give them a specific charge to allow for electrostatic adsorption of the first polyelectrolyte (Caruso et al., 2000). An advantage of this direct coating method is that the encapsulation efficiency is likely to be higher since drug elution from the core, a problem associated with the pre-loading method, is entirely circumvented.

To assist with the release of the drug, once the capsules have been internalised, the capsules are usually manufactured from enzyme-cleavable polyelectrolytes e.g. poly-L-arginine and dextran sulfate. These layers can easily be degraded by intracellular proteases, resulting in the release of the drug (De Geest et al., 2006). Crucially, experiments have revealed that the phagosomal membrane which encapsulates the microcapsule ruptures upon capsule disintegration, thus releasing the drug into the cytoplasm of the cancer cell (Skirtach et al., 2008).

In order to be a viable method of drug delivery, microcapsules must be tested in an *in-vivo* environment to ensure that unwanted side effects associated with interactions with biological tissue are not experienced. The tissue response was tested by De Koker et al.

(2007). Commonly used poly-L-arginine and dextran sulphate microcapsules were subcutaneously injected into a mouse. An inflammatory response was detected by an increase in the level of macrophages and fibroblasts at the site of injection. A pronounced reaction was recorded 18 days after the injection with a significantly high occurrence of new vascularisation Interestingly, there was no mention of the capsules being sterilised prior to use, however, the reaction is assumed to be a direct result of the microcapsules which are detected as foreign bodies by the immune system (De Koker et al., 2007). This immune response, albeit moderate, may be reduced by functionalising the surface of the microcapsules with polyethylene glycol (PEG). Researchers speculate that this so-called PEGylation could have a profound desensitising effect on the immune response, however, this is yet to be elucidated (Vergaro et al., 2011).

This thesis herein presents research that has been conducted in order to further the development of targeted drug delivery using microcapsules, an area that has been given little attention with respect to layer-by-layer fabricated polyelectrolyte microcapsules. Specifically, chapters 2 and 3 focus on controlled release of molecules from biodegradable microcapsules in order to demonstrate the ability to fine-tune the release kinetics of the encapsulated contents. Chapters 4, 5 and 6 focus on methods of functionalising polyelectrolyte microcapsules in order to achieve exclusive binding to protein substrates. The final chapter explores the use of functionalised microcapsules in an *ex-vivo* setting in order to determine their viability as a potential drug carrier.

2. Controlled release of protein from biodegradable polyelectrolyte microcapsules

2.1 Introduction

A major factor, which is often critical in drug delivery systems is the ability to control the release of the drug. As explained in the previous chapter, restenosis of arteries after surgical intervention is one such complication that requires a sustained release of therapeutic drug to control the disease. Polyelectrolyte microcapsules are porous, and therefore offer a degree of control over the release of the encapsulated drug. This can be further enhanced by incorporating biodegradable polyelectrolytes into the layer-by-layer structure, as explained in the previous section.

Following preliminary tests, it was determined that Poly-L-arginine and Poly-L-glutamic acid were ideal materials to fabricate biodegradable microcapsules. Both polypeptides are cleavable by proteases within the body and therefore should biodegrade *in-vivo* and release its contents accordingly. The aim of this chapter is to develop a system by which one can easily measure the effects of enzyme concentration on the release of encapsulated contents. It is assumed that a higher concentration will lead to more degradation of the capsule shell and subsequently, more release of the encapsulated material, thus highlighting the sensitivity of these potential drug carriers.

2.2 Materials

Bovine serum albumin (cat. no. A2153), poly-L-arginine hydrochloride (15-70 kDa) (cat. no. P7762), poly-L-glutamic acid (kDa) (cat. no. P4761), protease from streptomyces grisius (cat. no. P5147), Rhodamine B isothiocyanate (cat. no. R1755), boric acid (cat. no. 202878) were purchased from Sigma Aldrich Co.

2.3 Method

Bovine serum albumin (BSA) was selected as the protein to be encapsulated in order to test the release kinetics of the biodegradable polyelectrolyte microcapsules. This serum protein was chosen as it is an inexpensive protein which can be easily labelled fluorescently by using isothiocyanate derivatives of fluorescent dyes. To label the protein, BSA was dissolved in a borate buffer, made from 0.1M boric acid and 0.15M sodium chloride. 1mg Rhodamine-B isothiocyanate was dissolved in 5ml ethanol and added to the protein solution. After 24 hours of incubation at room temperature, under gentle stirring, the solution was dialysed using cellulose dialysis tubes to remove any unconjugated Rhodamine-B. The external water was replenished daily until diffusion of Rhodamine ceased.

2.3.1 Microcapsule preparation

The capsules were fabricated via the well-established layer-by-layer technique. Briefly, calcium carbonate cores embedded with Rhodamine-labelled BSA were co-precipitated by adding 24ml Rhodamine-BSA (1.8mg/ml) to 24ml 0.33M $CaCl_2$ and finally adding 24ml 0.33M Na_2CO_3. The mixture was stirred vigorously for 30 seconds and the resulting $CaCO_3$ was left for 5 minutes to allow the formation of a monodisperse

population of spherical cores with diameters ranging between 4 and 6μm. The cores were washed by centrifugation at 1500 rpm for 1 minute, followed by aspiration of supernatant and subsequent re-dispersion in deionised water. After 3 of these wash/centrifuge cycles, the $CaCO_3$ cores were coated by immersing the cores in 10ml of 1mg/ml Poly-arginine. To allow the sedimentation process to occur, and to ensure complete coverage of cores, the solution was placed on a vortex machine for 20 minutes. This was followed by 3 wash/centrifuge cycles to remove the excess polymer that had not been adsorbed. The same procedure was applied for the next layer (Poly-glutamic acid), resulting in the formation of a single bilayer. The process was continued until four bilayers were made. To dissolve the calcium carbonate cores and hence complete the fabrication process, ethylenediaminetetraacetic acid (EDTA) was used. 5ml of 0.2M EDTA was added to the capsules for 7 minutes and an additional 5ml for a further 7 minutes. This was followed by 3 wash/centrifuge cycles using EDTA and 3 wash cycles using deionised water.

2.3.2 Encapsulation efficiency

The supernatants of each wash cycle performed throughout the fabrication process were collected to determine the encapsulation efficiency of the capsules which is governed by the following equation:

$$\left(\frac{M_i - M_l - M_d}{M_i}\right) \times 100$$

where M_i is the initial mass of BSA added, M_l is the mass of BSA present in the supernatants during layer-by-layer deposition (including the supernatant collected after core formation) and M_d is the mass of BSA in the supernatants collected during the core dissolution. BSA was assayed using a fluorescence spectrometer. Emission and

excitation slits were set to 1nm and the excitation wavelength and emission detection range was set to 540 nm and 580 – 640 nm, respectively, in accordance with the excitation and emission wavelengths of Rhodamine B. A calibration curve was generated by testing known concentrations of BSA

2.3.3 Fluorometry analysis

The bulk microcapsule sample was divided into 35 aliquots. Solutions of protease from Streptomyces Griseus (Sigma Aldrich, UK) of concentrations 1mg/ml, 100µg/ml, 10µg/ml, 1µg/ml, 100ng/ml and 10ng/ml were made. Each of the enzyme concentrations were placed in 5 eppendorf tubes with microcapsules. The remaining 5 microcapsule samples were immersed in water as a control. All samples were stored in the refrigerator at 4°C. A sample was taken from each protease concentration groups after 24hrs. After centrifugation, the supernatants were analysed using fluorescence spectroscopy (Perkin Elmer LS 55) to determine the amount of Rhodamine-BSA released. This process was repeated for 5 consecutive days to build a protein release profile. A calibration curve was created by analysing 5 samples of known BSA concentration to determine the concentration of BSA in each experimental sample.

2.3.4 Scanning electron microscopy analysis

Scanning electron microscopy (SEM) images were taken using a FEI Inspect-F scanning electron microscope. Samples of biodegradable microcapsules were taken after 5 days of incubation to determine their morphology after degradation. Control samples, devoid of enzyme exposure were analysed to confirm whether the degradation was purely a result

of enzymatic action. Samples were gold-sputtered to render the surface electrically conductive. SEM images were subsequently acquired using a 10 kV beam.

2.4 Results and Discussion

The calibration curve generated from Rhodamine-BSA calibration can be seen in Figure 8. Known concentrations of BSA were made by weighing BSA using a microbalance and dissolving it in known volumes of PBS. As expected, an increase in BSA concentration led to an increase in fluorescence intensity recorded by the fluorometer. This confirms that the BSA had been successfully labelled with Rhodamine.

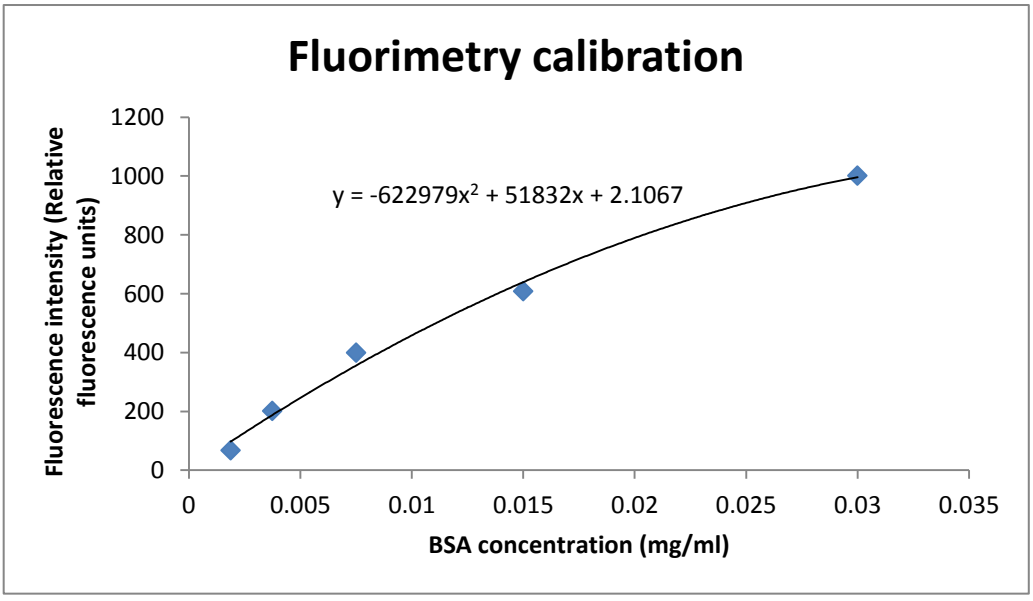

Figure 8. Fluorometry calibration. BSA-Rhodamine was assayed using fluorescence spectroscopy.

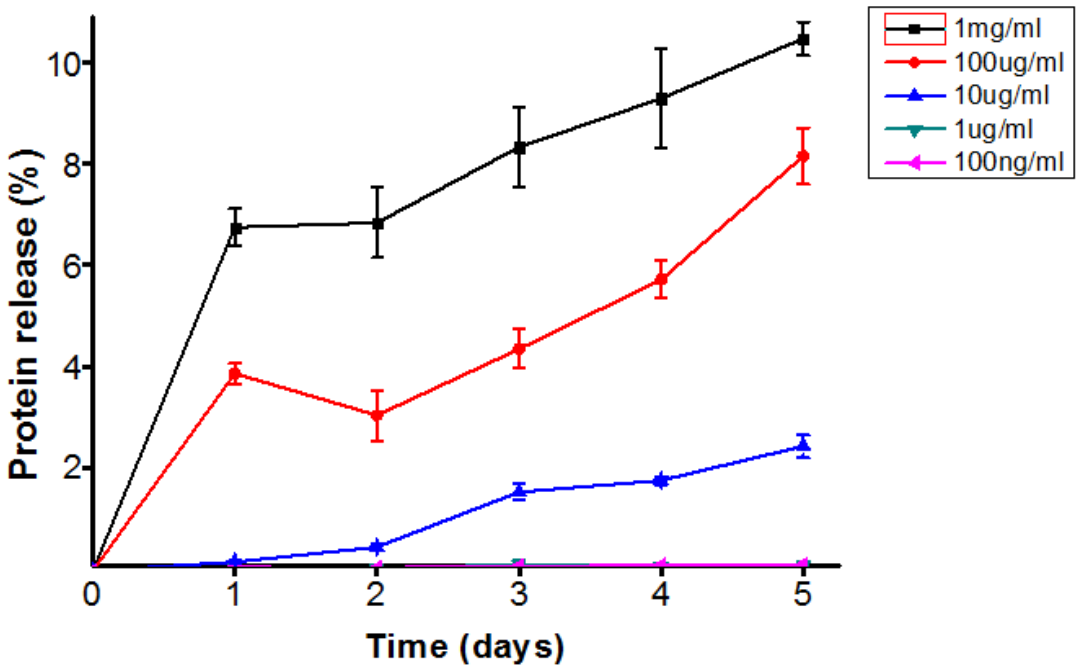

Figure 9. Cumulative protein release profiles obtained from biodegradable microcapsules under different external enzyme concentrations (highlighted by key). Protein release is given as a percentage of the initial mass of encapsulated BSA (n = 3).

The results shown in Figure 9 clearly highlight a more pronounced protein release in samples with high concentration of proteinase (1mg/ml, 100mg/ml and 10mg/ml). Furthermore, results show that at enzyme concentrations of 100ng/ml and below, there is no significant enhancement of protein release since the supernatants of these samples contained similar levels of protein to the control sample throughout the 5 days of testing.

Protein release for the 1mg/ml and 100µg/ml samples appeared to decrease on day 2. Theoretically, this is impossible since the capsule dispersant can only accumulate more protein after another 24hrs, unless the protein re-entered the intra-capsular space, which is highly unlikely. These apparent anomalies can be explained by the fact that the day 2 samples of these concentrations had less microcapsules to begin with, hence even after an

additional 24hrs, the samples appeared to release less than what they released on the first day. Indeed it was assumed that by shaking the bulk sample, the microcapsules were uniformly dispersed in solution and therefore by separating the solution into aliquots of equal volume, each sample would contain the same amount of capsules. In reality it is impossible to obtain a perfectly uniform capsule dispersion due to gravitational effects as well as aggregation of microcapsules. To avoid this in the future, samples should be weighed to ensure that capsule concentration is approximately the same.

Another characteristic of this protein release profile that does not bode well with typical findings published in the literature is the significant difference in the end point protein release values. This suggests that the protein is still being liberated at day 5. It can also be an indication that the pores of the capsules were occluded due to the accumulation of BSA on the inner surface of the capsules. With regard to the 1mg/ml sample, it is clear that the protein concentration is still rising to a degree, although the low gradient of the line between days 4 and 5 suggest that these capsules have almost reached the point where protein release ceases.

Scanning Electron Microscope Results

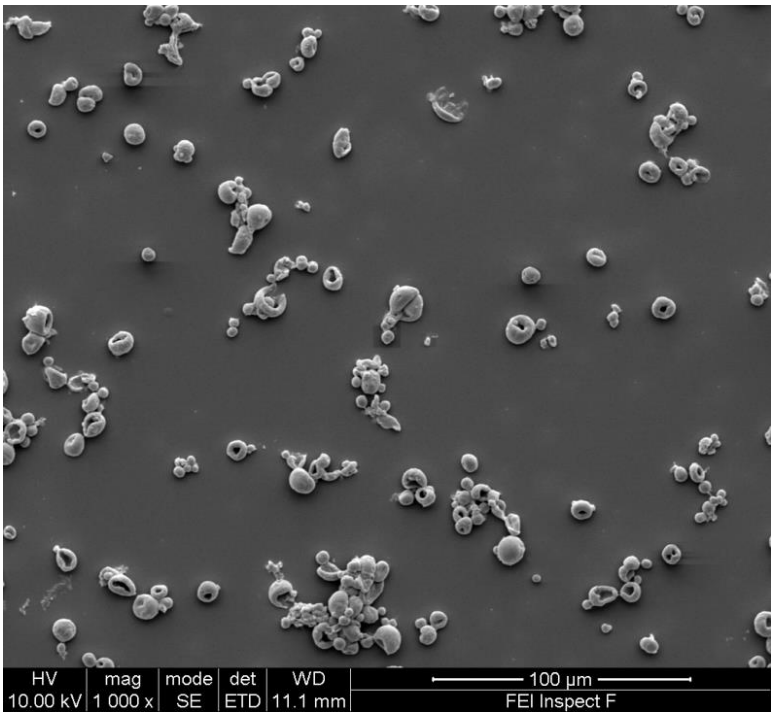

Figure 10. SEM image of BSA-loaded microcapsules without exposure to proteinase. T = 5 days.

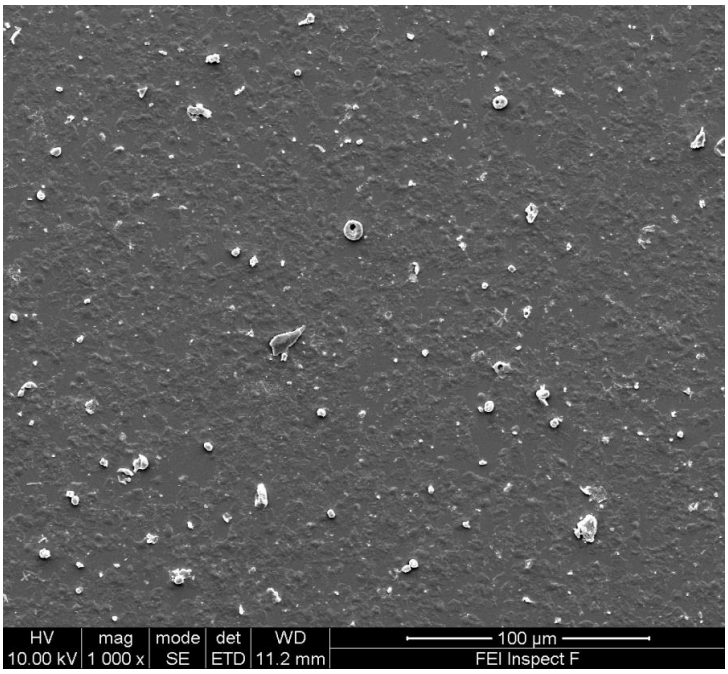

Figure 11. SEM image of remnants of BSA-loaded microcapsules after 5 days exposure to a 1mg/ml solution of proteinase

It is clear from the micrographs that higher concentration enzyme solutions led to the degradation and rupture of capsules. There was significantly less capsules in the 1mg/ml sample in comparison to the 100μg/ml sample, after 5 days. Incidentally, this decrease was noticed with an increase in material on the surface of the slide. This material is undoubtedly the residual polymer from the capsules that have been completely degraded, as shown in Figure 11.

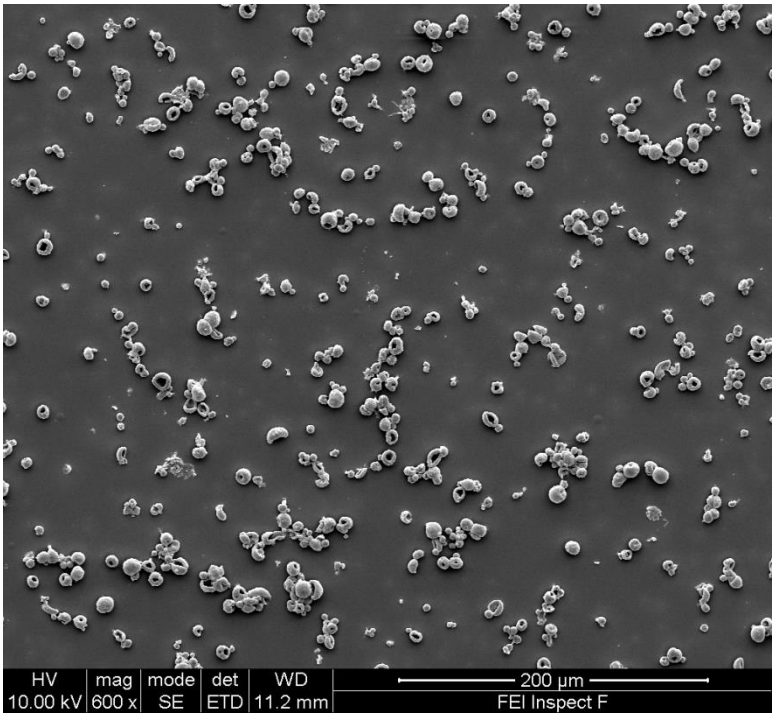

Figure 12. SEM image of BSA-loaded microcapsules after 5 days exposure to a 100ng/ml proteinase solution.

Analysis of the acquired micrographs reveal that more than 50% of the microcapsules resemble tori and have apparent holes in them. This phenomenon is consistent with all samples, even in the control sample where no enzyme is present. It may be that these are not holes and in fact these are deep folds of the capsule membrane leading to a concave structure. If they are holes, it is unlikely that these holes manifested due to enzymatic

action since these holes are even noticed in the control sample. Furthermore, the surface topology is more regular than surfaces noticed on microcapsules that have been convincingly degraded by high enzyme concentrations. Also if these holes were a result of peptide hydrolysis, higher concentrations of BSA would have been detected in the low enzyme concentration samples. However, no such burst release was shown suggesting that this burst release occurred during the manufacturing process, before enzymes were introduced to the capsule.

Another possible explanation could be insufficient coating of the calcium carbonate cores during synthesis due to an insufficient polymer. To prevent the occurrence of this, a sample of calcium carbonate cores were counted using a haemocytometer, and the total surface area of the cores was calculated. According to G. Sukhorukov, 1mg of polymer has the ability to cover a surface of approximately $1m^2$, thus the calculated total surface volume of $0.35m^2$ should adequately be covered by the 10mg of polymer used in each layer. Taking this in consideration, it can be concluded that these are not holes and are in fact folds in the capsule membrane.

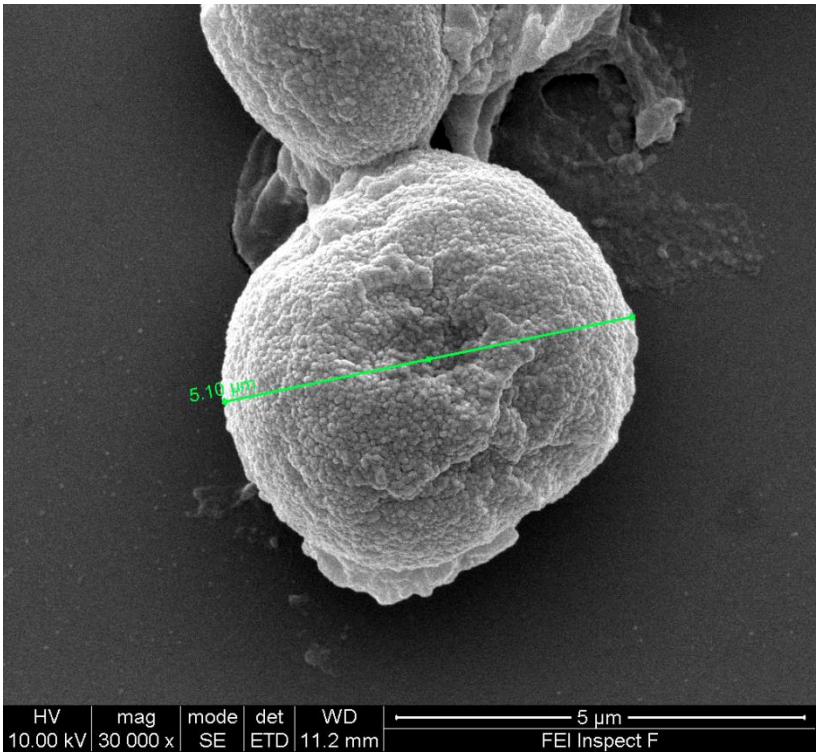

Figure 13. A single microcapsule from the control sample i.e. not exposed to proteinase (Diameter 5.1µm).

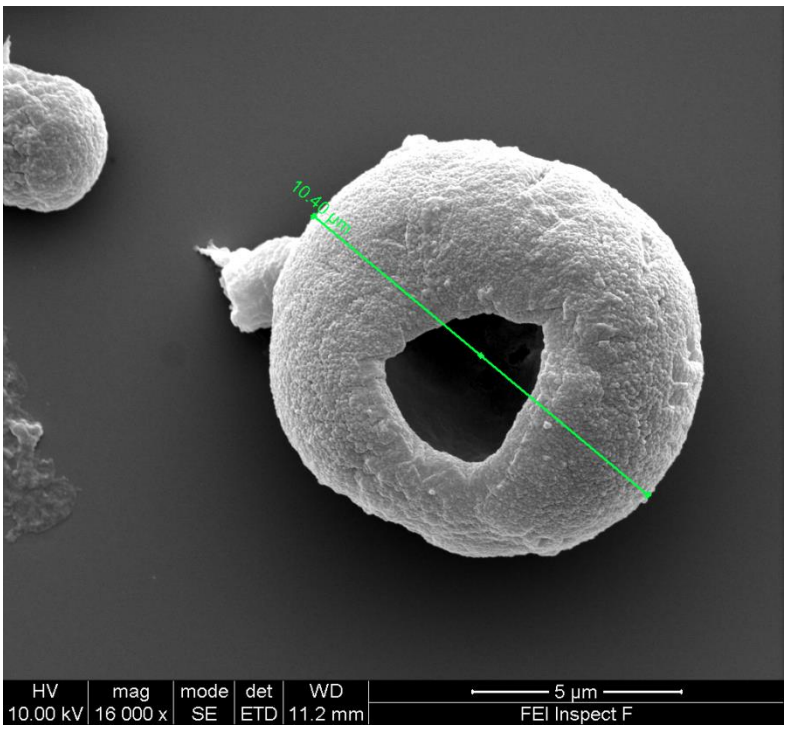

Figure 14. A single microcapsule from the control sample i.e. not exposed to proteinase, showing an apparent hole (Diameter 10.4µm).

From Figure 13 and Figure 14 it is clear that the capsules are polydisperse with microcapsule diameters ranging from 5-10μm. This resulted due to the formation of polydisperse calcium carbonate cores. It is unclear why this occurred. In future experiments, the cores shall be left to crystallise for a shorter time period to prevent the formation of excessively large cores.

Encapsulation Efficiency

Taking into consideration the number of layers and associated washing cycles applied, an encapsulation efficiency of 79.7% highlights the excellent retention properties of the fabricated capsules. It was noted that after each poly-L-glutamic acid layer, a high concentration of Rhodamine-BSA was found in the supernatant after deposition. No such burst-release was noticed in the supernatants collected from poly-L-arginine deposition. To maintain enzyme stability and to prevent the occurrence of microbial infection, the protein release study was conducted at 4°C. However, this temperature is not representative of the environment *in-vivo*. Indeed, at this temperature the protease activity is likely to be low. It will be challenging to maintain enzyme stability at body temperature for 5 days. With the aid of metabolic inhibitors such as sodium azide, this may be feasible.

2.5 Conclusion

In conclusion, biodegradable polyelectrolyte microcapsules were successfully fabricated using the layer-by-layer technique. As shown in the protein release profile, an elevated concentration of enzyme in the supernatant led to a higher rate of release of BSA,

unquestionably as a consequence of polyelectrolyte shell degradation. The microcapsules, constructed of 4 bilayers, are able to encapsulate high molecular weight molecules, as shown by a high encapsulation efficiency of BSA (79.7%). Significantly, the largest amount of BSA was lost in the core-dissolution step. Comparatively fractional liberation was noticed during layer deposition. This will be taken into consideration when approximating encapsulation efficiency for future experiments.

3. Self-degradable microcapsules

3.1 Introduction

The previous chapter has demonstrated that biodegradable microcapsules can be synthesised to be responsive to an enzymatic environment. In a situation where enzymes are not present, or not in abundance, these microcapsules may not be able to release their payload as efficiently as desired. Previous studies have been reported on "self-degradable microcapsules", highlighting possible mechanisms to overcome this. This chapter consists of a study conducted with the purpose of fine-tuning the response of "self-degradable" microcapsules for desired release rates, where the environment is devoid of enzymes.

As highlighted in chapter 1, current techniques of controlling the rate of release require some form of external stimuli. This may be unfeasible under certain circumstances. For example, changing the pH in a biological environment may lead to the denaturation of proteins. The previous section relies on external triggers i.e. enzymes within the dispersant, to break down the capsule shell and release the contents. This limitation can be circumvented by encapsulating enzymes within the microcapsules so they can be degraded from the inside. Proteases have been used in the pilot study in the previous chapter. In order to utilise them effectively, their structure and function must be fully understood.

3.1.1 Proteases

Proteases are a family of enzymes which have the ability to break down proteins i.e. they facilitate proteolysis. More specifically, they target the amide bonds within proteins and catalyse the hydrolysis reaction, ultimately breaking the protein down into smaller peptides/oligopeptides and amino acid residues. In doing so, proteases regulate the vast majority of chemical reactions that take place within cells. Proteases, themselves, are proteins, synthesised by ribosomes in the traditional manner. They are usually secreted as a latent form, known as a zymogen, which effectively has the active site "shielded" by a peptide domain, known as the pro-domain (Barrett et al., 2012). This so-called active site is the area where cleavage of the protein substrate occurs.

Working principle

With the pro-domain intact, the active site has no physical access to the cleavable regions of the protein i.e. the peptide bonds. In order to be activated, the pro-domain must be cleaved by another enzyme. Once this is removed, the protease is in its active form. In a similar fashion to all enzymes, proteases have an optimum working temperature. For the gold standard protease mixture, pronase, this temperature lies between 30-40 °C. At a temperature above 60°C, the proteases, themselves, begin to denature, rendering them dysfunctional (Potier et al., 1990).

There are many different types of proteases, each with a different crystallographic structure, and different mechanisms for catalysis of peptide bond hydrolysis. The differences in structure, particularly at the active site, complement their specific

substrates. This is often described as the lock and key theory, as proposed by Hermann Emil Fischer in 1890. In essence, this theory states that in order to achieve enzyme-substrate complexation, and subsequent peptide bond cleavage, there must be a degree of complementarity, both electrostatically and geometrically.

Self-degradable microcapsules have been previously synthesised and studied within the last decade (Borodina et al., 2007). This particular work effectively proves that the presence of proteinase (a mixture of proteases from Streptomyces griseus) increases the degradation of the capsule shell and hence increases the rate of release of the encapsulated DNA within the microcapsules. These particular microcapsules were constructed from two polypeptides, namely, poly(L-arginine) and poly(L-aspartic acid). The study concluded that without co-encapsulation with protease, the DNA remained trapped within the microcapsules after 40 hrs. In contrast, when protease was encapsulated, the entire payload was liberated within 2.5 hours, with 80% liberated within 1 hour. The concentration of proteinase encapsulated during the fabrication process was 3mg/ml. Taking into consideration the aggressive release kinetics associated with these microcapsules, one can conclude that this is an extremely high concentration of protease.

If a more sustained and controlled release profile is desired, the concentration of the encapsulated enzyme should be reduced drastically. Indeed, prior research has indicated that reducing the concentration of encapsulated enzyme alone, the drug release rate can be increased from seconds to days (Borodina et al., 2007). A major limitation of this method of encapsulation is the restriction of the type of drugs that can be loaded which is

limited to species that are not reactive to, or cleavable by the encapsulated enzyme. For example, if a protein, with a specific structure and function, suited for a particular treatment, is co-encapsulated with protease, the protease is likely to denature the therapeutic protein, rendering the treatment useless.

The aim of this chapter is to create self-degradable microcapsules similar to the kind used in the study by Borodina et al., (2007) and demonstrate the ability to fine-tune the release of encapsulated contents within these microcapsules. This will be achieved by a combination of creating microcapsules of different number of polyelectrolyte layers and encapsulating different quantities of proteinase. Instead of encapsulating DNA, the release of the proteinase itself, will be monitored to show whether the capsule shell is permeable to larger molecular weight species. Microcapsules, of different thickness and different constituents (biodegradable and non-biodegradable) will be produced, in order to demonstrate the ability to control the release of the encapsulated proteinase. This shall be monitored using UV-vis spectrophotometry.

3.1.2 UV-vis spectrophotometry:

Ultraviolet-visible (UV-vis) spectrophotometry is a routinely used spectroscopic technique which utilises ultraviolet light within the visible range (380nm to 750nm) and the invisible range (190-380nm). UV light of a predetermined wavelength is passed through a sample contained within a clear glass or PMMA cuvette, where a certain amount of light is absorbed due to the solutes within the sample, e.g. protein or DNA. More specifically, the non-bonding electrons within the molecule absorb the light and consequently become excited to a higher energy level orbital (Skoog et al., 2013). For

this reason it is often referred to as UV absorption spectroscopy. The level of absorbance by the sample is proportional to the concentration of the solute, hence this technique can provide quantitative data with respect to the concentration of a sample (Skoog et al., 2000). This study will be monitoring the level of proteinase, a protein. Proteins characteristically absorb ultraviolet light at approximately 240-300nm (Grimsley and Pace, 2004). More specifically, tryptophan, tyrosine and cysteine residues within the protein give rise to absorption at 280 nm. The differences in concentration and ratios of these residues create a shift in the peak absorbance of a protein, which is evidently unique for each individual protein. For the purposes of this study, the specific optimal properties which correspond to the peak of the absorbance graph is not important, since there is only one protein i.e. proteinase which is being analysed. The use of UV spectroscopy is much preferred than the previously used fluorescence spectroscopy, as used in the previous chapter. By using UV spectroscopy, effects such as photobleaching of the sample are eradicated. Furthermore, the sample doesn't require labelling which is time consuming and could lead to inaccuracies.

3.2 Materials

Calcium chloride dihydrate (CaCl2.2H2O), sodium carbonate (Na2CO3), ethylenediaminetetraacetic acid disodium salt dihydrate (C10H14N2Na2O8·2H2O), dextran sulfate sodium salt (Mol. Wt. ~40 kDa), poly-L-arginine hydrochloride (mol wt 15−70 kDa), Poly(allylamine hydrochloride) (mol wt 65 kDa), Poly(sodium 4-styrenesulfonate) (mol wt 70 kDa), Protease from Streptomyces griseus, were purchased from Sigma Aldrich Co.

3.3 Method

3.3.1 UV spectroscopy protocol

A Perkin Elmer Lambda 35 UV-vis spectrophotometer was used to analyse the samples. The slit width and data acquisition intervals were kept constant throughout (at 1 unit). Absorption detection range was set to 190-300 nm in accordance with the absorption wavelength of protein. A calibration curve was generated by measuring absorbance values for 14 samples with known concentrations ranging from 1 μg/ml to 1 mg/ml.

3.3.2 Microcapsule fabrication

Microcapsules were fabricated in a similar fashion to those made in chapter 2. The polycationic and polyanionic constituents of the layer-by-layer assembly were poly (L-arginine) and dextran sulphate, respectively. Dextran sulphate, a member of the polysaccharide family was chosen to monitor the effects of release, in the case where only one of the layer-by-layer constituents is cleavable by the encapsulated enzyme. For control purposes, synthetic microcapsules, comprised entirely by non-biodegradable polyelectrolytes, were produced. The polycation, and polyanion for these microcapsules were PAH and PSS, respectively. Microcapsules synthesised for this study were loaded via a preloading technique, previously described in section 2.2. 6 and 12 layer microcapsules were synthesised in order to determine the effects of the number of layers on the protein release profile. Each supernatant during the fabrication process was collected and analysed for proteinase content to determine the encapsulation efficiency.

3.3.3 Sample preparation and proteinase concentration analysis.

Once the cores had been dissolved, the 6 and 12 layer microcapsules were re-suspended in water. The concentration of each sample was measured using a haemocytometer, an apparatus traditionally used for determining the red blood cell count. The concentrations were equalised by dilution to allow a direct comparison to be made between the proteinase release profiles for the 6 and 12 layer biodegradable/non-biodegradable microcapsules. At various time points after initial incubation: t= 0.25, 0.5, 0.75, 1, 1.25, 1.5, 1.75 and 2 hours, the samples were centrifuged at 1500 rpm for 1 minute. In addition to these time points, the 12 layer samples were analysed up to t = 24 hours. The supernatant was then carefully transferred to a cuvette ensuring that no capsules were taken in the process. After UV spectroscopy analysis of the supernatant, the supernatant was promptly returned to their respective Eppendorf tubes and the capsules were re-suspended to allow further release of the encapsulated enzymes. After checking the supernatant at different time points over a period of 21 hours, a proteinase release profile was generated to demonstrate the release kinetics of the 6 and 12 layer microcapsules. The samples were kept at room temperature throughout the study to ensure the proteinases remained active.

3.3.4 Encapsulation efficiency

The encapsulation efficiency for the 12 layer microcapsules was calculated, to determine whether there is a significant amount of proteinase within the microcapsules at the end of the fabrication process. Previous experience, from the encapsulation efficiency calculation performed in chapter 2 suggests, that there are specific steps within the manufacturing process, where significant levels of encapsulated contents are lost. The supernatants were subsequently analysed by UV spectrophotometry as previously

described. The total amount of protein lost during the synthesis of the microcapsules was subsequently calculated to determine the encapsulation efficiency.

3.3.5 Epifluorescence imaging of microcapsules

Fluorescent 6 layer microcapsules were fabricated by replacing the second polyarginine layer within the LbL structure with FITC-labelled polylysine. As per usual, these microcapsules were preloaded with protease and left to incubate for 1 hour. Images were taken in order to visualise the integrity of the polyelectrolyte shells. Micrographs were taken using a Leica DMI4000B epifluorescence microscope, coupled to a Leica DFC300FX digital colour camera. The excitation wavelength of the FITC used was 488 nm, hence the excitation beam was filtered with a blue prism.

3.4 Results

3.4.1 Haemocytometry

Haemocytometry analysis of each sample highlighted a significant difference between the 4 different samples. These differences are likely to have arisen due to human error, particularly during the washing steps of the fabrication process, where capsules may accidently be removed during pipette aspiration of the supernatant after centrifugation. The recorded microcapsule counts can be seen in Table 1. The suspensions were diluted accordingly to equalise the microcapsule concentrations.

Table 1. Haemocytometry calculations.

	Biodegradable capsules (millions)		**Non-biodegradable capsules (millions)**	
	6 layer	**12 layer**	**6 layer**	**12 layer**
Capsule concentration (caps/ml)	10.68	29.5	44.4	88.4
Desired concentration (caps/ml)	10.68			
Volume of sample required (ml)	2	0.72	0.48	0.24
Volume of DI H_2O for dilution (ml)	0	1.28	1.52	1.76

3.4.2 Calibration

As expected, the UV absorbance peak measured at 280 nm, increased in amplitude as the concentration of proteinase increased. This confirms that the UV spectrophotometer is responsive to the presence of proteinase within a deionised water solution. Furthermore, the apparatus is responsive to concentrations as low as 1 μg/ml, confirming the apparatus as a viable means of measuring proteinase release. Once the calibration curve was plotted, a trendline for the curve was added, with the equation displayed in Figure 15. The intercept for the trendline is set to zero to satisfy the condition of zero absorbance for a solution void of proteinase.

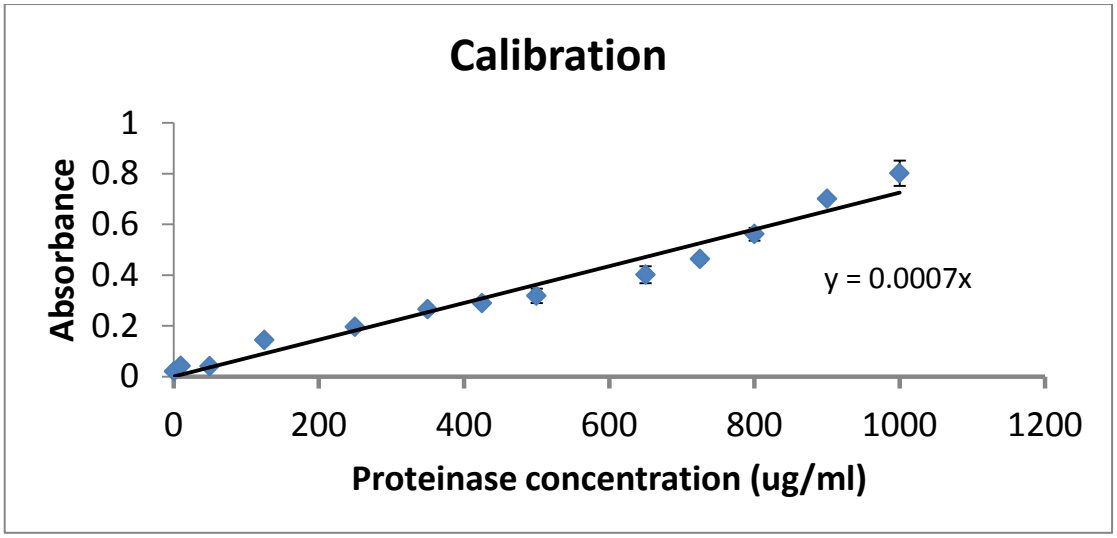

Figure 15. Calibration graph for proteinase absorbance calculated using UV-vis spectroscopy. Error bars indicate standard deviation (n = 3).

3.4.3 Protein release profiles

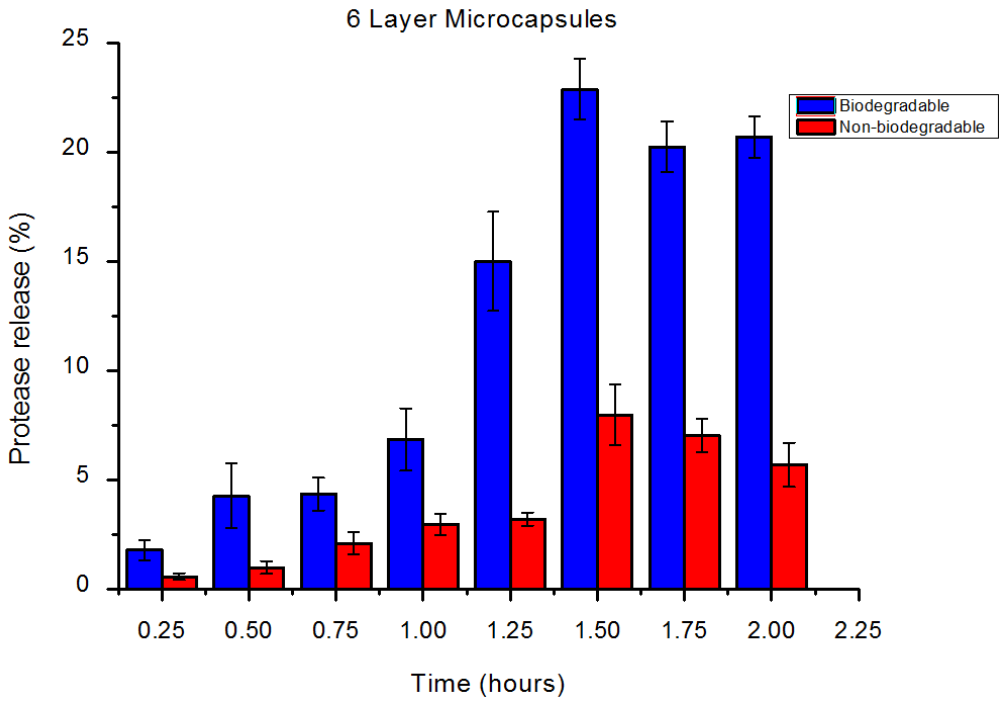

Figure 16. Protein release profile for 6 layer microcapsules. Protein release is expressed as a percentage of total protease encapsulated at t = 0. Error bars indicate standard deviation (n = 5).

As depicted in Figure 16, the level of released proteinase generally increases for both groups. The decrease in protein release for the non-biodegradable microcapsules is undoubtedly an anomalous result, since the accumulated proteinase diffused into the supernatant is unlikely to be reduced. At all time points, the biodegradable microcapsules released more proteinase than the non-biodegradable microcapsules. The most significant increase was noticed at t = 1.25 hours where a 5-fold increase in protein release was observed.

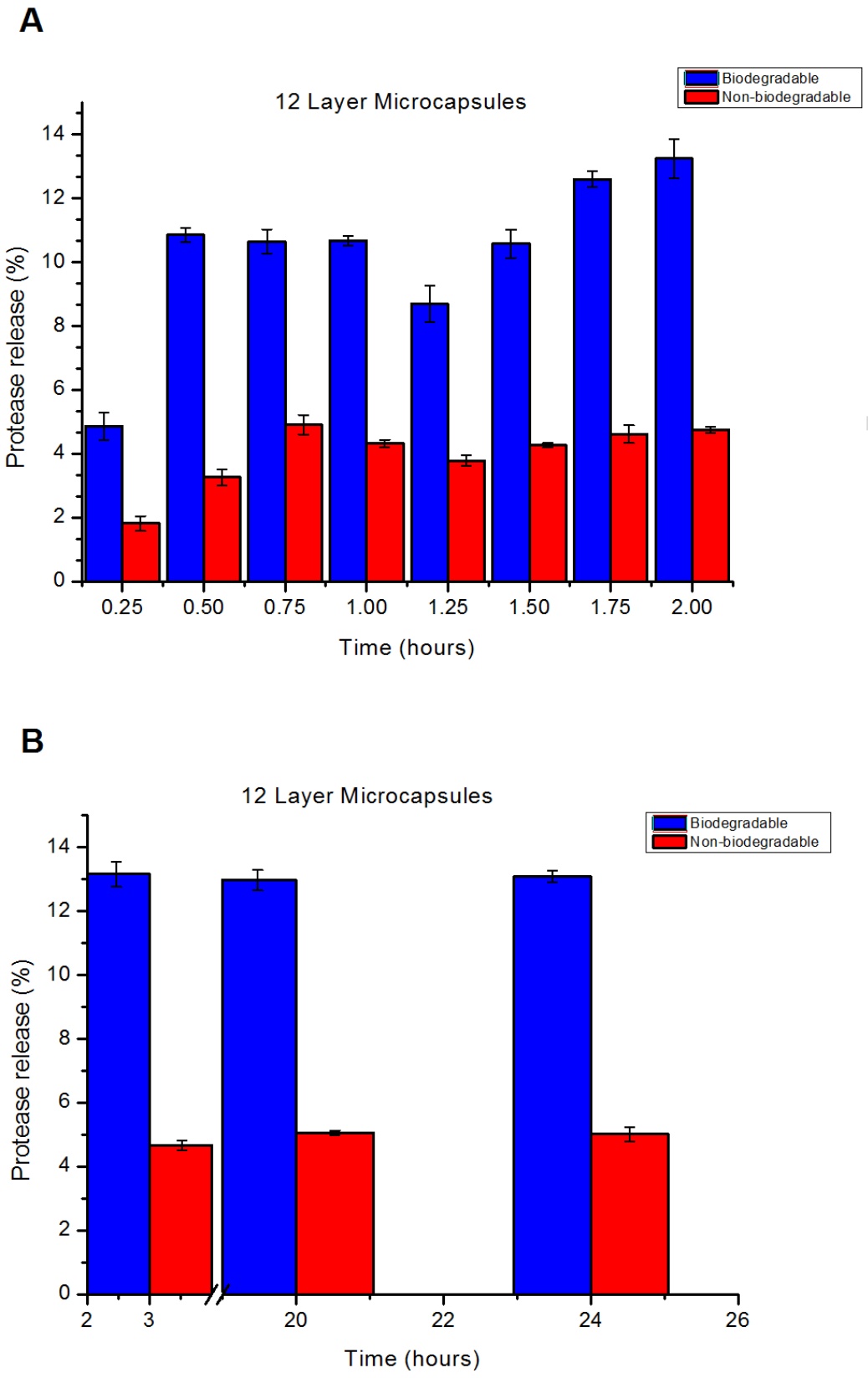

Figure 17. Protein release profile for 12 layer microcapsules between t=0 and t=2 hours (Panel A). Panel B shows a long term release profile. Error bars indicate standard deviation (n = 5)

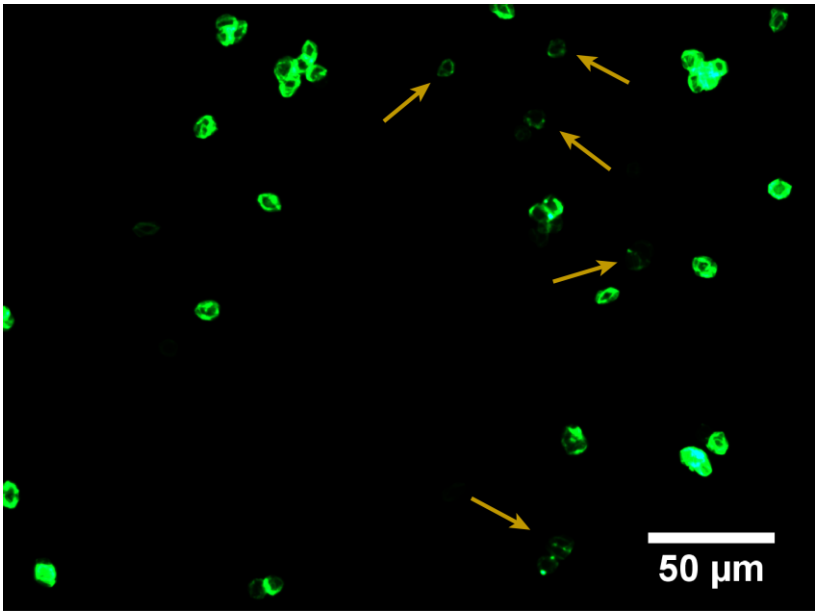

Figure 18. Fluorescent micrograph of 6 layer biodegradable microcapsules after 1 hour of incubation, highlighting the presence of partially degraded microcapsules (shown by yellow arrows). Green fluorescence is achieved by a single PLL-FITC layer was incorporated into the layer-by-layer construct.

Results obtained from the 12 layer microcapsules, as shown in Figure 17, indicate that in general, less proteinase was released, when compared to the thinner 6 layer microcapsule. With reference to the biodegradable microcapsules, despite an extremely long incubation time of 24 hours, only 13.1% of the encapsulated protease was liberated. When compared to the 6 layer biodegradable microcapsules, it is evident that after just 2 hours, 21% of the contents were liberated. Similarly to the proteinase concentrations recorded from the 6 layer microcapsules, the biodegradable 12 layer microcapsules also show a higher degree of liberation than the non-biodegradable 12 layer microcapsules, with a three-fold increase in protease liberation recorded at t = 0.5 hours. Furthermore, at t = 2 hours, the protease liberation seems to plateau at approximately 13% and 4% for the biodegradable and non-biodegradable samples respectively.

3.4.4 Encapsulation Efficiency

The encapsulation efficiency was determined by accumulating the masses of proteinase recorded after each significant stage in the manufacturing process, where significant levels of proteinase will be liberated, as displayed in Table 2. This was measured by UV-spectrophotometry. This total value is then subtracted from the original proteinase amount incubated during core formation (2000 µg per sample) to determine the amount taken up by the microcapsules. It is then displayed as a percentage of the original amount, i.e. the encapsulation efficiency, as shown in Table 3.

Table 2. Measured proteinase concentration after each significant step of the LbL process.

Biodegradable microcapsules		Non-biodegradable microcapsules	
Stage	Concentration (µg/ml)	Stage	Concentration (µg/ml)
Core formation	94.64	Core formation	94.64
Core wash 1	87.26	Core wash 1	87.26
Core wash 2	38.72	Core wash 2	38.72
Core wash 3	96.55	Core wash 3	96.55
Core dissolution	71.88	Core dissolution	9.56
EDTA wash 1	59.25	EDTA wash 1	0.95
EDTA wash 2	85	EDTA wash 2	0.15
EDTA wash 3	55.94	EDTA wash 3	0.67
H_2O wash 1	2.67	H_2O wash 1	0
H_2O wash 2	1.28	H_2O wash 2	0
H_2O wash 3	1.76	H_2O wash 3	0

Table 3. Encapsulation efficiency calculation for 12 layer microcapsules.

	Biodegradable microcapsules	**Non-biodegradable microcapsules**
Total proteinase lost	1189.9 µg	603 µg
Total remaining in capsules	810 µg	1397 µg
Encapsulation efficiency	40.5%	69.85%

3.5 Discussion

The main purpose of this study was to determine whether the rate of content release of biodegradable microcapsules could be altered in an environment where enzymes were not present. This was achieved by pre-encapsulating proteinase within the microcapsules so they can be degraded from the inside, rather than externally. Unlike previous studies, this study uses microcapsules, synthesised of both polyaminoacids and polysaccharides, hence only one component within the layer-by layer structure is cleavable by the encapsulated proteinase.

Encapsulation efficiency calculations were performed on the synthetic and biodegradable 12 layer microcapsules, to determine whether there was any proteinase left within the capsules. Most of the contents are naturally liberated during the core dissolution step, since the cores trap the contents within their porous surface, releasing a vast amount through the microcapsule membrane as the core is disintegrated and dissolved. Another more important step with respect to encapsulation efficiency is the step where the protein/drug is taken up (absorbed and adsorbed) to the cores i.e. during core production. It is very feasible to find a large proportion of the protein/drug left in the supernatant formed immediately after core preparation. Washing during the layer-by-layer process is unlikely to liberate much proteinase, since the vast majority of the proteinase will be adsorbed and absorbed to the surface of the calcium carbonate core. Taking this into consideration, the supernatants were removed and retained at the core preparation and core dissolution stages. Determination of the encapsulation efficiency is essential for determining whether the microcapsules, are indeed, self-degradable. If all of the proteinase was liberated, the efficacy of the self-degrading mechanism would be severely

reduced, and hence the quantity of drug released, in a clinical setting, would be heavily reduced. Encapsulation efficiencies of 40.5% and 69.85% were calculated for the biodegradable and non-biodegradable microcapsules, respectively. The lower encapsulation efficiency of the biodegradable microcapsules, suggests that the proteinase enzymes were acting on the capsule shell even at this early stage. Larger losses of proteinase were found once the cores were dissolved. During this step, the proteinase is released from the confinements of the cores, thus allowing the active sites of the proteinase to contact the inner surface of the capsule shell, and subsequently hydrolyse the peptide bonds within the Poly (L-Arginine) component of the capsule wall.

In contrast, the synthetic PAH/PSS microcapsules, are non-biodegradable, hence they remain relatively sealed when the proteinase makes contact with the inner capsule shell. Some proteinase, however, is lost during the core dissolution and subsequent washing steps of the synthetic microcapsules. This is likely to have occurred as a result of passive diffusion of the proteinase through the porous capsule shell. Studies have shown that the capsule wall of polyelectrolytes are porous to proteins of molecular weights similar to that of the proteinase (16-27 kDa) used in this study (She et al., 2010a). Another explanation for this loss could be the incoherence of the capsules themselves. During the layer-by-layer process, some cores are incompletely covered by the polyelectrolytes. This commonly occurring phenomenon could result in a burst in proteinase release during this part of the fabrication process. Furthermore, this dissolution step results in the formation of carbon dioxide from the EDTA complexion with the calcium ions from the calcium carbonate core. This sudden increase in pressure has been shown to shock the capsules, often resulting in capsule rupture, ultimately leading to the complete liberation of all its internal contents. Care was taken, when dissolving the cores to prevent the occurrence of

ruptured capsules, by agitating the suspension gently and opening the Eppendorf tube to allow the CO_2 gas to vent freely. This undoubtedly helped reduce the loss of proteinase at this step remained low (19.12 µg). Regardless of these losses, both synthetic and biodegradable microcapsules retained a significant level of proteinase.

When comparing Figure 16 and Figure 17 it is clear that the 6 layer microcapsules released a greater amount of proteinase than the 12 layer microcapsules at all time points. Neglecting the effects of the proteinase, this is likely to occur naturally under normal conditions due to the presence of a thicker, less porous polyelectrolyte shell. The action of the proteinase within the capsules is only realised when the biodegradable and synthetic microcapsules are compared. There is a relatively large increase in amount of proteinase released in the 6 layer biodegradable microcapsules, compared to the 12 layer biodegradable capsules. This large increase is not noticed in the non-biodegradable samples. This suggests that the non-biodegradable capsules remain well-sealed and have not been degraded by the proteinase, as expected i.e. these are not technically self-degradable microcapsules. Taking this into consideration, the reduction in proteinase release in the 12 layer biodegradable capsules with respect to the 6 layer microcapsules may also have occurred as a result of the enzymes not being able to digest the capsule shell as effectively.

Further analysis of the 6 layer proteinase release profile, indicates that the 6 layer biodegradable microcapsules liberated most of its total amount lost during the early stages of incubation (within 1.5 hours). This was not noticed with the synthetic microcapsules. This notion offers further proof that the proteinase begins to act upon the

capsule shell from the onset. The epifluorescence image show in Figure 18 may provide evidence to support this statement. A number of capsules (highlighted) seem to have a lower fluorescent intensity than others. Irregularities are noticed in the fluorescence of the capsule wall of these particular capsules. This may indicate that the wall is being partially degraded. In contrast, these discrepancies may have arisen due to incomplete coverage of PLL-FITC during the layer-by-layer process.

As expected, the most stable and well-sealed capsules were the 12 layer synthetic batch. The capsules within this sample are comprised of a thick shell that is non-responsive to enzymatic treatment. Indeed, research has shown that when PAH/PSS layer-by-layer assemblies are placed within a biological environment, the layers remain fully intact virtually indefinitely (Kerdjoudj et al., 2008). The supernatant corresponding to this batch of capsules showed no significant increase, after the initial burst, even after 24 hours.

The general trend of all proteinase release profiles as shown in Figure 16 and Figure 17 is well described by the hypothesis of the mechanism behind the self-degradable microcapsules. However, on closer inspection, there are some inconsistencies with the graphs. In theory, the total amount of proteinase in the supernatant should not decrease, as the same supernatant is used at each time point where the sample was analysed. Furthermore, the concentration gradient between the proteinase inside and outside of the microcapsules should dictate the outward diffusion of the proteinase, hence the supernatant concentration should not decrease. The slight decrease in supernatant proteinase content, noticed in all profiles could be a result of the accidental aspiration of

microcapsules while transferring the supernatant to the cuvette for UV spectrophotometry. If this were to occur, the measured absorbance will be the total absorbance of the proteinase within the supernatant as well as the absorbance attributed to the microcapsules with encapsulated proteinase. This would ultimately produce a higher than expected supernatant proteinase concentration. If the next transfer of the supernatant from the capsule sample to the UV cuvette resulted in a pure supernatant without contamination with microcapsules, the perceived absorbance will be lower than the previous measurement. Another explanation for the slight decline in proteinase supernatant concentration towards the end of all release profiles could be due to the adsorption of proteinase on the Eppendorf tubes that contain the sample. It is a well-known fact that proteins adsorb to plastics over time largely due to electrostatic and hydrophobic interactions (Karlsson et al., 2005). The Eppendorf tubes used are constructed from polypropylene. It is likely that over time, the proteinase in the supernatant may have deposited to the surface of the tubes, resulting in a slightly lower proteinase supernatant concentration.

In the case of both 12 layer microcapsule samples, the total amount of proteinase released into the supernatant, once stability had been established (t = 24), was less than 10% of the encapsulated proteinase, determined by encapsulation efficiency calculations, suggesting that the surface of the microcapsules were not as porous as envisaged, even in the case of the biodegradable microcapsules. This apparent decrease in porosity may have arisen due to the proteinase adsorbing to the inner surface of the microcapsules and aggregating to the point where the pores would become partially/fully occluded. This is likely to restrict further diffusion of proteinase into the supernatant.

Interestingly, it was discovered that the 6 layer biodegradable microcapsules reached maximum proteinase secretion in approximately 2 hours, which is roughly the same amount of time taken for the medium concentration, microcapsule sample to reach maximum secretion of DNA, in the study by Borodina et al. (2007). The main differences between these two samples are 4-fold. Firstly, the amount of proteinase per capsule in the former study was 0.808 pg versus 0.037 pg in the present study. Secondly the dextran sulfate used in this study is replaced with poly (L-aspartic acid) in the former study. Thirdly, the capsule shells in the study by Borodina et al. (2007) had an extra layer of polyelectrolyte. Most crucially, however, the species being measured in the former study, is DNA. More specifically, the study used double-stranded DNA from herring testes. This form of DNA typically ranges between 12 and 1000 kDa. Unfortunately, the molecular weight of the DNA used was not disclosed in the paper. The similarity of the results found could be attributed to the DNA used in the study by Borodina et al., (2007), providing that low molecular weight DNA was used. If this were the case, the present study has encapsulated contents of a significantly higher molecular weight (typically between 20 and 60 kDa). By intuition, it is clear that the proteases would take longer to diffuse through the capsule shells. This notion leads to further evidence to suggest that the proteinase diffusion was halted by blockage of the pores by the large protease molecules within the microcapsule shell. Indeed, the study analysing DNA secretion showed that almost 100% of the DNA was secreted within 2 hours.

3.6 Conclusion

In conclusion, self-degradable microcapsules have been successfully prepared and tested. The protein release profiles coupled with visual evidence from epifluorescent microscopy clearly indicate that the microcapsules made from cleavable polypeptide (poly-L-arginine) have been degraded by the proteinase encapsulated within. Furthermore the release is progressive in nature, with significant protease being liberated after t = 1.5 hours for 6 layer self-degradable microcapsules. This progressive release profile has manifested through peptide hydrolysis of the poly-L-arginine component of the capsule shell. This is confirmed by low levels of protease being liberated from the non-biodegradable PAH/PSS control sample. In addition, microcapsules with a thicker shell were less susceptible to degradation by the encapsulated protease. Three main parameters are key to controlling the rate of release of encapsulated contents, namely: the amount of encapsulated protease, the thickness of the shell and the proportion of shell constituents that are biodegradable. By adjusting these parameters, self-degradable microcapsules can be tailor-made for specific applications that are dependent on the rate of release and external protease concentrations.

4. Targeted delivery of polyelectrolyte microcapsules

4.1 Introduction

As mentioned in the introductory section, targeted delivery of polyelectrolyte microcapsules is an essential requirement for the treatment of site-specific diseases. This chapter aims to develop mechanisms by which microcapsules can increase adsorption to collagen type IV, in attempt to help the microcapsules target the basement membrane. Furthermore, an investigation into the suppression of non-specific adsorption to endothelial cells will be conducted in order to prevent microcapsules from adsorbing to the undamaged regions of the endothelium.

4.1.1 Protein adsorption

Non-specific protein adsorption is the key contributor to the unspecific adhesion of polyelectrolyte microcapsules to protein and cellular surfaces. For these reasons, the mechanisms of protein adsorption must be fully understood.

Adsorption refers to the action by which substances accumulate and adhere to surfaces. Specifically, proteins adsorb through a variety of mechanisms including: intermolecular forces, ionic bonding, electrostatic interactions and hydrogen bonding (Kurki et al., 1989). These mechanisms arise directly from the intrinsic structure of proteins. As discussed earlier, proteins are long polyamino acid chains that have come together in a bundle which is maintained by hydrogen bonding, electrostatic interactions between

charged amino acids, and disulphide bonds (Hautanen et al., 1989). Due to their hydrophilicity, charged amino acids within a protein preferentially locate towards the periphery of the molecule, thus allowing these charged amino acids to interact with surfaces (Launes and Hautanen, 1988). These electrostatic forces are more prominent when the surface is charged e.g. a polyelectrolyte. Surface energy and texture of the surface also influence the degree of protein adsorption.

Conditions also have a profound effect on adsorption. By changing the pH, the overall charge of proteins can be altered (Pierschbacher and Ruoslahti, 1987). Proteins can be described as amphoteric i.e. they have regions of cationic and anionic charge. Most charges from proteins arise from dissociation/association of hydrogen ions from carboxylic acids and amine groups respectively. These mechanisms are driven by the amount of hydrogen atoms (H^+) and hydroxide ions (OH^-) ions there are in the solution. If the pH of the solution were to be near the isoelectric point (pI) of the proteins, protein adsorption should be largely reduced since this is one of the main adsorption mechanisms.

Proteins are relatively large polymers (MW usually greater than 10,000) with a complex tertiary structure. They are comprised of amino acids. In total, there are 20 naturally occurring amino acids each of which has a specific charge. This gives rise to anisotropic charges within the protein superstructure. Instead, a net charge is used to describe the overall charge of the protein. It is important to realise that should a protein have a net positive charge, it is not impossible for this protein to be absorbed to a positively charged surface since some regions of the protein may be negatively charged. The region where

this attachment may occur is commonly referred to as a charge patch. This explains why proteins readily adsorb to charged surfaces.

Other factors that affect protein adsorption include the concentrations of the protein solutions involved as well as the molecular weight of the proteins. Lower molecular weight proteins exhibit higher mobility and thus adsorb at a faster rate. These proteins may then be displaced at a later stage by heavier proteins which have a higher affinity to this particular surface. This time-dependent competitive adsorption is known as the Vroman effect (Vilaseca et al., 2012).

4.1.2 Basement membrane anatomy

Since the ultimate aim of this study is to create microcapsules which adhere to sites of endothelial damage i.e. where the basement membrane is exposed, this structure must be studied in depth.

The vascular basement membrane serves as a foundation for which the endothelial cells reside on. The primary function of basement membrane is to provide structural support to the cells. The main components of basement membrane include heparan sulphate proteoglycans (e.g.perlecan), nidogen/entactin, laminin and type IV collagen, the latter being the most abundant protein (50% of basement membrane proteins) (Kalluri, 2003). This is therefore a potential target for microcapsule delivery in cases where the endothelial lining has been damaged, and the underlying basement membrane is exposed.

The second most abundant protein is laminin. Both collagen and laminin have the ability to self-assemble into three dimensional structures. It has been discovered that although perlecan, nidogen and entactin do not possess the ability to form such suprastructures, they are essential in providing complexes between type IV collagen and laminin (Aumailley et al., 1993). Figure 19 illustrates thenidogen and perlecan-dependent binding of laminin to collagen type IV.

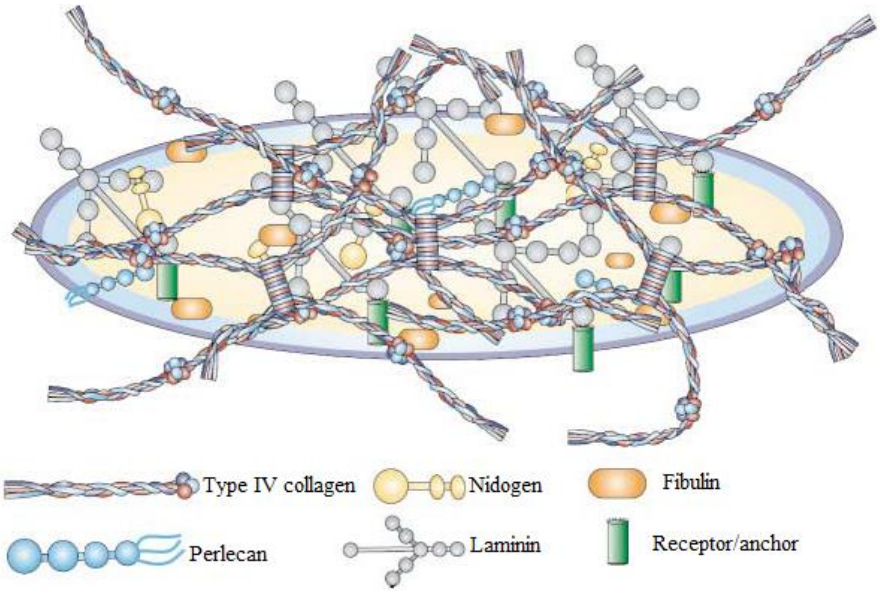

Figure 19. Basement membrane structure. Adapted from (Kalluri, 2003).

Collagen type IV structure

In order to find suitable collagen type IV binding polymers, it is important to understand the structure and chemical components of the protein which differs vastly from other interstitial collagens. Collagen is the main component of connective tissue in mammals. It is also the most abundant protein in animals (Friedman et al., 2000). The protein is composed of a collagenous region (1400 residues long) and a non-collagenous region

(230 residues long). The majority of collagen proteins are made up of three alpha chains which each have the following amino acid repeat unit in their collagenous domains:

$[Gly\text{-}Xaa\text{-}Yaa]_n$

where Gly is a glycine residue and Xaa and Yaa are other residues (usually either proline or hydroxyproline.

The glycine is an essential part of collagen which contributes to the triple helical structure (also known as tropocollagen). Its small size allows the alpha chains to be tightly packed to create a robust structure. The highly abundant proline and hydroxyproline residues are also essential in maintaining such a rigid structure since these residues form hydrogen bonds between the chains. A suprastructure is formed by dimer and tetramer bonds at the C termini and N termini respectively. Intermolecular bonds come in the form of disulphide bonds which are able to form due to the presence of cysteine in the non-collagenous ends of the tropocollagen molecules (Leinonen, 1999).A bundle of these tropocollagen molecules are called a collagen fibril. When combined, they form a structure with high tensile strength.

As all collagens, the amino acid repeat unit is also found in type IV collagen; however the sequence is interrupted 25 times along a single chain with regions that are unable to form a triple helix due to lack of hydroxyproline, an essential amino acid which provides hydrogen bonding. This gives rise to the flexible sheet-like structure of type IV collagen as shown in Figure 21 (Hudson et al., 1993).

Figure 20. Schematic drawing highlighting the triple helical structure of a tropocollagen molecule. Adapted from (Kalluri, 2003).

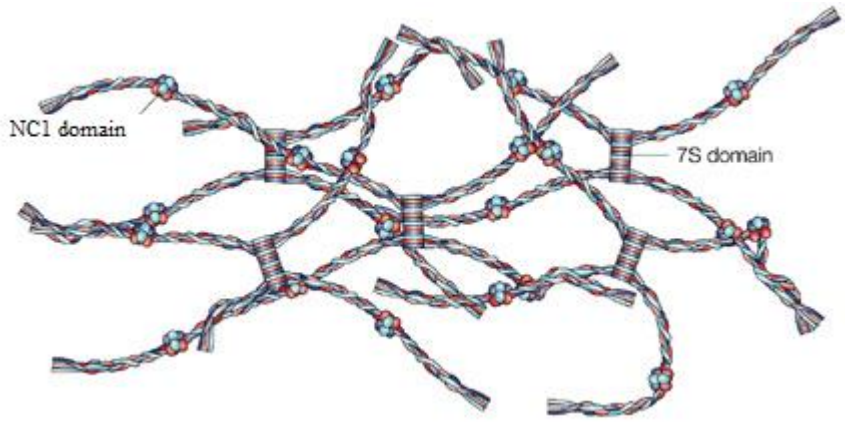

Figure 21. Schematic drawing highlighting the suprastructure of type IV collagen showing the dimer (NC1 bonds) and tetramer bonds. Adapted from (Kalluri, 2003).

As mentioned earlier, we are required to target the basement membrane of damaged blood vessels. Using the technique discussed earlier, we aim to functionalise the biodegradable microcapsules with the heptapeptide that has a specific affinity to collagen type IV.

4.2 Suppression of capsule retention by endothelial cells

As mentioned earlier, polyelectrolyte microcapsules are typically made from PAH and PSS. These polymers are known to have strong adhesive properties due to their

electrostatic charges. Since the aim of this project is to produce microcapsules which do not stick to cells, weakly charged polyelectrolytes were used. The polymers tested are listed below.

4.2.1 Materials and Methods

Dextran sulphate (DexS), a negatively charged polysaccharide was used to make $[PArg/DexS]_4$ capsules with dextran sulphate used as the terminal layer.

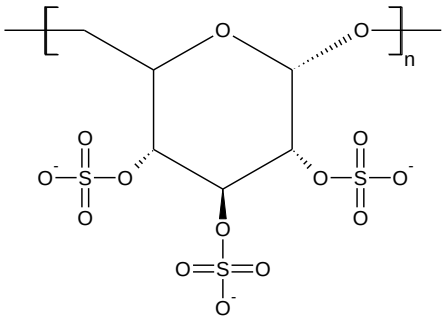

Figure 22. Skeletal structure of dextran sulfate.

Poly-L-arginine (PArg) terminated microcapsules were made with the structure $[PArg/DexS]_3$-PArg.

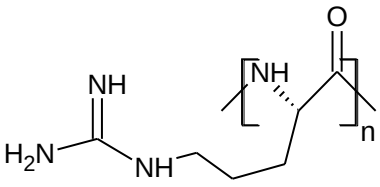

Figure 23. Skeletal structure of poly-L-arginine.

Poly-L-glutamic acid, a negatively charged polyamino acid was used along with poly-L-arginine to make microcapsules with the following conformation: $[PArg/PGlut]_4$.

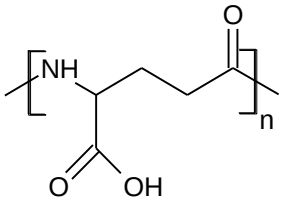

Figure 24. Skeletal structure of poly-L-glutamic acid.

As a control, **polyethylene glycol (PEG)** terminated capsules were synthesised by adsorbing poly-L-lysine-grafted PEG onto $[PArg/PGlut]_4$ capsules. The positively charged PLL side chains of the PLL-PEG serve to anchor the PEG to the negatively charged terminal layer (poly-glutamic acid) via electrostatic binding. PEG, also referred to as poly(ethylene glycol) is insusceptible to unspecific binding to proteins. The non-fouling properties of PEG manifest from the existence of a stable interfacial water layer which acts as a physical barrier and effectively prevents direct contact between the protein and the PEG surface (Boughton, 1985, Yang et al., 2012b).

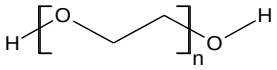

Figure 25. Skeletal structure of PEG.

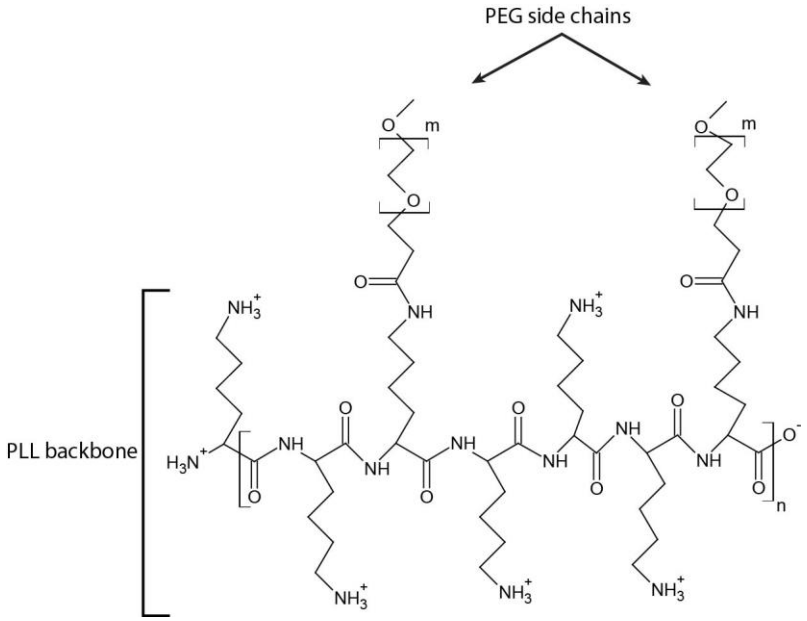

Figure 26. Skeletal structure of PLL-Grafted PEG. Adapted from (Müller et al., 2003).

Additionally, the dense PEG brush layer that is formed on the surface of the microcapsules help shield the electrostatic charges of the underlying polyelectrolyte layers. This prevents electrostatic interactions between the surface and proteins, a force which is assumed to be one of the major contributors of protein adsorption (Lvov et al., 1995). By functionalising the microcapsules with PEG, they should not bind to collagen type IV or endothelial cells (Benhabbour et al., 2008).

To see whether the number of layers has an effect on the adhesion properties of the microcapsules, 4 layer and 8 layer microcapsules were prepared. Microcapsules were synthesised as described in chapter 2.

4.2.2 Experimental procedure

Endothelial cells (HUVEC) were seeded onto a 40mm diameter petri dish at a concentration of 30 kcell/ml with cell culture medium and fetal bovine serum (10%). The

cells were subsequently incubated at 37°C in air supplemented with 5% carbon dioxide. Cell culture medium and fetal bovine serum was replenished every 48 hours. 2ml microcapsule suspension samples at a concentration of approximately 5 million capsules/ml were pipetted onto the cells once they had reached confluence. The size of the microcapsules produced ranged between 3 and 6 μm. The cells were then incubated for 15 minutes at 37°C to allow the capsules to sink to the bottom and come into contact with the cells. After the incubation period, images were taken using an optical microscope in bright-field mode before and after washing. Briefly, the washing protocol consisted of three wash/aspiration cycles with HEPES buffer (3x2ml). The numbers of capsules before and after washing were quantified using ImageJ software. From this data, percentage retention was calculated. For comparison, the same batch of 8 layer microcapsules were tested on collagen type IV substrates for the same length of time. Substrates were prepared by preparing a 1mg/ml collagen type IV solution with PBS and immersing glass slides in the solution for 1 hour. Excess collagen was removed by pipette-washing.

4.2.3 Results

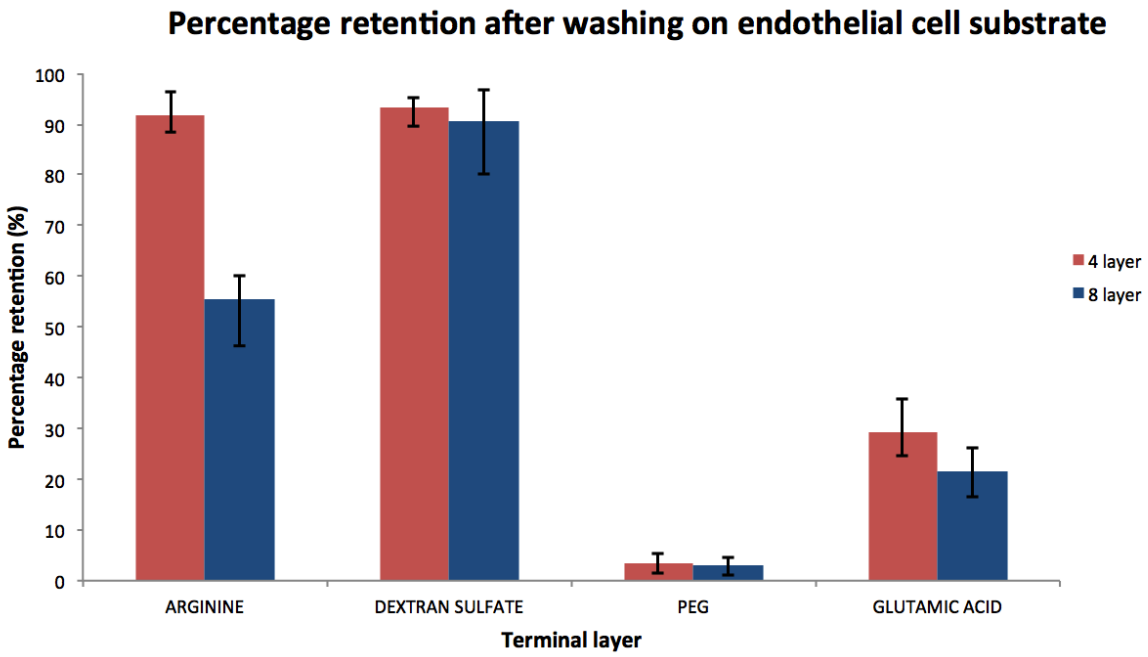

Figure 27. Percentage retention of capsules with different terminal layers incubated on endothelial cells. Error bars indicate standard deviation (n = 5).

The adsorption assays performed on the HUVECs as shown in Figure 27, indicate that the PEGylated microcapsules predominantly refrained from adsorbing to cells, with an average percentage retention of 3.4% and 2.9% for 4 and 8 layered microcapsules respectively. There was no significant difference between 4 and 8 layered microcapsules bar one, namely the polyarginine-terminated microcapsules, which showed a 64.5% increase in retention when the number of layers used were halved.

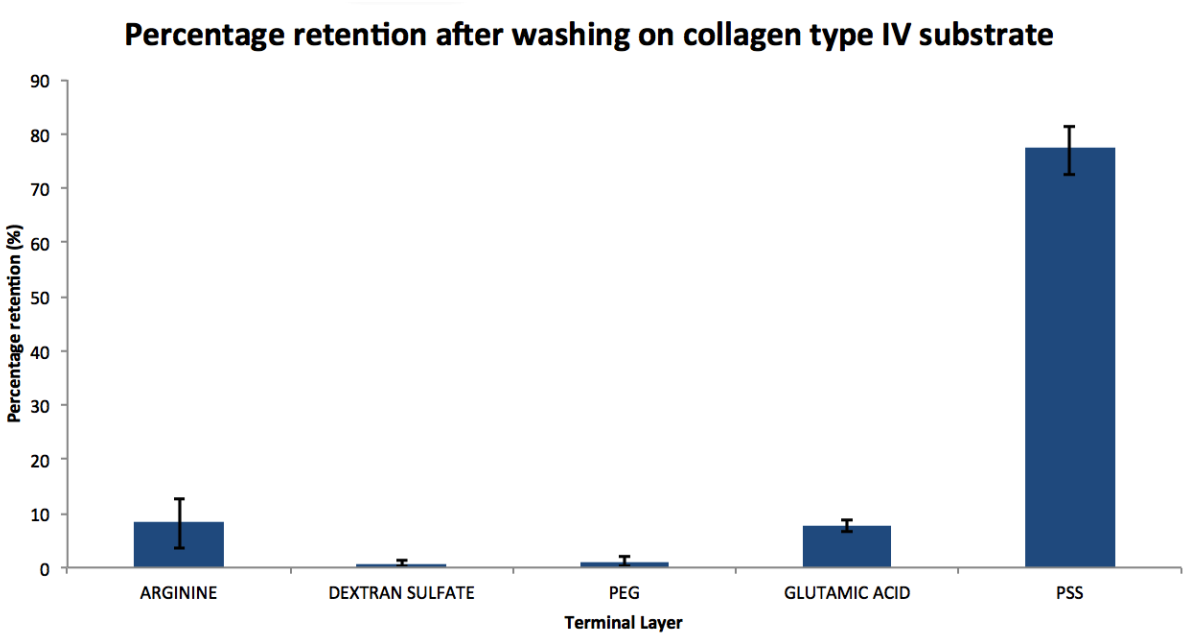

Figure 28. Percentage retention of capsules with different terminal layers, incubated on collagen type IV. Error bars indicate standard deviation (n = 5).

Similarly to the adsorption assays performed on HUVEC cell cultures, the assays performed on collagen type IV substrates revealed a negligible degree of binding from PEGylated microcapsules (1%). Retention on all other microcapsules were less than 10%, with the exception of PSS which displayed a high affinity for collagen type IV (77.5%).

4.2.4 Discussion

From the results, it is clear that the difference in adsorption onto the cells using 4 layers and 8 layers is largely insignificant except for the arginine terminated microcapsules which showed an increase in percentage retention of 65%. It is unclear how this increase manifested. It may be that the 4 layer microcapsules offered more flexibility, allowing more of the surface of the capsule to contact the endothelial surface. In contrast, an

increase in the number of layers has been shown to improve the integrity and density of the terminal layers, which should in theory increase the positivity of the terminal layer. This should lead to an increase in binding of microcapsules to the anionic surface of the cells. However, the results presented contradict this statement.

As expected, the PEG-terminated microcapsules showed negligible adhesion to both the cells and the collagen type IV. Therefore this is not a suitable terminal layer. Despite this shortcoming, PEG should not be disregarded since its protein resistance is key to reducing unspecific protein binding, especially since it does this by shielding strong electrostatic forces. Instead, ways of functionalising PEG with anti-col IV shall be investigated.

The primary advantage of functionalising PEG-terminated microcapsules with anti-col IV is that it should theoretically result in a drug carrier system that is extremely specific to collagen type IV. The combination of the protein resistance and reduction of PEG coupled with the high specificity of anti-col IV should ensure the capsules have a high affinity for collagen type IV whilst at the same time have a much lower affinity to other protein-based substrates as well as cell cultures.

4.3 Microcapsule surface modification for the enhancement of cell targeting

4.3.1 Introduction

It is a well-established fact that in an *in-vitro* environment, polyelectrolyte microcapsules adhere to cells (Liu et al., 2014). This fact is supported by the data represented in the previous subchapter (Figure 27). This phenomenon is believed to occur as a result of the non-specific electrostatic interactions between the layer-by-layer polyelectrolytes and the cell membrane. Research into specific targeting of polyelectrolyte microcapsules is scarce. If the cell membrane structure is fully understood, it may be possible to enhance the binding of microcapsules to cells to improve the efficacy of drug delivery. For this reason, the detailed structure of the cell-membrane, is henceforth examined.

4.3.2 Cell membrane structure

The eukaryotic cell is primarily composed of a phospholipid bilayer, which is a bilayer made out of phospholipid molecules. The phospholipid molecule, as shown in Figure 29 is made out of a hydrophilic (polar) head and a hydrophobic (non-polar) tail.

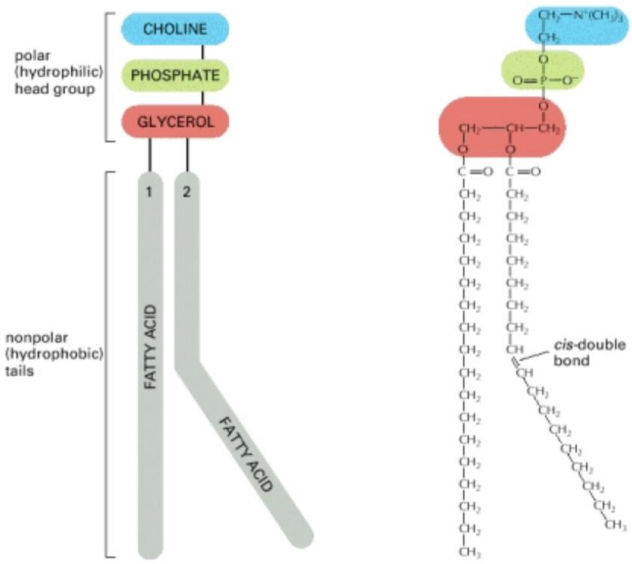

Figure 29. Diagram showing a schematic (left) and formulative (right) representation of the phospholipid molecule. Adapted from (Alberts et al., 2002).

More specifically, the hydrophilic head is comprised of three subunits, namely, choline, phosphate and glycerol. The lipid-based tail is composed of fatty acids and contribute to 50% of the mass of the cell membrane. The bilayer is spontaneously self-assembled as a result of the hydrophobicity of the fatty acid tails resisting contact with water, while the hydrophilic heads naturally favour the water-based extracellular fluid. This results in a bilayer configuration where the non-polar tails are orientated inwards and the polar heads are orientated externally, as shown in Figure 30. The abundant negatively charged phospholipid, phosphatidylserine, is believed to contribute to the anionic charge of cell membranes (Yeung et al., 2008).

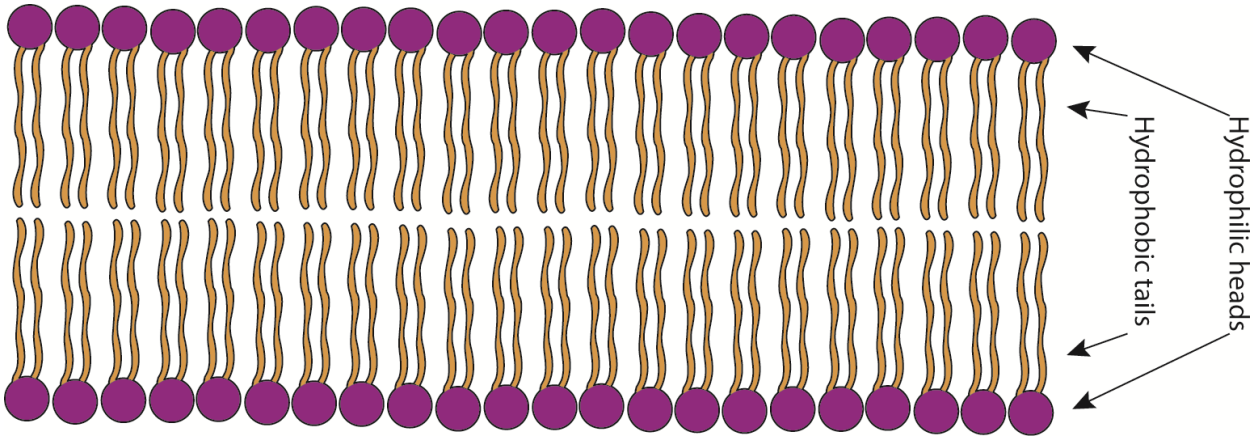

Figure 30. Schematic diagram representing the tightly-packed phospholipid bilayer.

Cell membranes are also comprised of various proteins. The protein component of the cell membrane accounts for 50% of the membrane volume (Alberts et al., 2002). Located within the phospholipid bilayer are embedded proteins, known as transmembrane proteins. These proteins, as suggested by their name, cross straight through the membrane and in some cases, create a channel, where ions and small molecules can diffuse through via passive diffusion or active transport. In addition to these transmembrane proteins, there exist surface proteins which are located peripherally on the cell. As a result of their location, these particular proteins are more relevant to this study and shall therefore be explained in more detail.

Cell adhesion molecules

Cell adhesion molecules (CAMs), are responsible for cell-cell and cell-extracellular matrix interactions. These are the proteins that help anchor a cell to its environment.

These are therefore vital in terms of cell attachment and may offer a potential binding site for microcapsules. The types of CAMs are henceforth described.

Integrin

Integrins are proteins which are classed as transmembrane receptors. In essence, these proteins are responsible for sensing external triggers, usually by binding to trigger molecules. Subsequently, this triggers the integrin to send a chemical message to the interior of the cell, which triggers an appropriate response i.e. they are signal transducers (Tarone et al., 2000). Integrins bind various extracellular matrix proteins including: laminin, collagens and fibronectin, hence they also function as cell-anchoring proteins (Ruoslahti, 1991).

Cadherin

Cadherins are cell surface glycoproteins. They serve as adhesive proteins which are able to bind cells to one another both *in-vitro* and i*n-vivo.* A member of the glycoprotein family, their structure is primarily based on a protein with short sugar molecules (oligosaccharides) covalently bound to the polypeptide side chains. Their function is an active process which can only take place in the presence of calcium ions, Ca^{2+} (Halbleib and Nelson, 2006). As a result of their function, the location of cadherins is restricted to the cell-cell junctions, and hence this is not an ideal target for microcapsule delivery.

Selectin

Unlike the aforementioned proteins, selectins are a type of lectin, and hence have the ability to sugar groups. In particular, E-selectin, a protein involved in the inflammatory response, is expressed on endothelial cells and is therefore the relevant molecule to analyse for this particular application. E-selectin loosely binds to sialylated carbohydrates present on the cell surface of leukocytes. The low affinity of this interaction leads to the formation and breakage of bonds, which, in turn contribute to the characteristic rolling action of leukocytes at the inflammatory site (Kunkel and Ley, 1996). For this reason, this would not be an interaction worth exploiting. A high binding affinity would be more desirable.

Glycocalyx

In addition to the earlier described proteins, there exists a significant structure on the periphery of the luminal cell membrane, namely the glycocaylx which can be seen in Figure 31.

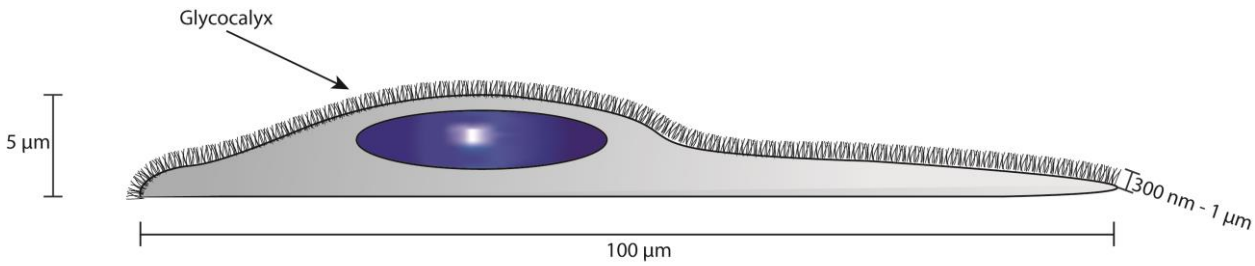

Figure 31. Schematic drawing of an endothelial cell showing the glycocalyx on the apical side.

This densely packed “brush-like” assembly, is expressed in all cells, including endothelial cells. Within an *in-vivo* environment, the endothelial glycocalyx undergoes deformation due to the shear stress exerted by the blood flow. The glycocalyx in turn transduces this signal to the internally located cytoskeleton and subsequently triggers an intracellular response e.g. an inflammatory response (Weinbaum et al., 2007). Other research has shown the glycocalyx to play a role in the regulation of vascular permeability and the prevention of erythrocyte build-up on the vessel wall (Kolářová et al., 2014). Previous studies have shown it to be a very stable component of the cell membrane, with a full regrowth time of 14 days after degradation via neuraminidase, in an *in-vitro* environment (Bai and Wang, 2012).

The structure of the glycocalyx can be clearly seen in Figure 32. It is made up of various sugar chains, including heparan sulfate, a glycosaminoglycan (GAG). These GAG chains are found covalently bound to core proteins, to create structures known as proteoglycans. This is the most abundant GAG in the glycocalyx, is heparan sulfate proteoglycan, which contributes to 50-90% of the total proteoglycan content (Ihrcke et al., 1993).

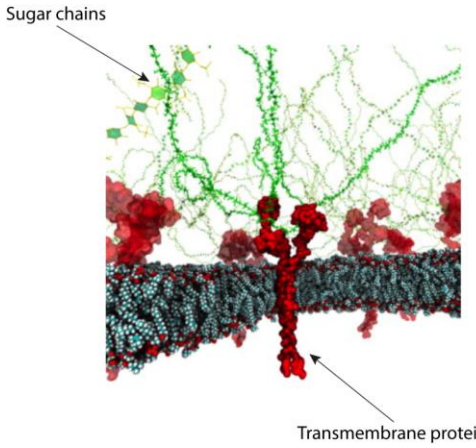

Figure 32. Schematic drawing of the glycocalyx highlighting the sugar chain and transmembrane protein components. Adapted from (Cruz-Chu et al., 2014).

Heparan sulfate proteoglycans are made up of a core protein which is primarily linked to heparan sulfate GAG side-chains as well as chondroitin sulfate side-chains. The glycocalyx has an overall anionic charge, due to the presence of sulfate groups on the GAG chains. This electrostatic charge, combined with the negatively charged phospholipid bilayer, unquestionably renders the entire cell surface negatively charged. If the cells were to be targeted via electrostatic force, it is essential to have a cationic outer layer or functional group.

Potential ligands

Currently, many biocompatible polycationic polymers are used in microcapsule fabrication. Examples include polysaccharides such as chitosan and dextran-spermine conjugate, (Azzam et al., 2002) and polypeptides such as poly-l-arginine and poly-l-glutamic acid and poly-l-lysine. For a stronger electrostatic affinity, poly-allylamine hydrochloride or Polydiallyldimethylammonium chloride (PDADMAC) could be used, as these polymers have been characterised with zeta potentials of +20 mV and +35 mV respectively, on planar surfaces (Michel et al., 2012) (Decher and Schlenoff, 2012).

However, these polymers are non-biodegradable and therefore would not be as efficient in terms of drug release, as shown in chapters 2 and 3.

Instead of tackling the problem from an electrostatic approach, it may be beneficial if a more specific approach was used. As explained earlier, there are many proteins on the surface of the cell membrane. Each of these proteins may be targeted by functionalising the microcapsules with specific antibodies, however, this would be costly. Furthermore, surface of the cells are not entirely covered with these surface bound proteins. Instead it would be more beneficial to target a structure that surrounds the entire exposed area of the cell membrane i.e. the glycocalyx.

Integrins are transmembrane proteins that are involved in interactions between cells and the extracellular matrix. A group of integrins including αV and 2 β1 integrins (α5 and α8) have the ability to interact with a specific tripeptide group found within protein structures, namely the RGD (Arginine-Glycine-Aspartic acid) sequence (Xiong et al., 2002). To mimic the adhesive function of these cell-binding proteins, short peptides containing the RGD sequence can be synthetically manufactured. These peptides are often coated on cell substrate surface in order to promote cell adhesion. Interestingly, synthetic peptides containing this sequence e.g. GRGDSP derived from Fibronectin, have a reported affinity of up to 1000 fold less than fibronectin (Ruoslahti, 1996). Nevertheless, this interaction is highly specific since if the central glycine residue is replaced with alanine, the binding is reduced by 100 fold (Hautanen et al., 1989). Specificity is also demonstrated by the lack of activity when the aspartic acid residue is

in the D isomer conformation (Pierschbacher and Ruoslahti, 1987). Although specificity is a key element of cell targeting, the markedly reduced binding affinity of these peptides suggests that RGD peptides are not the best candidate for microcapsule functionalisation.

Wheat-germ agglutinin

Wheat germ agglutinin (WGA) is a lectin with a molecular weight of 23.5 kDa (Nagata and Burger, 1972). This protein specifically binds specifically to sialic acids. This includes N-acetyl glucosamine, a component of the hyaluronan and heparan sulfate GAG chains found on the proteoglycans of the glycocalyx (Salmon et al., 2012).

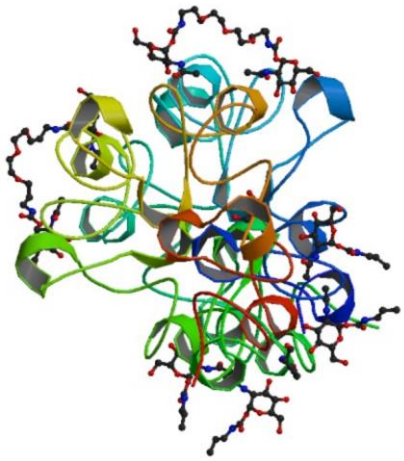

Figure 33. Ribbon structure of wheat germ agglutinin.Adapted from (Schwefel et al., 2010).

The binding of WGA to the glycocalyx arises due to the high degree of complementarity between the carbohydrate-binding site of WGA and N-acetyl glucosamine and its associated oligosaccharides (Peters et al., 1979). As a protein, it has the potential of adsorbing onto the surface of polyelectrolyte microcapsules. More precisely, WGA has an isoelectric point of 8.7, implying that it is positively charged at pH=7 (Schaeffer et al.,

1982). Therefore microcapsules with a negatively charged polymer should readily adsorb WGA, resulting in WGA-terminated microcapsules. Furthermore, WGA is a protein and therefore can be fluorescently labelled, thus the researcher could ascertain whether the WGA has been adsorbed onto the microcapsules with ease.

4.3.3 Materials

Primary pooled Human Umbilical Vein Endothelial Cells (HUVEC), were acquired from a commercially sourced cell-line (Lonza Cologne AG, Germany). Cell culture medium (cat. no. M199) and fetal bovine serum were purchased from Invitrogen, UK. B-endothelial cell growth factor (1 ng/ml) and penicillin (100 U/ml), Lectin from *Triticum vulgaris* (wheat) (cat. no. L4895), Poly-Lysine-FITC labelled (15-30 kDa) (cat. no. P3543) and neuraminidase from *Clostridium perfringens* (cat. no. N2876) were purchased from Sigma Aldrich Co. Synthetic polyelectrolyte microcapsules were manufactured in the laboratory (for individual materials see section 3.2).

4.3.4 Method

Capsule preparation

PSS and PAH polyelectrolyte layers were sequentially deposited on calcium carbonate cores, as described in section 3.3.2 to produce microcapsules with the structure $[PSS/PAH]_3$-PSS. A WGA-FITC solution (200 μg dissolved in 2 ml PBS) was added to the Eppendorf tube containing the polymer-coated cores and incubated at room temperature for 1 hour, ensuring that the cores remained well suspended in the solution. Three washing cycles with PBS were administered to the sample to remove excess

WGA. Finally the cores were dissolved using an EDTA solution which had an adjusted pH of 7 in order to maintain the integrity and structure of the WGA and avoid denaturation of the carbohydrate-binding site. For control purposes, microcapsules terminated with PSS and PAH were synthesised to determine whether the WGA-glycocalyx interaction is more potent than electrostatic interactions. For visualisation, these microcapsules had a single PLL-FITC polymer layer incorporated in the layer-by-layer assembly, in a similar way as described in section 3.3.2.

Cell preparation

Human umbilical vascular endothelial cells were cultured on coverslips placed in a 24-well plate at a concentration of 40 kcell/ml with cell culture medium and fetal bovine serum (10%) as nutrients. Cells were incubated in an incubator set at 37°C and 5% CO_2. Cell culture medium and fetal bovine serum was replenished after 2 days. Once confluence had been reached, half of the wells were treated with neuraminidase, an enzyme that cleaves the carbohydrate components of the glycocalyx including: heparan sulfate, chondroitin sulfate, hyaluronic acid and sialic acid (Pahakis et al., 2007). A 1 U/ml solution was incubated with the cells for 45 minutes in a similar fashion to previous studies (Barker et al., 2004). This was performed to remove the glycocalyx and determine whether the interaction between the WGA-terminated microcapsules and the cells is based on the binding of the WGA to the sialic acid component of the glycocalyx. The medium was then removed and replaced with WGA capsule suspension. After incubation at room temperature for 1 hour, the cell cultures were thoroughly washed 3

times to remove any unbound microcapsules. All cells were labelled with CellTracker Red in accordance with the relevant protocol. Cells were subsequently fixed by paraformaldehyde for 15 minutes. Epifluorescent images were acquired to determine microcapsule retention on the each sample. For consistency, the middle of each coverslip was analysed.

4.3.5 Results

Microcapsule adsorption

All micrographs were taken after 3 washing cycles with PBS. The cells are stained with CellTracker Red. All samples analysed contained a large number of microcapsules on both neuraminidase-treated and untreated HUVEC cell cultures. WGA-terminated microcapsules experienced the largest degree of aggregation.

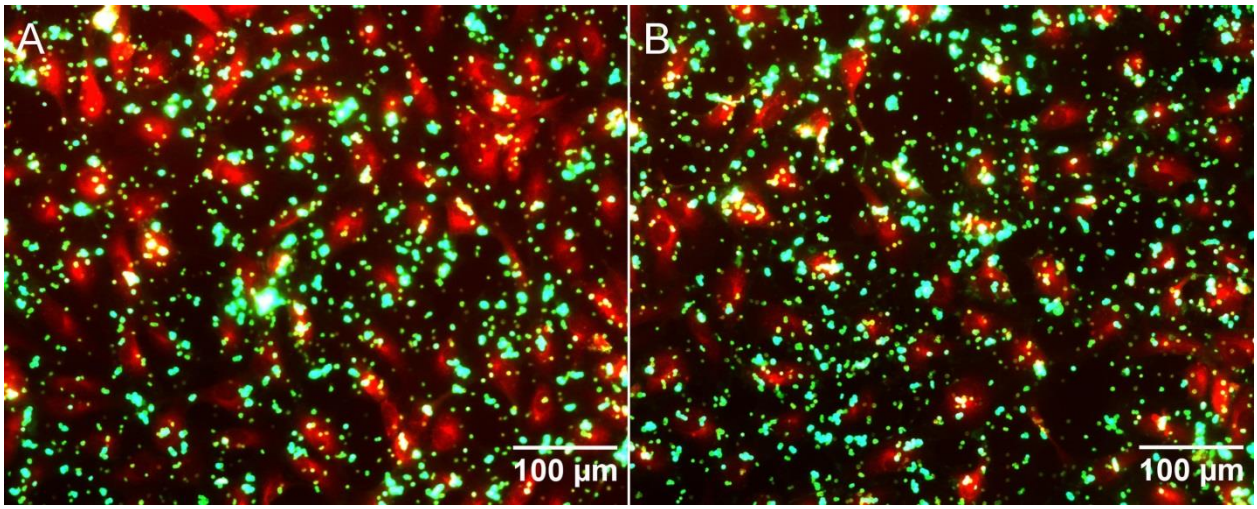

Figure 34. FITC-labelled WGA capsules (green) on endothelial cells, stained with CellTracker™ Red (Panel A) and neuraminidase treated cells (Panel B).

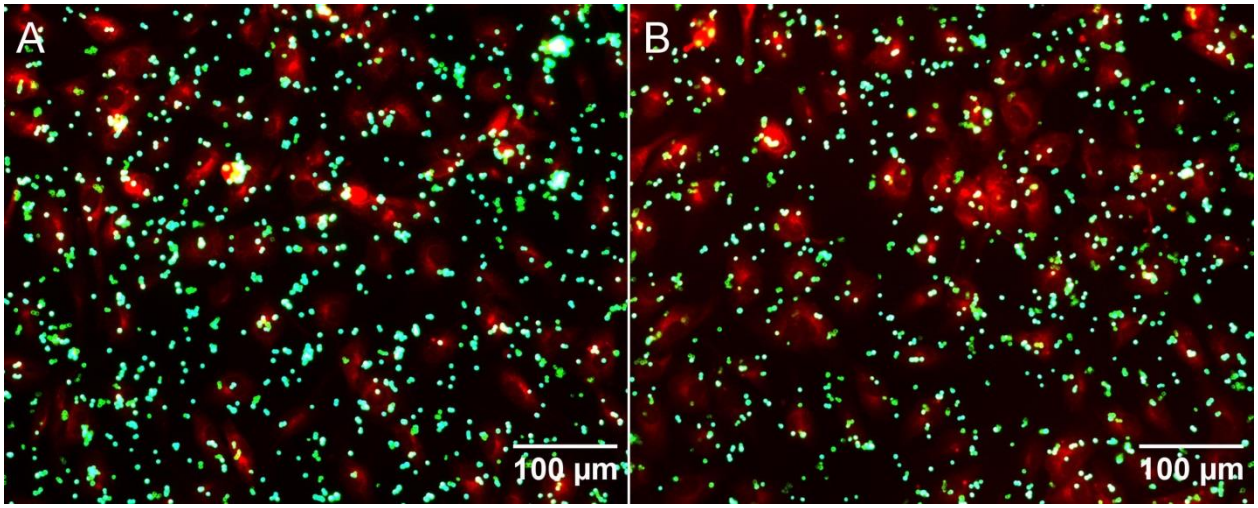

Figure 35. FITC-labelled PAH capsules (green) on endothelial cells, stained with CellTracker™ Red (Panel A) and neuraminidase treated endothelial cells (Panel B).

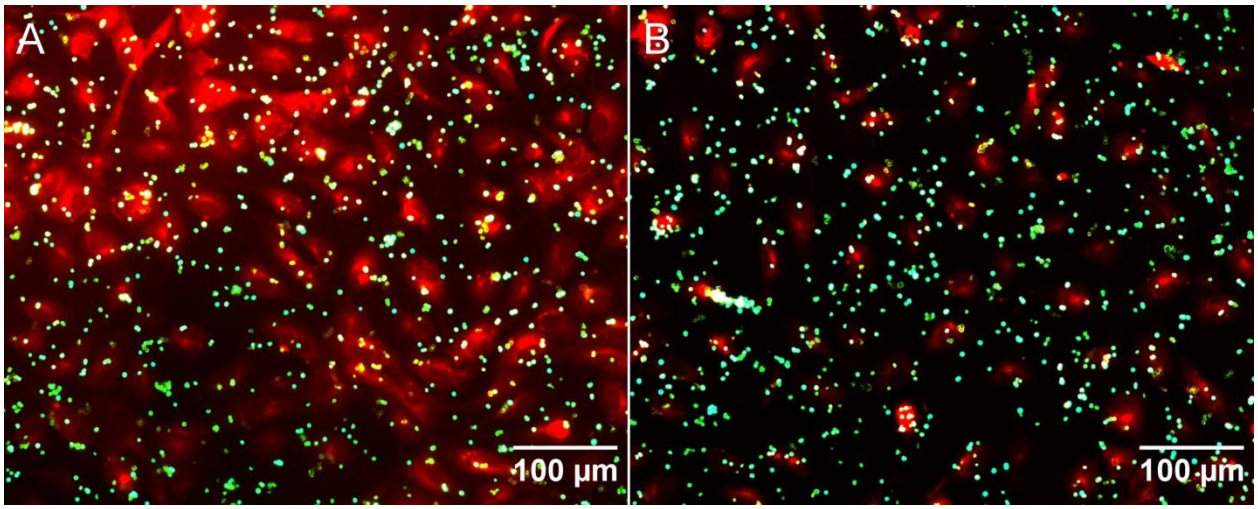

Figure 36. FITC-labelled PSS capsules (green) on endothelial cells, stained with CellTracker™ Red (Panel A) and neuraminidase treated endothelial cells (Panel B).

Neuraminidase validification

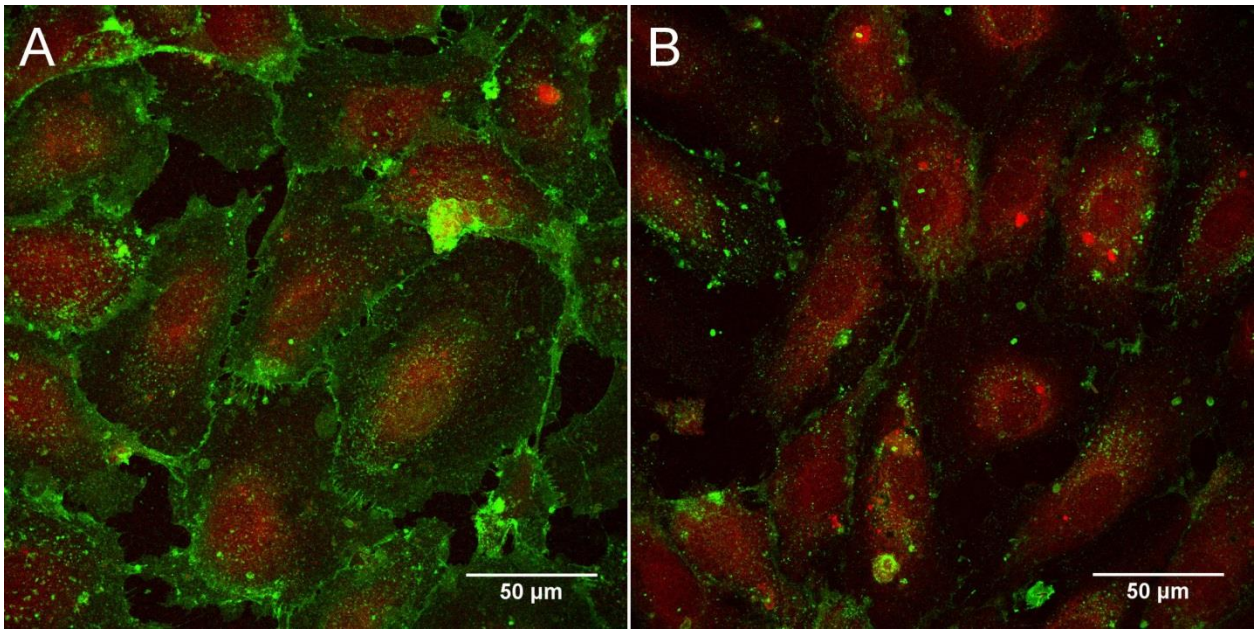

Figure 37. Stacked confocal image of endothelial cells (stained red by CellTracker Red. (Panel A) and neuraminidase treated endothelial cells (Panel B) Cells were stained with WGA-FITC (green) to detect the presence of the glycocalyx.

WGA-FITC staining of the glycocalyx revealed an intact uniform glycocalyx on untreated cells, as expected for mature cells. As expected, upon neuraminidase treatment, it appears the glycocalyx has been degraded, as illustrated by a diminished level of green fluorescence in Figure 37B.

Capsule adsorption summary

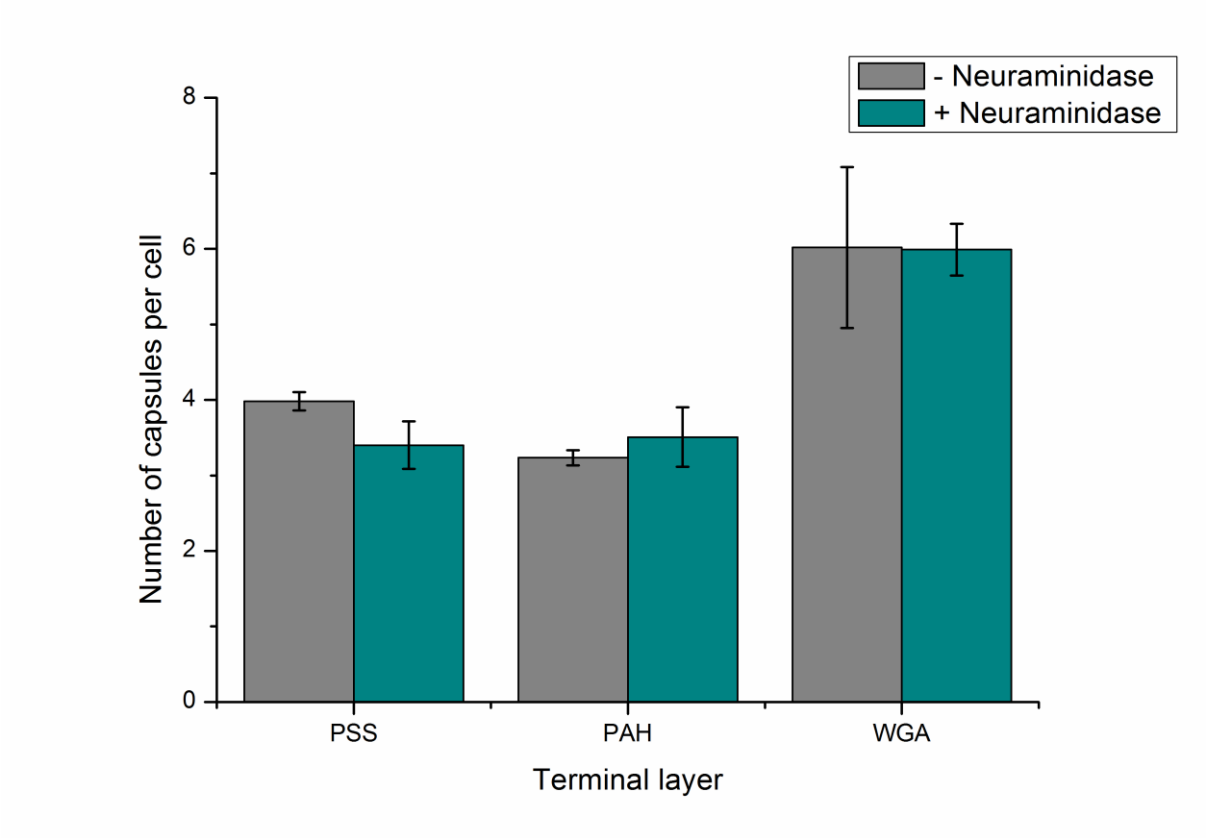

Figure 38. Capsule retention on endothelial cells treated with and without neuraminidase. Error bars indicate standard deviation (n = 5)

Cleavage of the glycocalyx by neuraminidase treatment was confirmed by confocal microscopy, as shown in Figure 37. After the enzymatic treatment, the green signal shown in Figure 37B, corresponding to the glycocalyx (labelled with WGA-FITC), was markedly reduced compared to Figure 37A.

The summary of capsule retention on endothelial cells treated with and without neuraminidase reveal that by terminating the microcapsules with WGA, capsule adsorption was marginally increased by approximately 50%. A one-tailed t-test was performed to determine whether the difference between results obtained with WGA

capsules with and without neuraminidase were statistically significant. The computed values for t and p were 0.043561 and 0.483671 Indicating that the difference was not statistically significant at the $p < 0.05$ level.

4.3.6 Discussion

From the data obtained, it is clear that on all occasions, the microcapsules, regardless of their structure, adhered to the cells quite convincingly, as expected. This is undoubtedly due to the non-specific electrostatic interactions between the highly charged polymers and the cell membrane surface. With reference to the WGA-terminated capsules, the cell affinity was markedly higher. At first glance, one may presume that this enhancement of capsule binding is indeed a result of the aforementioned glycocalyx-WGA interaction. However, once the glycocalyx is removed via neuraminidase treatment, the capsules are still equally well-retained on the cell membranes. The absence of change in capsule retention may have arisen due to the use of an inactive/denatured batch of neuraminidase. The neuraminidase was tested using confocal microscopy. By labelling the glycocalyx with WGA-FITC, one can determine whether the glycocalyx is present on the cell membrane before and after neuraminidase treatment. As seen in Figure 37 (Panel A), the entire surface of the cells are highlighted green confirming the presence of an intact and densely packed glycocalyx layer. In contrast, Figure 37 (Panel B) indicates that after neuraminidase treatment the green fluorescence signal is significantly weaker, suggesting that the glycocalyx has been considerably destroyed. This confirms that the neuraminidase is an adequate enzyme for glyocalyx removal. Thus it would appear that the binding of the WGA capsules to the cells is not purely acquired through WGA-glycocalyx interactions. Another force must be contributing to the adhesion of WGA to

the cell membrane. Since WGA doesn't significantly bind to neuraminidase treated cells, one must assume that the surface of the capsules is not entirely coated with WGA. Indeed, the polymers deposited never entirely form a continuous layer on the templates, hence the underlying polyelectrolytes may be exposed. However, this still would not account for the abnormally high level of interaction.

Another factor to consider is the environment within which the capsules are incubated i.e. the cell culture medium. This cocktail of nutrients contains proteins from the fetal bovine serum component. A major constituent of fetal bovine serum is BSA, a negatively charged protein (Loughney et al., 2014). This BSA would have had ample time to electrostatically adsorb to the positively charged protein thus resulting in BSA-coated microcapsules. Other proteins including growth factors are also likely to contaminate the surface of the capsules. These proteins are involved in the promotion of cell proliferation and hence have a high affinity to cells (Shah, 1998). This theory could also explain why the negatively charged PSS-terminated microcapsules also significantly bind to the cells. By observation of Figure 34, it is clear that the WGA microcapsules are significantly more aggregated than their polylelectrolyte-terminated counterparts. This may account for the increase in apparent cell adsorption.

4.4 Collagen type IV binding pilot study

4.4.1 Introduction

In order to localise microcapsules to the site of endothelial injury, the type IV collagen-rich basement membrane shall be targeted. A recent study led to the discovery of a type IV collagen-binding heptapeptide ligand (Chan et al., 2010). By functionalising microcapsules with this ligand, they should specifically adhere to collagen type IV and therefore the exposed basement membrane of a damaged vessel. The authors of this study successfully functionalised tailor made nano particles, aptly named nanoburrs, with heptapeptide ligands which have a strong affinity to collagen type IV, a highly abundant protein found in the basement membrane of human vasculature. This particular heptapeptide which boasts a two fold increase in nanoparticle retention *in-vivo* compared with a random heptapeptide library, would be an ideal ligand to functionalise the proposed microcapsules of this study. These ligands (KLWVLPK) were attached to the PEG surface of the nanoburrs via maleimide thiol conjugation chemistry. With regard to the polyelectrolyte microcapsules fabricated by the LbL technique, this complex chemistry would not be applicable. Instead, the heptapeptide ligands could be conjugated to the surface of the microcapsules in a similar fashion to Taublan (2006) whereby a short polylysine chain is attached to the ligand to serve as an electrostatic adhesive. In this case, it is essential to terminate the LbL process with a polyanion that will electrostatically bind to the polylysine chain. This proposed peptide chain can be manufactured by FMOC solid-phase peptide synthesis, a well-established technique (Stuber et al., 1989).

4.4.2 Materials and Methods

In the original study, Chan et al, 2010 functionalised the PEG surface of the nanoparticles with the ligand via maleimide thiol conjugation chemistry. With regard to the polyelectrolyte microcapsules fabricated by the LbL technique, this complex chemistry would not be applicable. Instead, the heptapeptide ligands could be conjugated to the surface of the microcapsules in a similar fashion to Taublan (2006) whereby a short polylysine chain is attached to the ligand to serve as an electrostatic adhesive as shown in Figure 39. In this case, it is essential to terminate the LbL process with a polyanion that will electrostatically bind to the polylysine chain. This proposed peptide chain can be manufactured by fmoc solid-phase peptide synthesis, a well-established technique (Stuber et al., 1989). Once this peptide was synthesised, polyglutamic acid/poly-L-arginine microcapsules were synthesised as described in section 2.3.

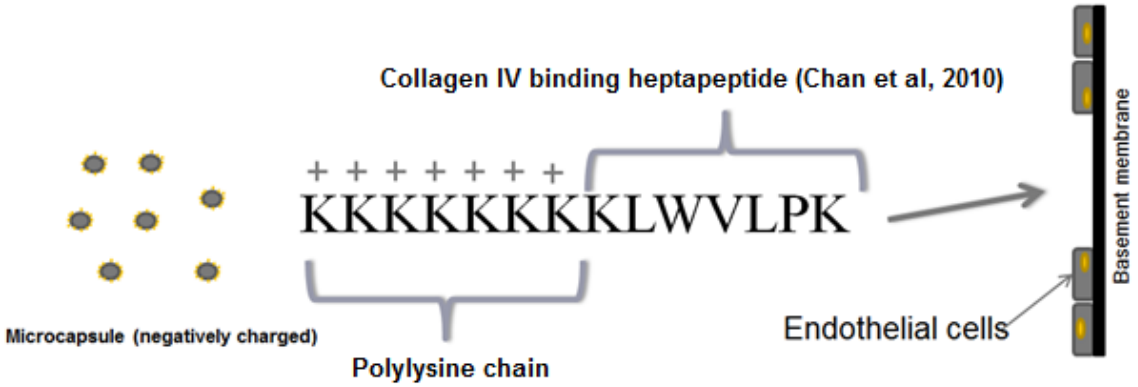

Figure 39. Proposed mechanism of basement membrane targeting.

A solution of the above peptide was made by Cambridge Peptides Ltd. and dissolved with deionised water to a concentration of 2mg/ml. The polyglutamic acid-terminated microcapsules were then suspended in this solution. After 30 minutes of vigorous

shaking, the suspension was centrifuged and microcapsules were washed three times. After washing the capsules were tested for their affinity for collagen type IV by introducing them to a collagen type IV-coated glass slide. This substrate was prepared by immersing a glass slide in a 1 mg/ml solution of collagen type IV (prepared in PBS). After incubating at room temperature for 1 hour, the slide was washed with PBS to remove any non-adsorbed collagen. 200µl of functionalised capsule solution was then pipetted onto a marked out volume on the glass slide. For control, polylysine-terminated microcapsules were tested against collagen type IV. After 24 hours, the samples were washed three times using deionised water and the slides were viewed under an optical microscope to assess capsule retention. Initial results were negative as shown in the micrographs below.

4.4.3 Results and Discussion

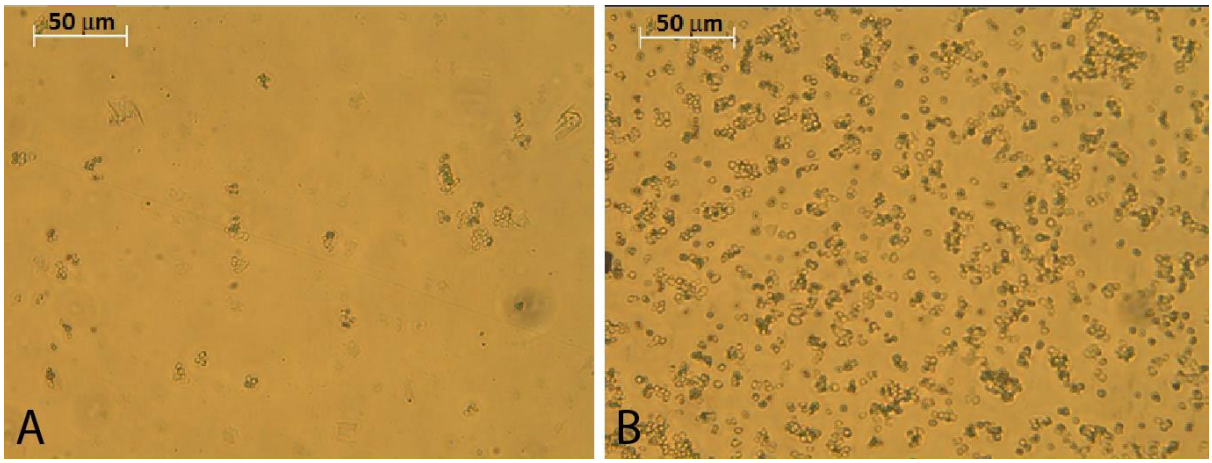

Figure 40. Micrographs showing the retention of Microcapsules with heptapeptide ligand (Panel A) and control microcapsules terminated with Poly-L-lysine (Panel B) on collagen type IV-coated glass.

Evidently, the control microcapsules displayed a higher affinity to collagen type IV than the specifically functionalised microcapsules. The high binding rate noticed in the control sample could be explained to an insufficiently coated glass slide. Therefore in reality, what is being observed is the electrostatic attraction between the positively charged microcapsules with the negatively charged glass. To verify this explanation, a collagen type IV-coated 8 well slide was acquired from Ibidi GmbH. The same procedures were carried out on this reliable substrate, however, the results were similar. The functionalised microcapsules may not have been sufficiently coated with the heptapeptide in order to have a noticeable effect on microcapsule retention. In normal practice, large polymers are used to coat the surface of microcapsules. In the presence of an ionic solution e.g. NaCl, the large size of high molecular weight polymers contribute to a thicker, denser layer. It is likely that the underlying robust polyglutamic acid layer was in fact interacting with the collagen type IV. Unfortunately the production of custom made high molecular weight polypeptides is very costly and due to lack of funding and not enough scientific evidence to justify such purchase, this idea was terminated.

On reflection, 2 major requirements were necessary for a ligand to be a viable candidate in the proposed polyelectrolyte microcapsule system:

- The ligand must have a high molecular weight (>10kDa) in order for sufficient coating of microcapsules
- The ligand must be easily attached to the surface of microcapsules e.g. could have an electrostatic charge.
-

In addition to collagen type IV, the basement membrane contains proteoglycans such as perlecan which is high in heparan sulfate, a glycosaminoglycan. These biomolecules bind

in-vivo as depicted in Figure 19. Furthermore, research has also shown that they also bind *in-vitro*. Unfortunately, this proteoglycan is extremely expensive. Instead, the use of a cheaper alternative, namely heparin, was investigated. Heparin is very similar to heparan sulfate. The glycosaminoglycan features similar disaccharide units to heparan sulfate. Due to these similarities, heparin also possesses the ability to bind to collagen type IV, as shown in previous studies (Koliakos et al., 1989). It is believed to bind to three major sites, the site with the highest affinity being the NC1 domain. Other biopolymers capable of binding to this site include chondroitin sulfate and dermatan sulfate. These glycosaminoglycans do not possess the ability to bind to the other two heparin binding sites which are located 100nm and 300nm from the NC1 domain. For this reason, heparin would be the most ideal polymer to use in a type IV collagen binding study. Another advantage of using heparin as a ligand is that it is extremely negatively charged. This will easily allow it to attract to a positively charged polyelectrolyte used in microcapsules, thus satisfying the 2nd criterion. Furthermore, heparin has a large molecular weight (>12kDa), therefore it should adequately coat the surface of the capsule membrane.

4.5 Heparin study

Since the main aim of this study was to develop microcapsules which have the ability to bind to collagen type IV, the biodegradable polymers were substituted for cheaper, more traditional synthetic polymers (PAH/PSS) in the layer by layer process. 2 samples of 8 layer microcapsules were manufactured. One sample was terminated with heparin by suspending 7 layer microcapsules (PAH terminated) in a 2mg/ml heparin solution. As a control, the other sample was terminated with the negatively charged PSS polyelectrolyte. All samples were labelled with tetramethylrhodamine isothiocyanate

(TRITC) by incorporating a singleTRITC-labelled PAH layer within the layer-by-layer assembly (layer 3). 300µl of each sample was introduced to 2 wells on a collagen type IV 8 well slide and left for 48 hrs. This would allow the capsules to sink to the bottom and contact the collagen type IV.

Results:-

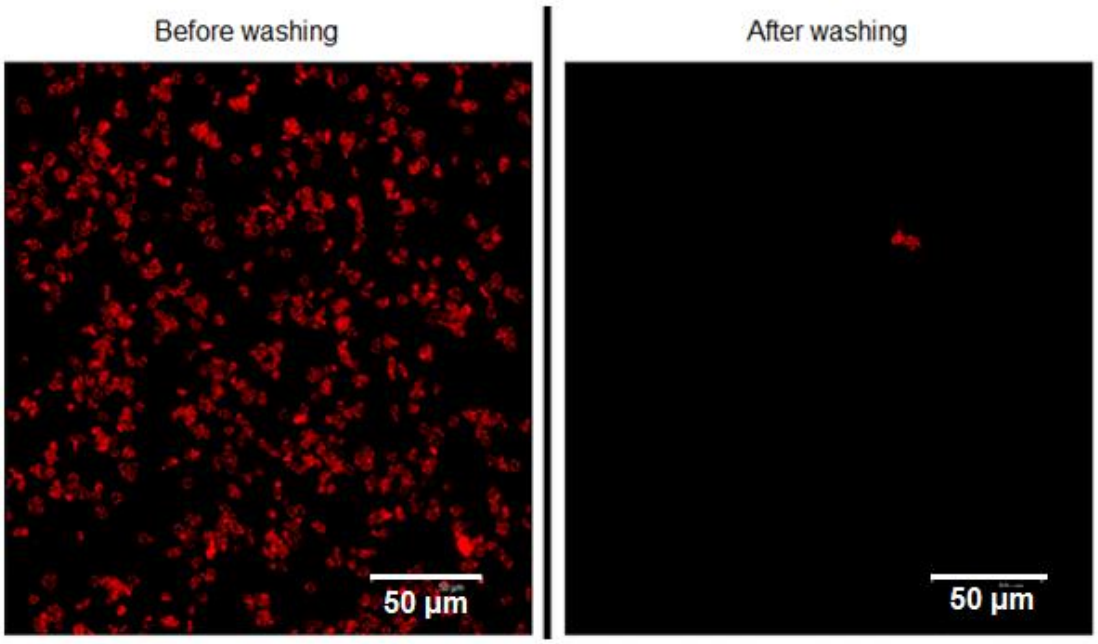

Figure 41. Confocal images of heparin-terminated microcapsules labelled with TRITC on collagen type IV glass slide before and after washing (Scale bar: 50 µm).

Clearly after 3 wash cycles, the majority of capsules were washed away, indicating that the manufactured microcapsules do not bind to collagen type IV. This did not bode well with previous studies that claim that heparin does indeed bind with type IV collagen (Koliakos et al., 1989). An explanation for this negative result could be that the size of

the heparin isn't large enough to create a thick substantial heparin layer. This led to research into creating a denser layer by applying the concept of heat-shrinking.

Heat shrinking

Microcapsules fabricated by specific polymers have been shown to undergo an irreversible shrinking process upon heat treatment. Studies have proved that the density of the materials used doesn't reduce therefore suggesting that material has not been lost during the annealing process. It has been proposed that the increase in temperature causes the ionic bonds to temporarily break. This softens the capsule shell which allows for the reformation of the polyelectrolyte layers into a more preferred structure (Song et al., 2009a). The polymers assume a more uniformly coiled structure due to this formation possessing a higher entropy. The ionic bonds are reformed once the structural changes are made, as shown in Figure 42.

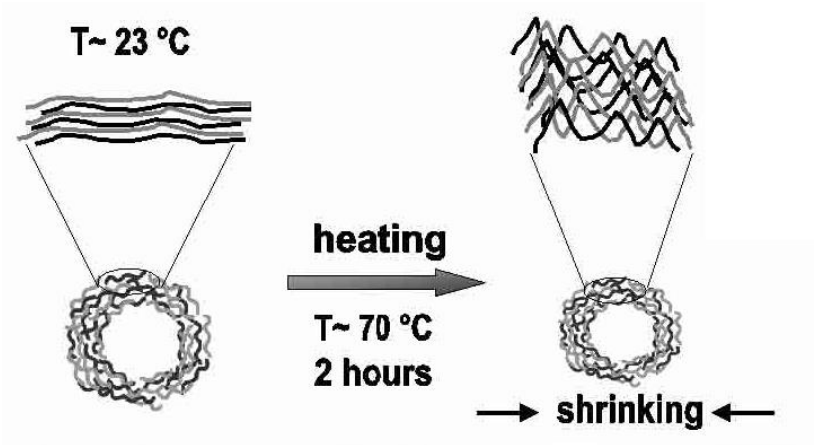

Figure 42. Schematic showing the structural changes of PAH/PSS microcapsules upon annealing. Adapted from (Leporatti et al., 2001).

Microcapsules have been reported to shrink by up to 30%. It has also been reported that microcapsules terminated with a negative polyelectrolyte tend to shrink less than those terminated with a positive polyelectrolyte. Although the microcapsules under investigation in this study are terminated with a negative polymer, the annealing process was trialled in order to create a thicker outer coating. After fabricating microcapsules in the same way as previously described, they were placed in a dryer at 70°C for 2 hours. After this period, SEM images were taken, as shown in Figure 43.

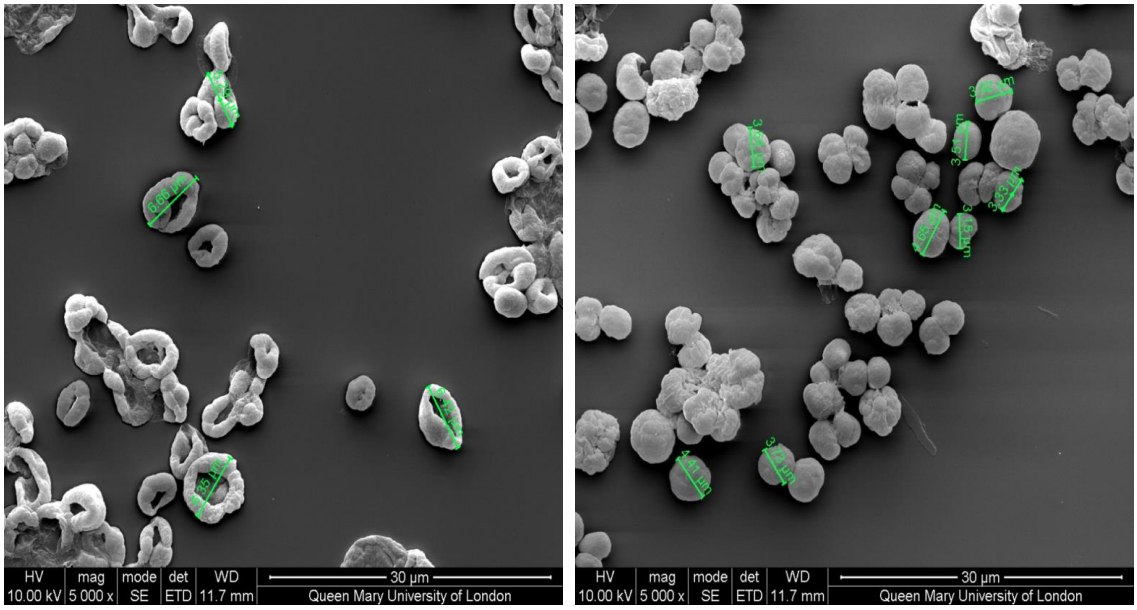

Figure 43. SEM images taken before (left) and after (right) heat-shrinking treatment with diameters displayed. Diameter range before shrinkage: 5.35 – 6.66 µm. Diameter range after shrinkage: 3.33 – 4.41 µm.

After heat-shrinking treatment, the microcapsules shrunk by an average of 35.5% by diameter. This was not as significant as predicted. Nevertheless, these microcapsules were introduced to a collagen type IV well slide and left for 48 hours. As a control PSS terminated microcapsules were subjected to the same annealing process and placed in an identical collagen type IV well slide at an identical microcapsule concentration (10^6

capsules/ml). After 48 hours, both slides were visualised using a fluorescent microscope, washed three times, then visualised again to quantify microcapsule retention. The results, as seen below, differ vastly from the untreated microcapsules.

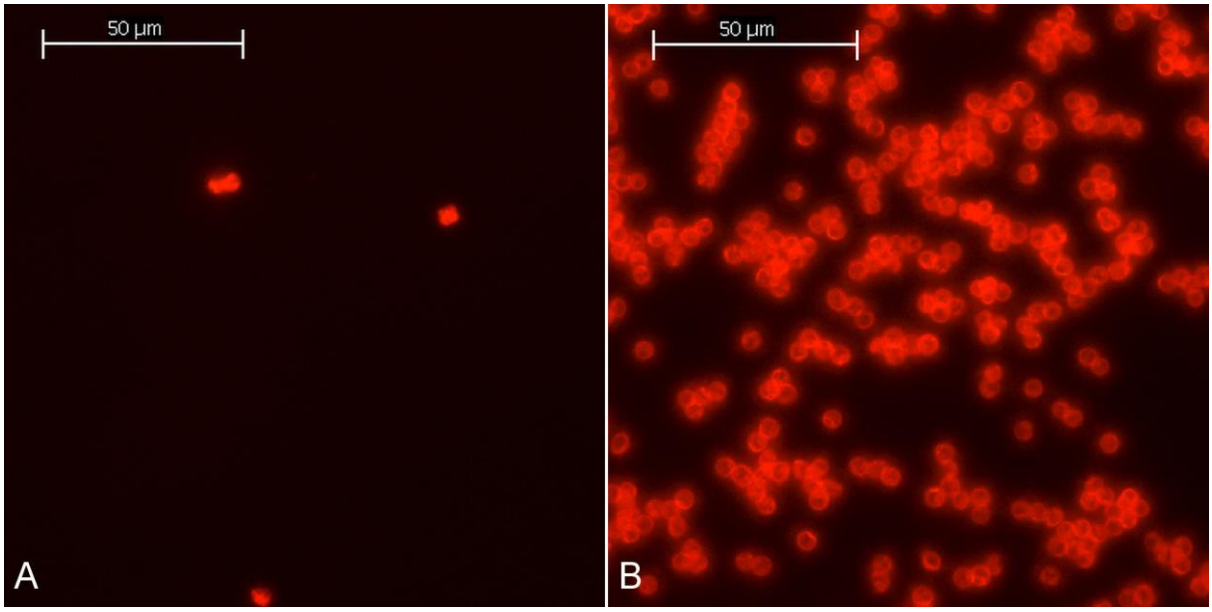

Figure 44. PSS terminated capsules (left) and heparin terminated capsules (right) on collagen type IV slide after 3 washing cycles.

The notion that PSS is a relatively strong polyanion, leads one to believe that the interaction between heparin (a strong polyanion) and type IV collagen cannot be based purely on electrostatic attraction since the PSS terminated microcapsules did not adhere to the collagen type IV. Indeed, type IV collagen is weakly positive at a neutral pH. This evidence proves that there is indeed a more specific interaction between heparin and type IV collagen. Literature suggests that heparin-collagen type IV interactions are at least partially dependent on electrostatic attraction (Tsilibary et al., 1988). The result shown in Figure 44 appear to be in agreement with the literature since the fluorescent microphotographs clearly show that annealed heparin-functionalised microcapsules have

the ability to adhere to type IV collagen. Unfortunately, this experimental procedure was repeated 5 times and all other occasions revealed negligible binding of heparin-terminated microcapsules.

4.6 Cell culture study

In order to verify that the heparin-terminated microcapsules do not bind to intact endothelium, a simple *in-vitro* study was conducted involving human umbilical vein endothelial cells (HUVECs). It is important to mention that the capsules were not synthesised under sterile conditions and were therefore sterilised prior to introducing them to the cells. UV sterilisation was used as oppose to autolclave sterilisation since the high temperatures involved in the autoclave process would most likely denature the microcapsules. Microcapsules were exposed to the ultraviolet light for 1hr. To determine whether UV irradiation had an effect on the adsorption of microcapsules, untreated microcapsules were introduced to cell cultures. These capsules were fabricated under sterile conditions under the cell culture hood. Microcapsules with the following structure were synthesised:

$[PAH/PSS]_3[PAH/Heparin]$

$[PDADMAC/PSS]_3[PDADMAC/Heparin]$

Polydiallyldimethylammonium chloride is a strong cationic polymer. It was selected to determine whether a stronger polyelectrolyte would lead to a denser terminal layer of heparin and ultimately a higher retention of capsules on collagen type IV.

The cells were cultured on a 40 mm petri dish (10% Fetal bovine serum, 90% cell culture medium). When fully confluent, 100µL of heparin terminated microcapsule

suspension was added to the cell culture. The capsules and cells were incubated for 24 hours to allow the microcapsules to sink to the bottom of the petri dish and allow them to contact the cells. After 24 hours, images were taken using an optical microscope. The cells were washed three times with phosphate buffered saline solution to remove the capsules. Images were taken after this was done to see if the capsules were successfully washed away. To determine the biocompatibility, capsules and cells were incubated for 3 days. For control purposes, the following microcapsules were fabricated:

$[PSS/PAH]_4$

$[PSS/PDADMAC]_4$

Results

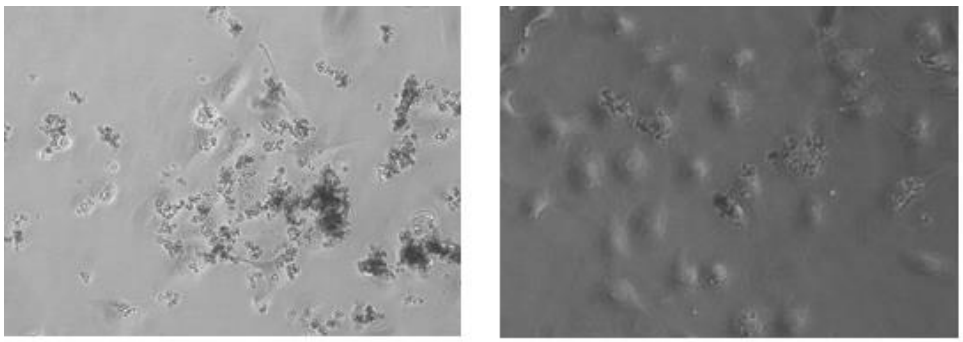

Figure 45. $(PAH/PSS)_3$-PAH/Heparin microcapsules on HUVECs before (left) and after (right) washing.

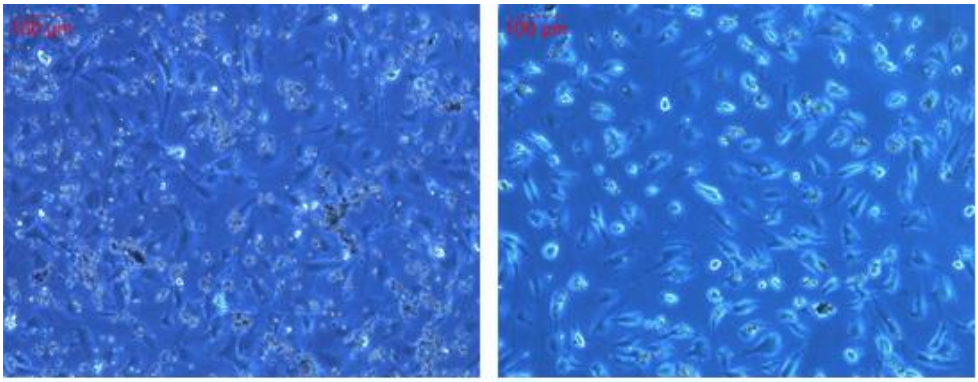

Figure 46. $(PDADMAC/PSS)_3$-PDADMAC/Hep microcapsules on HUVECs (UV treated) before (left) and after (right) washing.

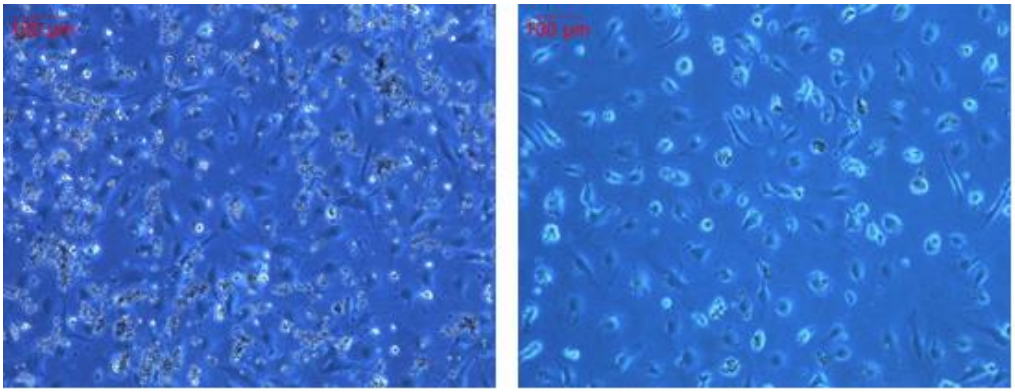

Figure 47. (PDADMAC/PSS)3-PDADMAC/Hep microcapsules on HUVECs (no UV) before (left) and after (right) washing.

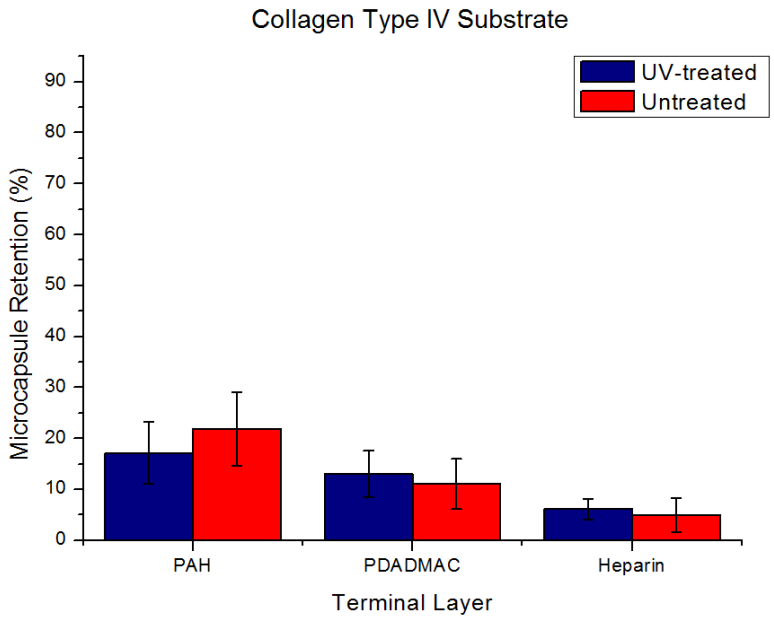

Figure 48. The effect of the terminal layer on microcapsule retention on collagen type IV substrates. Microcapsules were counted after washing sample three times. Heparin terminated capsules were fabricated with 3 PDADMAC/PSS bilayers (n=5).

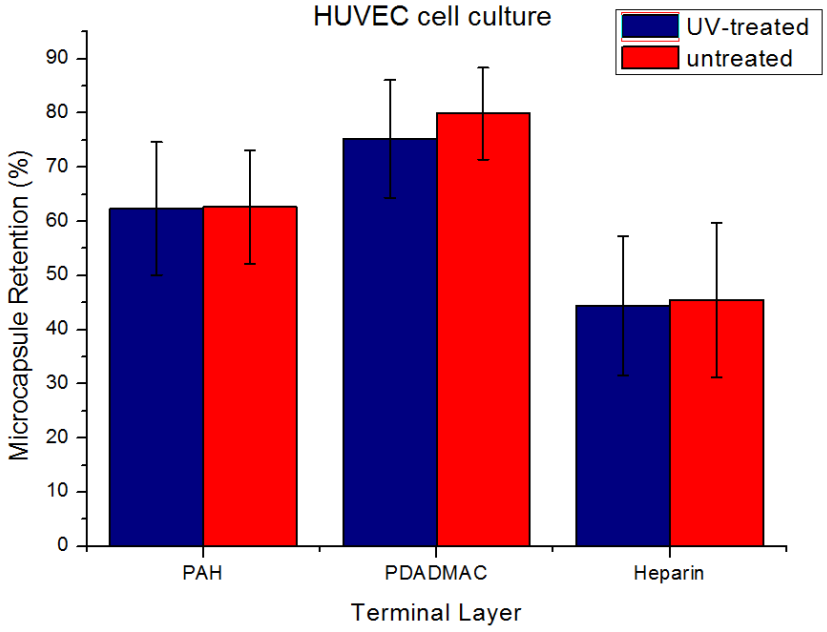

Figure 49. The effect of the terminal layer on microcapsule retention on a confluent HUVEC cell culture. Microcapsules were counted after washing sample three times. . Heparin terminated capsules were fabricated with 3 PDADMAC/PSS bilayers (n=5).

4.7 Discussion

After 3 days of incubation with a complete monolayer of capsules, the endothelial cells remained viable and an endothelial monolayer was maintained. It is clear that for all samples, non-specific adhesion was noticed after washing. This was only apparent on a fraction of cells within each culture. The attraction was more noticeable in the capsules fabricated from PAH and PDADMAC which showed capsule retentions of 64.2% and 75.2%, respectively. This was expected since both of these polyelectrolytes are positively charge, resulting in electrostatic attraction to the anionic cell surface. The degree of retention is consistent with the strengths of PDADMAC and PAH (Smith et al., 2004). Furthermore, heparin-terminated microcapsules were also retained on HUVECs, albeit at lower levels. This is particularly undesirable since ideally the capsules should refrain from binding to cells and specifically bind to the basement membrane, represented by collagen type IV in these experiments. Figure 48 and Figure 49 clearly show that there is no significant difference between results measured for UV-treated and untreated samples, indicating that the capsules are not sensitive to ultraviolet light. Moreover, the cells survived the 24 hour incubation period with unsterilised microcapsules, with no sign of elevated levels of cell death.

Type IV collagen binding studies were performed using these modified microcapsules. Ideally, the incorporation of a stronger polycation should serve to improve the integrity of the layer-by-layer formation, thus resulting in a more substantial terminal layer. The respective micrographs reveal that the microcapsules terminated with heparin on collagen type IV substrates appear to have in fact lost their adhesive properties, with a mean retention of 6.1% compared with 17.1% and 13% capsule retention for PAH and

PDADMAC, respectively. This leads one to believe that the heparin layer is not the main contributor to collagen type IV adhesion, and that the PAH polymer played a significant role in this adhesion. A reason for this lack of adhesion could be that the molecular weight of the heparin (unknown) could be too low. Moreover, cell culture grade heparin was not used, rendering the sample used impure. This could also have an effect on layer integrity.

4.8 Conclusion

Despite many attempts of functionalising microcapsules with ligands that recognise collagen type IV, a suitable candidate for exclusive binding to the basement membrane protein has not been determined. One of the major limitations of all experiments carried out in this chapter is the presence of unspecific binding. Without its suppression, exclusive binding simply cannot be achieved. A more intricate solution must be found which allows specific binding to collagen type IV surfaces whilst simultaneously supressing unwanted non-specific binding.

5. Exclusive binding of polyelectrolyte microcapsules to streptavidin

5.1 Introduction

Targeted drug delivery is a term used to describe the specific localisation of drugs to the site of where the drug is required. By achieving targeted drug delivery, one can increase the efficacy of the drug as well as reduce various unwanted side effects which may be attributed to the drug acting on normal unaffected areas of the body. With respect to microcapsules, targeted drug delivery research is scarce, largely due to the fact that the polyelectrolyte multi-layer shell outer surface is difficult to modify in such a way that provides specific binding to a particular surface. Furthermore, polyelectrolyte microcapsules typically adsorb to protein surfaces via non-specific adsorption due to the presence of charged polymers (Kayitmazer et al., 2013). This is evident when using the well-established PAH/PSS polymer conformation (Heuberger et al., 2005b). Polyelectrolyte microcapsules are therefore inherently incapable of achieving specific adsorption without some form of surface modification.

Thus far, this thesis has only focused on ways of targeting a particular protein and has not addressed the problem of unspecific binding. This chapter aims to initiate the exploration into the use of polyelectrolyte microcapsules in targeted drug delivery of specific protein substrates. In order to achieve specific adsorption, the microcapsules must refrain from adsorbing to all surfaces, other than the target surface. The work conducted in section 4.2 has effectively demonstrated the non-fouling properties of Polyethylene glycol in terms

of cell resistance. This PEGylation procedure is clearly an efficient way of "shielding" the electrostatic effects of the polyelectrolytes. There are a number of biomolecules that have a high and specific affinity to various proteins e.g. antibodies and cadherins. One such specific interaction, is the well-established affinity of the vitamin, biotin, and streptavidin, a protein produced by Streptomyces avidinii. This chapter aims to produce biotin-functionalised microcapsules which have a highly specific affinity to streptavidin substrates, purely to highlight the ability to specifically target proteins with microcapsules. The performance of these microcapsules will be assessed by assaying them against 3 control proteins: collagen type IV, fibronectin and bovine serum albumin.

5.1.1 Literature review on targeted drug delivery

The incentive for studying and developing targeted drug delivery systems is twofold. Firstly, by localising the treatment to the site where it is required, the efficacy of the therapy is largely increased as a result of a higher concentration of drug at the diseased site. Secondly, by administering a drug at the site of the disease and retaining it within the confinements of the diseased area, one can circumvent the side effects associated with the oral/systemic route. Ultimately this improves the therapeutic index of a drug, which is defined as the ratio of the lethal/toxic dose divided by the therapeutic dose (Junutula et al., 2008).

Normal drug delivery modes consist of administration via a number of pathways including: oral, intravenous injection, absorption through skin and inhalation. These traditional modes of drug delivery are not specialised for targeting diseased areas. Indeed, skin adsorption is an effective way of delivering drugs to the skin, however,

where internal diseases are concerned; this is not a viable means of drug delivery. Smarter drug delivery systems have subsequently been introduced into healthcare services worldwide. The current methods of targeted drug delivery are henceforth reviewed.

Nanosponges

Nanosponges are nano-sized drug carriers that are manufactured from oligomers. These porous structures have been used in cancer therapy and have successfully been shown to reduce tumour growth. Their three-dimensional scaffold-like structure gives rise to a high degree of porosity which, in turn, results in a high loading capacity, increasing the overall efficacy of drug delivery. Nanosponges are non-membrane bound with an entirely open structure, hence substances are freely able to move from the interior to the local environment and vice versa, according to the concentration gradient. Their pore size range from 2 to 8 nm (Farrell et al., 2008) which is significantly smaller than the pore size of a typical calcium carbonate microparticle (30 – 50 nm) (Sukhorukov et al., 2004) hence they are less efficiently loaded than their calcium carbonate counterpart. This small pore size also equips them with self-sterilising properties since bacteria are too large to diffuse through the pores (Patel and Oswal, 2012). These structures are fabricated from a polymer backbone e.g. polystyrene, cyclodextrin and ethyl cellulose, which is then cross-linked by introducing the backbone to cross-linkers such as glutaraldehyde and dichloromethane (Yadav and Panchory, 2013).

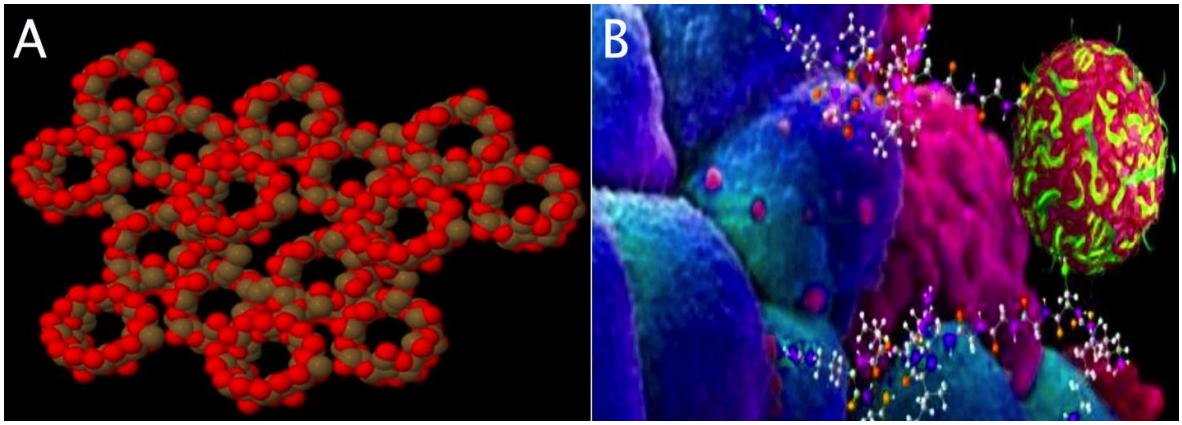

Figure 50. Molecular structure of cyclodextrin-based nanosponges (Panel A). Adapted from (Shringirishi et al.) Panel B is an illustration of a functionalised nanosponge interacting with a human breast cancer cell. Adapted from (Yadav and Panchory, 2013)

Nanosponges have been shown to successfully target and treat site-specific diseases, by functionalising the surfaces with targeting ligands, however, the modifications to overcome the limitations of the nanosponge system are extensively complicated. For instance, cyclodextrin-based nanosponges are inherently unable to form complexes with hydrophilic and large molecular weight species and must be chemically modified in order to circumvent this limitation (Trotta et al., 2012). One major limitation of the nanosponge system is the inability to retain larger molecular weight species e.g. the use of TIMPs for control of MMP activity in diseased tissue. In contrast, as previously explained, microcapsules are well-suited for carrying protein-sized molecules.

Liposomes

These vesicles are fabricated from a phospholipid bilayer, hence are therefore biodegradable, biocompatible and will not provoke an immune response i.e. they are non-immunogenic. They can be as small as 10 nm and can hence pass through the blood-tissue barrier (Manish and Vimukta, 2011). Their ability to transport both hydrophobic

and hydrophilic drugs highlights their versatility as drug vehicles (Medina et al., 2004). With respect to cell delivery, it is important that the liposomes are positively charged so it can interact with the negative cell membrane as well as negatively charged proteoglycans expressed on the surface of the cell. This, in turn, facilitates cell uptake (Wiethoff et al., 2001). By contrast, positively charged liposomes have been shown to be cytotoxic to cells (Lv et al., 2006). In order to achieve targeted drug delivery, liposomes can be targeted with ligands including: surface proteins, peptides (Juliano et al., 2009), antibodies and lectins, as shown in Figure 51 (Kelly et al., 2011).

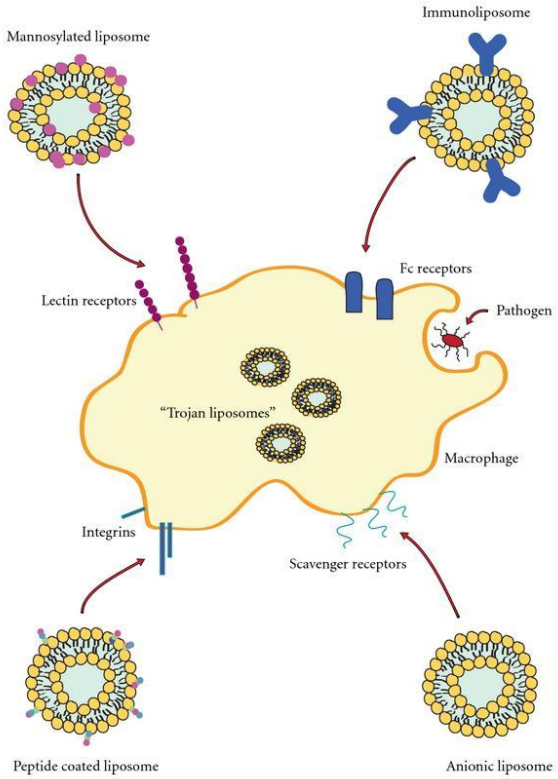

Figure 51. Schematic diagram showing the potential targeting ligands for liposome functionalisation Adapted from (Kelly et al., 2011).

It is important to realise that although liposomes have the ability to adsorb immunoglobulins, hence giving them apparent specific binding properties, they also adsorb other serum proteins *in-vivo* (Patel, 1991). This renders them useless since non-

specific adsorptions are inherently expected as a result. Furthermore, liposomes are impractical where controlled release is desired. These vesicles cannot be manipulated as easily as polyelectrolyte microcapsules to develop desired release profiles, as shown in chapter 2 and 3 (Barenholz, 2001). In addition, liposomes are quickly up-taken by a system of cells known as the reticular-endothelial system (RES). If the target for the drug was an extra-RES tissue, the drug is unlikely to reach its designated area as a result of adsorption into RES cells (Gabizon, 2001).

5.1.2 Biotinylation

The biotin-avidin and biotin-streptavidin complexes are widely used and well-characterised biochemical interactions. The bonds between these structures are extremely strong. The binding affinities (Ka) of avidin and streptavidin to biotin have been reported to be as high as 10^{15} M^{-1} and 10^{13} M^{-1} respectively. In comparison, a typical protein ligand interaction has an affinity of 10^{2}-10^{4} Ka (Boughton and Simpson, 1984). Furthermore, the complex is stable even under acidic and basic conditions (Boughton and Simpson, 1982). Through the use of specially derived reagents, biotin is also able to chemically conjugate to protein, allowing proteins, such as antibodies to be functionalised and adsorbed to surfaces coated with streptavidin/avidin. Biotin's high affinity to both avidin and streptavidin is a direct result of their chemical architecture.

Biotin

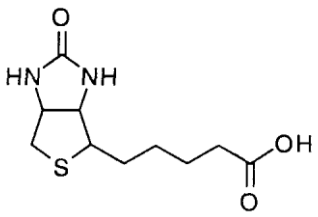

Figure 52. Structure of Biotin. Adapted from Patent number WO2000072802 A2(2000).

Biotin, also known as coenzyme R, is a B-vitamin which is based on a cyclic urea structure (Boughton et al., 1984). One of the important features of biotin is that each of the amino groups have carbon atoms which carry a hydrogen atom each, allowing hydrogen bonds to be formed with other structures.

Avidin, a protein isolated from egg white is composed of 4 amino acid chains made from approximately 128 residues each (Sochynsky et al., 1980). It is extremely thermo-stable with a protein-unfolding melting temperature (Tm) of 85°C. This is increased up to 132°C when bound to biotin (Prescott et al., 1999). Within each chain, there is a 'pocket' which allows biotin to bind to the protein effectively providing 4 biotin-binding sites, as shown in Figure 53. This is known as the biotin-binding site.

Figure 53. Ribbon structure of avidin with 4 bound biotin molecules.Adapted from (Tetramer of Avidin Binding the Biotin Ligands, 2011).

Streptavidin

Streptavidin is a protein isolated from the bacterium *Streptomyces avidinii.* Similar to avidin, streptavidin is composed of 4 identical amino acid chains. Each chain is 159 residues long (Aslan et al., 2007). Similarly to avidin, it has the ability to bind to 4 biotin molecules. These binding motifs strongly resemble the motifs found in avidin. The twisted barrels formed by the peptide chains are open-ended. This is where the binding of biotin occurs. Once bound to streptavidin, a surface loop folds over the binding site to effectively lock the biotin in place. This gives rise to a very low dissociation between the 2 structures (Green, 1990).

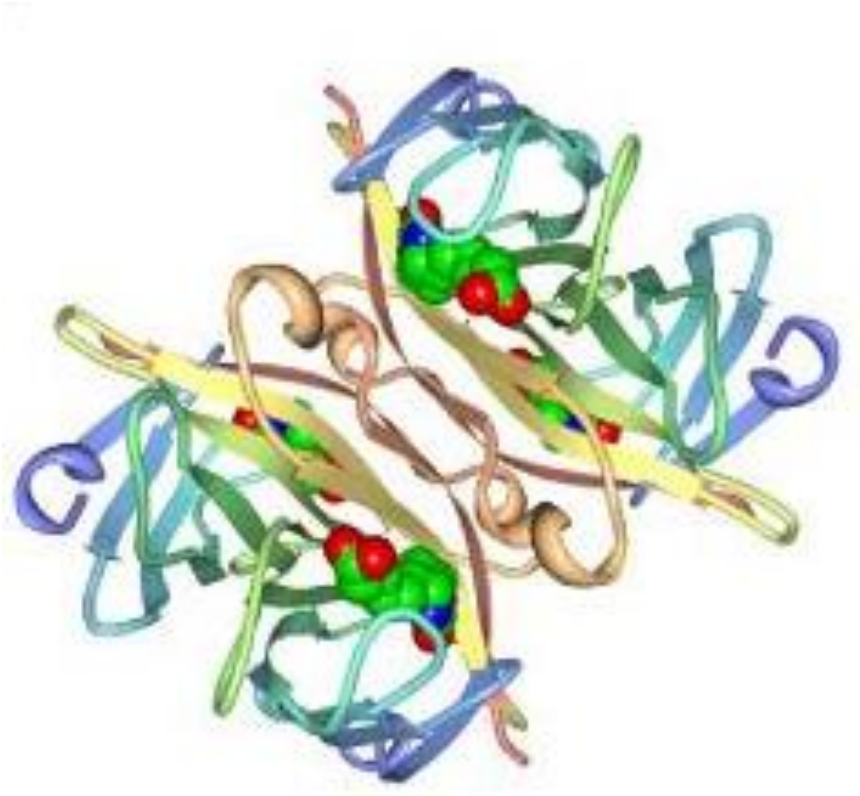

Figure 54. Ribbon structure of Streptavidin-biotin complex. Adapted from (Christov and Karabencheva-Christova, 2012).

Both proteins bind to biotin via a biotin-binding site, which has a size of 293 $Å^3$. This is complementary to the volume of biotin (242$Å^3$), allowing for a tight fit. Deep within the pocket resides a group of potential donors and acceptor residues including Serine, Threonine, Tyrosine and Asparagine, which are able to form hydrogen bonds with the hydrogen atoms on the polar ring of biotin. The presence of aromatic residues gives rise to a 'hydrophobic box', which aids biotin-binding. The combination of these parameters results in one of the strongest non-covalent bonds in the realm of biochemistry. Streptavidin has a slightly lower affinity to biotin than avidin, due to one less aromatic residue at the biotin-binding site. Furthermore, the hydrogen bonding between the carboxylic acid group of the pentanoic acid moiety of biotin is weaker in streptavidin since each oxygen is only able to form one bond with a hydrogen. Comparatively, 5

bonds are formed in avidin (Lindman et al., 2006). Nevertheless, the biotin-streptavidin complex is still an extremely strong interaction, rendering streptavidin a viable protein to adsorb biotinylated antibody. The control proteins must also be reviewed in order to justify why they were chosen. A variety of proteins were chosen, each with unique structural properties to prove that the binding to the target protein was specific. Their structures and functions are highlighted below.

5.2 Target proteins

5.2.1 Fibronectin

Fibronectin is a glycoprotein which is naturally found within the extracellular matrix. It is comprised of 2 quasi-identical domains, each of 220 kDa in molecular weight, giving rise to a combined molecular weight of 440 kDa. These domains are linked together by a pair of disulfide bridges located near the end of the C-terminal on both domains (Johansson et al., 1997). This protein is multifunctional in nature, playing important roles in migration, differentiation, cell adhesion and wound healing. With an acidic isoelectric point of between 5.6 and 6.1, fibronectin possesses a net negative charge at a neutral pH (Boughton et al. 1984). This will therefore be an ideal protein to determine whether the microcapsules will adhere to negatively charged proteins, perhaps due to exposed poly-L-arginine polymer on the surface of the capsules.

5.2.2 Collagen type IV

The structure and function of collagen type IV has been described in detail in section 4.1.2. With a basic isolelectric point of 9.28, it is the only positively charged protein used

in this study. This will allow one to determine whether the PLL-PEG-Biotin is effectively shielding electrostatic interactions between positive surfaces and the intrinsic dextran sulfate component of the capsules. Furthermore, the beta pleated sheet structure is different to the globular structure of the other control proteins used.

5.2.3 Bovine serum albumin

Bovine serum albumin (BSA) is a commonly used and ready available serum protein. An important characteristic of this protein is net negative charge at a neutral pH due to the acidic isoelectric point of 4.7 (Ge et al., 1998). Furthermore, it would be interesting to investigate the adsorption properties of the microcapsules with a non-human born protein.

5.3 Materials

Biodegradable microcapsules (see section 3.2 for individual materials). Fluorescein isothiocyanate-labelled Poly-L-lysine (cat. no. P3069), Collagen from human placenta (Bornstein and Traub type IV) (cat. no. C5533), Bovine serum albumin (cat. no. A2153), Fibronectin from human plasma (F2006) and Streptavidin (cat. no. S4762) was purchased from Sigma Aldrich Co. Poly-L-Lysine grafted with polyethylene glycol and polyethylene glycol-biotin(50%) (PLL(20 kDa)-PEG(2 kDa)/PEG-biotin (50%) (3.4 kDa)) and PLL-PEG (PLL(20 kDa) grafted with PEG(2 kDa)) was purchased from SuSoS AG.

5.4 Method

5.4.1 Microcapsule Preparation

Microcapsules were made using the previously described layer-by-layer technique. Briefly, dextran sulfate and Poly(L-arginine) layers were sequentially deposited on calcium carbonate templates until 3 bilayers were completed. At a later stage, the amount of adsorbed microcapsules on specific substrates would need to be quantified. For this reason, the 4th layer (i.e. the second Poly(L-arginine) layer was replaced with Fluorescein isothiocyanate-labelled Poly(L-lysine) (PLL-FITC), a fluorescein-labelled cationic polypeptide, in order to allow fluorescent visualisation of the capsules. All polymers were dissolved in deionised water at 1 mg/ml and the incubation time per layer was at least 15 minutes in order to allow sufficient time for a coherent layer to be established. The resultant architecture of the produced microcapsules can be seen below:

[DexS/Parg][DexS/PLL-FITC][DexS]

These biodegradable polymers were chosen since they are often associated with weaker electrostatic charges when compared with synthetic polymers such as PAH and PSS. This is an essential attribute to have when unspecific adsorptions must be suppressed as much as possible. Once the final, dextran sulfate layer was added, the capsules were deemed ready for PEGylation. PLL-PEG-Biotin, purchased from SuSoS AG, was reconstituted in PBS. This particular chemical is similar to the PLL-PEG previously described in section 4.2, however 50% of the PEG branches have been functionalised with biotin. The capsules were incubated in a 1mg/ml solution of PLL-PEG-Biotin for an hour to allow the cationic PLL backbone to electrostatically bind to the anionic dextran sulfate surface

of the cores. The cores were subsequently washed to remove any unbound complexes. Following this step, the entire surface was PEGylated with approximately 50% of the surface functionalised with biotin. Hence, in theory, this process should lead to the suppression of unwanted non-specific adsorptions as well as the functionalisation of the surface to specifically target streptavidin. Finally, the cores were dissolved using a 0.2M EDTA solution, using the dissolution protocol as described in section 2.3. A control sample, using non-functionalised PEG as the terminal layer of the microcapsules were prepared to demonstrate the non-fouling properties of PEG with reference to protein surfaces. The microcapsules were counted in a similar fashion as described in chapter 3, using a haemocytometer. The microcapsule concentrations of each suspension were equalised by dilution to avoid the occurrence of biased data. 4 proteins were used in the assay to determine the affinity of the capsules to various proteins. These included the target protein, Streptavidin, and 3 control proteins: BSA, fibronectin and collagen type IV.

5.4.2 Protein substrate preparation

The protein surfaces were prepared by simple adsorption onto a planar surface. Circular coverslips (diameter: 18 mm) were chosen as the material to be coated. The justification for this choice is twofold. Firstly, the coverslips are manufactured from silica glass, a material that has been proven to bind to proteins very effectively via non-specific adsorption (Kalasin and Santore, 2009). Secondly, these coverslips fit adequately within the wells of a 24 well plate, which can be used as incubation chambers. Briefly, 40 μg/ml protein solutions were prepared by dissolving the right amount of protein in PBS. This concentration was determined in accordance with previous protein adsorption studies, in order to produce a complete monolayer on the surface (Gautrot et al., 2010). After

placing a coverslip in each well on the 24 well plate, 200 µl of each protein solution was placed into the separate wells, ensuring that the entire surface was coated. Each protein was deposited on 2 wells to allow affinity assays to be conducted using both PEGylated capsules and biotin-functionalised PEGylated capsules. After incubation at room temperature for 1 hour, the wells were pipette-washed 3 times with PBS, ensuring that the surface was kept wet at all times. This was done to maintain the integrity and structure of the proteins and prevent crystallisation.

5.4.3 Microcapsule adsorption assay

200 µL of microcapsule suspensions were placed in each well, as shown below in Figure 55. This diagram clearly shows all of the experimental samples that were tested, including the control microcapsules and the control protein substrates.

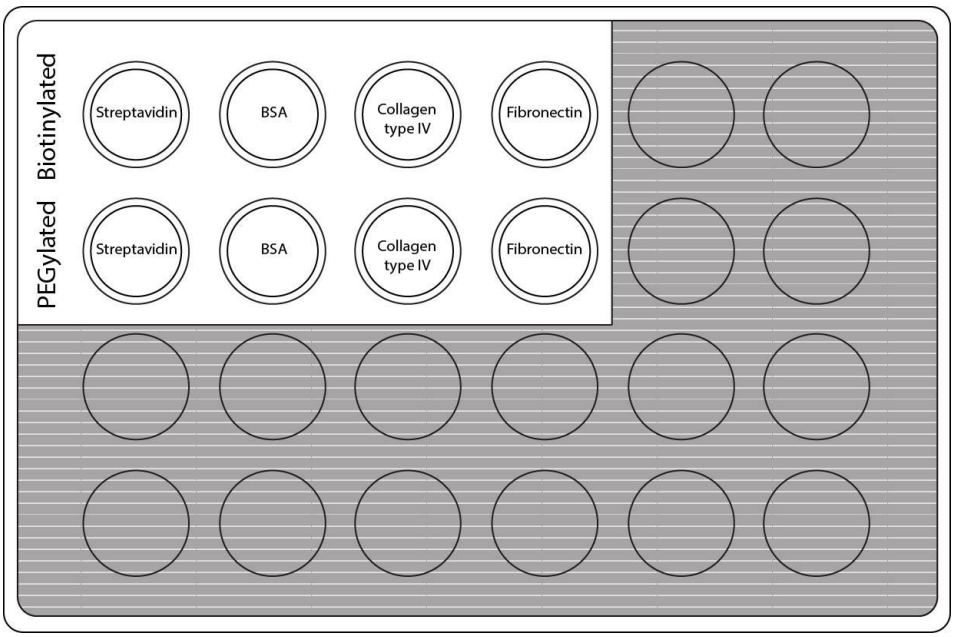

Figure 55. Schematic diagram showing the distribution of the samples in the 24-well plate.

The suspensions were left in the wells for 1 hour to allow the capsules within the suspension to sink and contact the protein substrates at the base of each well. Incubations were performed at room temperature. After incubation, the microcapsules were washed using a dilution/washing technique. This involved 3 dilution steps, where the microcapsule suspensions were diluted followed by the removal of approximately 50% of the diluted suspension, as described in a previous study (Gautrot et al., 2010). This was performed in order to prevent surface of the coverslip from drying out, leading to unspecific binding of the capsules as they dry onto the protein surface. After 3 dilutions, 3 washes were performed, removing all solutions after each cycle. The coverslips were then carefully removed using tweezers to ensure that the centre of the coverslips were untouched. They were then mounted face down onto a glass slide with mounting medium.

5.4.4 Epifluorescence microscopy analysis

The mounted coverslips were analysed using a Leica DMI4000B epifluorescence microscope, coupled to a Leica DFC300FX digital colour camera. The excitation wavelength of the FITC used is 488 nm, hence a blue filter was applied to the excitation beam. The intensity of the mercury lamp used was kept constant at 50% throughout all measurements. The micrographs acquired were then processed using an intensity calculator tool available from the open-source software, Image J. Briefly, each image was loaded into the software and the entire surface was selected and measured. The software was used to count each microcapsule that had remained adsorbed to the protein substrate after washing. This would provide an indication of the affinity of the microcapsules for that specific surface.

5.5 Results

After analysis of each sample, it became apparent that the edges of all samples were laden with microcapsules. Evidently, the microcapsules were not being washed effectively around the edges. For this reason, analysis was restricted to the centre of the coverslips.

5.5.1 Micrographs

The following images are examples of the micrographs obtained from different samples. On all occasions, where present, the microcapsules were clearly visible. They fluoresced green, in accordance with the emission wavelength of FITC (519 nm).

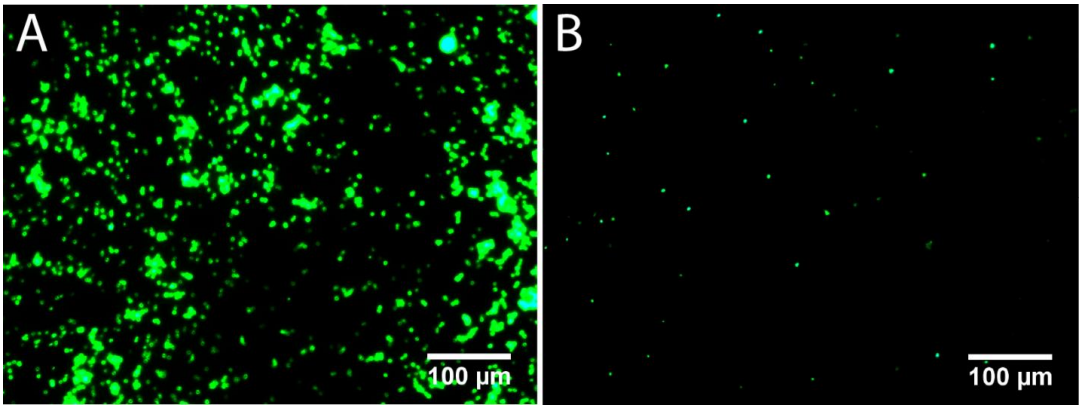

Figure 56. Images showing the adsorption of PEG-biotin terminated capsules (Panel A) and PEGylated microcapsules (Panel B) on Streptavidin coated coverslips.

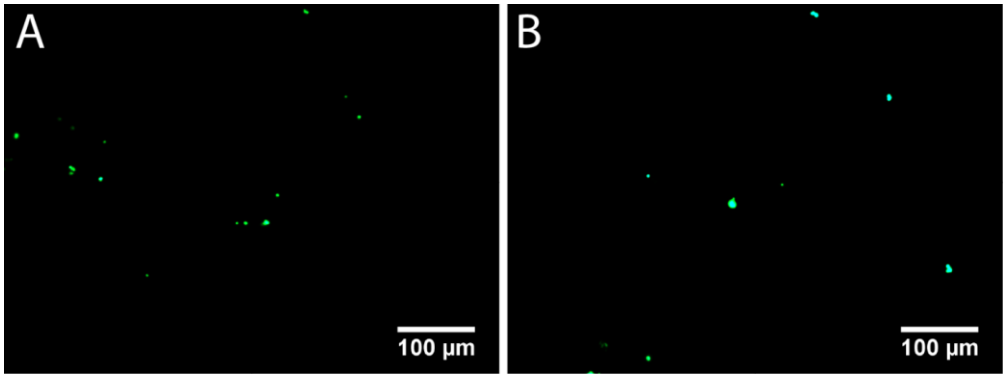

Figure 57. Images showing the adsorption of PEG-biotin terminated capsules (Panel A) and PEGylated microcapsules (Panel B) on collagen type IV coated coverslips.

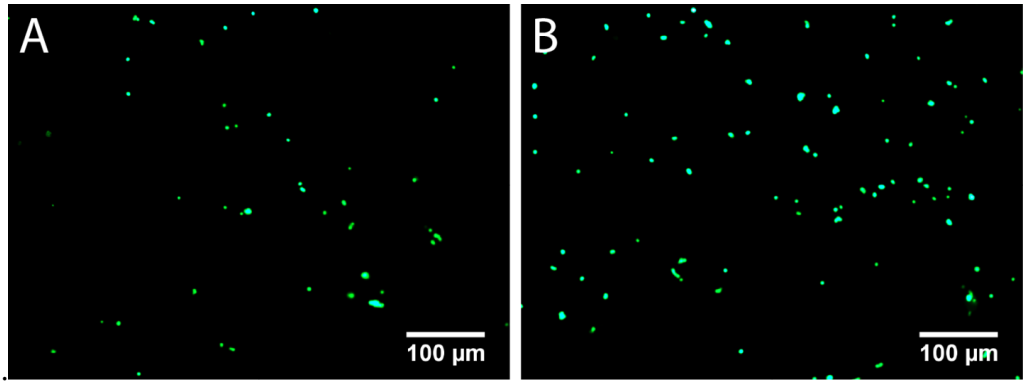

Figure 58. Images showing the adsorption of PEG-biotin terminated capsules (Panel A) and PEGylated microcapsules (Panel B) on fibronectin coated coverslips.

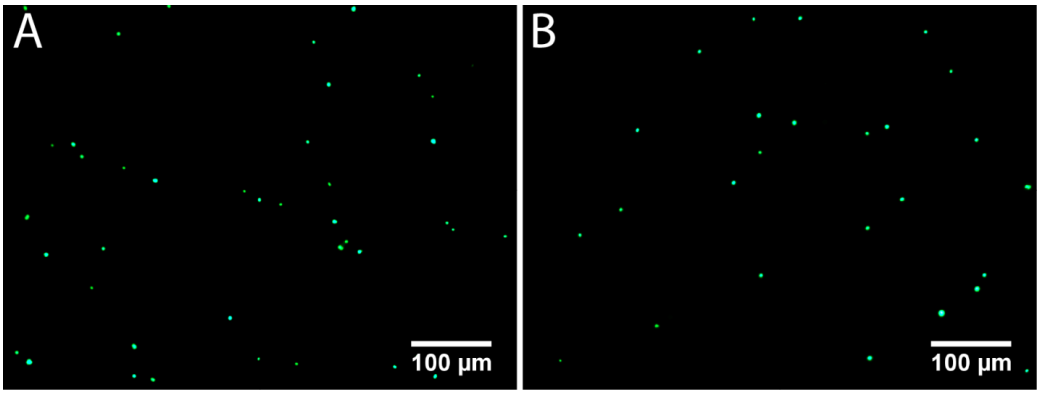

Figure 59. Images showing the adsorption of PEG-biotin terminated capsules (Panel A) and PEGylated microcapsules (Panel B) on BSA coated coverslips.

5.5.2 Adsorption summary

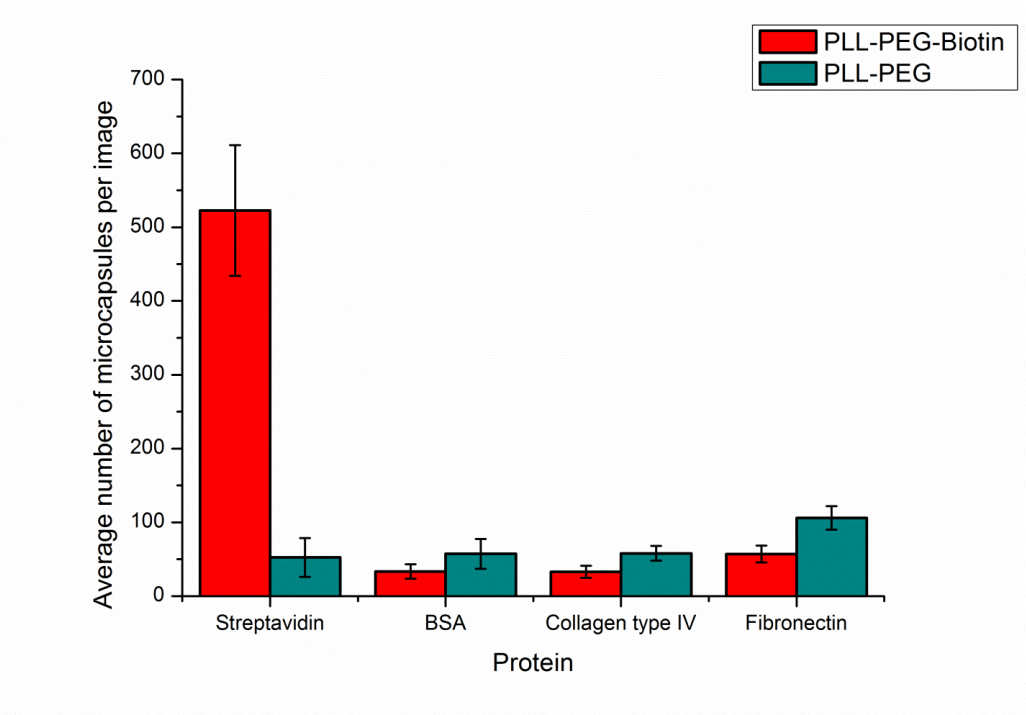

Figure 60. Summary of the effects of PEGylation (cyan) and PEGylation/biotin functionalisation (red) of Dextran sulfate/poly-l-arginine microcapsules on adsorption to protein substrates. Error bars indicate standard deviation (n = 10).

Results from the adsorption assay indicate that the degree of binding of the PEG-biotin functionalised microcapsules was 10 fold greater on the target protein (streptavidin) compared to the control proteins. Furthermore, computed t and p values for a one-tailed t-test performed on the PEG on streptavidin and PEG-biotin on streptavidin were 8.83 and 0.000454, respectively. Hence the data is statistically significant at the p = 0.01 confidence threshold. Furthermore, a long term study has successfully proven that PLL-PEG-Biotin terminated microcapsules are fully functional 7 days after synthesis, as shown by the micrograph depicted in Figure 61.

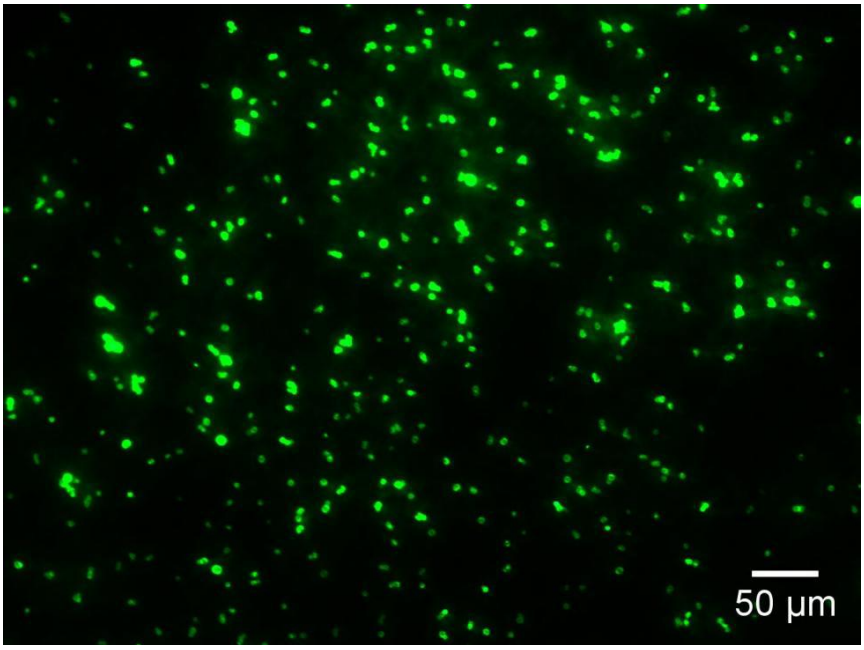

Figure 61. Epifluorescence image showing 366 capsules functionalised with PLL-PEG-biotin strongly bound to streptavidin. N.B. the capsules in this image were fabricated one week prior to this experiment.

5.6 Discussion

The affinity and specificity of PEGylated and biotin-functionalised microcapsules were tested against various proteins including the target protein, streptavidin. The micrographs obtained reveal that the PEG-Biotin microcapsules exhibited a high binding affinity towards streptavidin substrates, as shown in Figure 56A whereas a lower, in some cases negligible binding affinity was noticed on the remaining protein substrates. Furthermore, the PEGylated capsules showed insignificant binding towards streptavidin-coated coverslip. This statement is supported by a one-tailed t-test between the PEGylated and PEG-biotin microcapsules on streptavidin. The computed p value is lower than 0.05 (0.00366), hence the difference between the binding of the two groups are statistically significant. It is important to realise that the only difference between these capsules is that the control capsules are not functionalised with biotin. Combined, these findings

suggest that the non-covalent biotin-streptavidin complex is solely responsible for the binding of the microcapsules to the streptavidin.

The quantification method of capsule binding affinity was direct in nature. The capsules were simply counted with the aid of software. This should be relatively accurate, however, in some cases, the capsules would be found aggregated together on the surface of the protein substrate. This was circumvented by approximating the number of capsules within the agglomeration by estimating the total area covered. Since all capsule samples were relatively monodisperse, this was a sufficient method of estimating the total number of capsules within the images.

Upon closer analysis of all washed coverslips, the edges were laden with microcapsules. This is undoubtedly not a result of protein adsorption, since most of the middle of these substrates were largely empty. This phenomenon has most likely occurred due to the washing technique. During aspiration, suspended, unbound capsules would be removed by pipette aspiration, however, there is always some residual suspension left in the wells, usually confined to the edges. This results in the apparent adsorption of capsules around the perimeter of the coverslips. In the interest of validity, these areas were negated from the analysis.

Furthermore, the effects of the highly specific interaction between PLL-PEG-biotin microcapsules and streptavidin are still exhibited in long term assays. A sample of PLL-PEG-biotin microcapsules were kept in the fridge for 2 weeks. The results of testing

these microcapsules 2 weeks after fabrication, show a high degree of binding to the streptavidin substrate (Figure 61).

After washing all control protein samples, it was apparent that some microcapsules remained on the surface of these proteins despite PEGylation of all capsules. A possible explanation for this non-specific binding to protein surfaces could be the incomplete PEGylation of the surface of the microcapsules. Incomplete coverage of the underlying dextran sulfate layer could lead to unspecific interactions, as previously discussed. This non-specific adsorption may also be the result of incomplete aspiration of the suspensions during washing. However, the washing protocol consisted of 3 dilution and 3 washing cycles, hence the unbound capsules should have been sufficiently removed from the surface.

5.7 Conclusion

A system whereby microcapsules can be functionalised to specifically and exclusively bind to a streptavidin substrate has been successfully established. By preventing unspecific adsorptions via PEGylation and functionalising the capsules with biotin, the ability to produce microcapsules that are able to target a specific protein has been achieved. Results show at least a 9-fold increase in capsule retention when in contact with streptavidin, compared to control proteins. Furthermore, the capsules remain fully functional after 2 weeks, indicating good stability which is required for long-term use e.g. long-term therapy. The next step in this research topic would be to add flexibility to the system, in order to allow specific binding to a wider variety of target proteins.

6. Biofunctionalisation of PEGylated micro-capsules for exclusive binding to protein substrates

6.1 Introduction

One of the major challenges in modern medicine is the localisation of drugs within the body. Many drugs have been developed for chemotherapeutic use, however, they all exhibit side effects of varying degrees of severity. This is due to the fact that once a drug is injected into the blood stream, it becomes largely ubiquitous within the body, potentially affecting normal tissues and causing unwanted side effects. By generating a system whereby drugs can be delivered specifically to injury/carcinogenic sites in the body, one can significantly reduce side effects of drugs on normal tissues. Furthermore, site specific delivery decreases the amount of drug needed for adequate efficacy, which also potentially minimises costs incurred to the health service.

The concept of microencapsulation in drug delivery has been extensively studied (De Geest et al., 2009a), however, surface functionalisation of microcapsules to achieve site specific adsorption has not been fully explored. A number of recent studies have investigated the functionalisation of micro/nanoparticles, as the surface of these particles are more easily modified and unspecific protein adsorptions are less common (Singh and Lillard Jr, 2009, Azarmi et al., 2008, Chan et al., 2010). In contrast, microcapsules have higher loading capacities due to their larger size and hollow interior, which makes them

more suitable as carriers in drug delivery, providing that their functionalised surface enables site specific adsorption.

As previously shown in chapters 2 and 3, when biodegradable polymers, e.g. polyamino acids and polysaccharides, are used, one can manufacture biodegradable capsules that are able to degrade over time, resulting in a controlled release of the encapsulated drug (Wang et al., 2007a). . Potential applications of such microcapsules include delivery of vascular endothelial growth factor (VEGF) to promote endothelial cell proliferation and migration (Wang et al., 2008) and stromal cell-derived factor 1 (SDF-1) to promote homing of endothelial progenitor cells to lesions with damaged endothelium. These processes occur over a long period of time (months to years) and therefore require a sustained release of drugs, which can help to inhibit the progression of these diseases (Horlitz et al., 2002, Pastorino et al., 2011). Furthermore, these diseases are site-specific, therefore capsules will need to be selectively adsorbed to the regions where endothelial denudation has occurred after angioplasty, i.e. where the collagen type IV-rich basement membrane has been exposed (Kalluri, 2003). Consequently, the aim of this study is to produce microcapsules that have the ability to specifically adsorb to a collagen type IV substrate. Additionally, the system devised should be versatile enough to be applicable to other diseases that require specific localisation of drugs.

In order to achieve site-specific adsorption, a unique biomolecule that specifically recognises certain peptide sequences on the collagen molecule must be tethered to the microcapsule. Antibodies successfully fulfil this requirement as they specifically bind to the antigen that is present on their target protein. A study has demonstrated that one can

adsorb antibodies directly on the surface of PSS-terminated microcapsules via non-specific protein adsorption (Cortez et al., 2006). However, it is necessary to be aware that achieving specific adsorption between the capsules and the target (i.e. through antibody-antigen interactions) is not sufficient evidence to prove that the capsules have a specific affinity to a particular surface. One must also prove that the capsules refrain from adsorbing to other biological substrates. The study in question did not investigate whether their microcapsule adsorption would be suppressed on other biological surfaces. In order to determine whether the use of immunoglobulins would be a viable means of achieving specific adsorption of microcapsules, their structure and function should be fully understood.

6.1.1 Immunoglobulins

The use of antibodies as a means of achieving substrate-specific adhesion of polyelectrolyte microcapsules was investigated. In order to understand how antibodies achieve protein-specific adhesion, their structure must be studied.

Antibodies are large Y-shaped proteins and are often referred to as immunoglobulin molecules. Below is a diagram highlighting the major constituents of an immunoglobulin molecule.

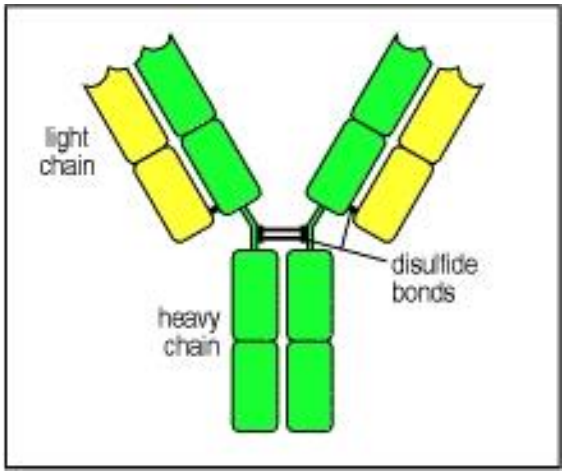

Figure 62. Antibody structure. Adapted from (Janeway, 2001).

Antibodies are made up of 4 major polypeptides which are interconnected via disulphide bonds. Two of them are known as light chain due to their low molecular weight of approximately 25kDa and their larger counterparts are known as heavy chains with a molecular weight of 50kDa. The stems of different antibodies from the same immunoglobulin family are almost identical. Conversely, the arms of the y structure are variable. Ultimately, this is what gives antibodies their binding specificity. Each arm has an identical tip known as the antigen-binding site which interacts and binds with an antigen. Therefore one immunoglobulin has the ability to bind to two identical antigen molecules (Janeway et al., 2001). Although the forces involved in antibody-antigen interactions are weak e.g. van der Waals, ionic and hydrophobic interactions, the summation of the large quantity of these interactions gives rise to a relatively strong interaction. Furthermore, the hinge region, located between the Fc (constant fragment) and Fab (antigen-binding fragment) region is flexible, giving rise to rotational and lateral movement, allowing the antibody to bind to epitopes that are positioned irregularly (Ruoslahti, 1996).

6.1.2 Polyclonal and monoclonal antibodies

Antibodies come in two different forms, namely monoclonal and polyclonal antibodies. To decide which type is ideal for this purpose one must understand how antibodies are synthesised and the difference between the two types.

Antibodies are formed from B lymphocytes (B-cells) *in-vivo* during an immune response. When an organism is injected with protein antigens, B-cells respond by producing antibodies at a single epitope of the antigen. An epitope is a specific amino acid sequence on the antigen, which binds to antibodies. Once an antibody has been produced, the B-cell then divides to give multiple B-cells which produce the same antibody. Typically, B-cells produce many different antibody clones which are able to bind to multiple epitope sites on the antigen. This is known as a polyclonal antibody. This type of antibody is particularly useful in providing a high binding affinity to the corresponding antigen, however, it can result in a lower specificity due to different antigens exhibiting similar epitopes (Anand et al., 2010). By contrast, monoclonal antibodies produced using hybridoma technology, are monospecific i.e. they will all bind to the same epitope of the antigen. Briefly, an antigen is introduced to the host which induces the production of B-cells which produce a complementary antibody. These B-cells are subsequently isolated from the spleen of the organism and fused with myeloma cells via electrofusion (Karsten et al., 1985). The so-called hybridoma cell can be easily cloned into identical daughter cells, all of which will produce identical monoclonal antibodies. This technique therefore produces antibodies which are highly specific to a single antigen; however, should the epitope not be available due to the orientation of the antigen, the antibody will fail to bind, giving rise to a compromised binding affinity.

As demonstrated in the previous chapter, by grafting polyethylene glycol chains onto the surface of polyelectrolyte microcapsules, one can reduce the non-specific adsorption associated with the polyelectrolytes (Wattendorf et al., 2008, Yang et al., 2012a). The protein-resistant properties of PEG have been well characterised in scientific research (Heuberger et al., 2005a). This characteristic effectively shields the electrostatic forces associated with the polyelectrolyte multilayers, resulting in a significant reduction in non-specific protein adsorption. An ideal solution to achieve selective adsorption to collagen type IV would be to tether the PEG chains with anti-collagen type IV antibody. Furthermore, to improve binding affinity, it is essential to orientate the IgG immunoglobulin in a manner that exposes the Fab fragments to facilitate antigen binding.

6.1.3 Interaction with Protein G and Antibodies Literature Review

Protein G has the ability to specifically bind to IgG with high affinity. More specifically, the protein binds predominantly to the Fc region of the IgG molecule. This immunoglobulin-binding protein possesses a weak affinity to the Fab region, although most of the commercially available protein G has been genetically modified to virtually eliminate this affinity. Interactions with this region may affect the activity of the antibody, thus reducing its affinity to bind to its respective antigen (Saha et al., 2003). To this end, protein G has the ability to both isolate and orientate antibodies on a surface. This method of immobilisation is superior to the use of a streptavidin-biotin complex where the biotin attached to the antibody has the potential to compromise the activity of the antibody (Koutsoukos et al., 1983).

Protein G and Protein A are well established immunoglobulin-binding proteins, which, when genetically engineered, exclusively bind to the Fc fragment of IgG. Consequently, when antibodies are adsorbed to a protein G surface, they are automatically orientated in such a way that the Fab fragments are available for antigen binding (Bae et al., 2005). In order to understand the binding of Protein G with the Fc fragment, the structure of both components must be understood.

Located on the heavy chain, the Fc domain is formed of two constant domains of similar length, namely C_H^2 (110 residues) and C_H^3 (106 residues). Protein G is made up of 600 amino acids. Each molecule of protein G has three identical Fc-binding domains located near the C terminus (Ruoslahti, 1996). These chains are made up of 55 amino acids each. These residues are arranged in a structure that consists of a four-stranded beta sheet with a single alpha helix positioned diagonally across. In theory, by incorporating protein G into the microcapsule structure, antibodies should be able to be absorbed and orientated uniformly with their epitopes available for antigen-binding. Furthermore, this method will selectively filter any stabilising proteins that may be present in the antibody solution, as it will only bind immunoglobulins. The end result should be a pure coating of antibody on the surface of the microcapsules.

Protein G has been reported to have a higher affinity to the IgG isotype than protein A (Saha et al., 2003). For this reason, protein G shall be used in this study. This PEG/antibody assembly will be applied to biodegradable microcapsules, made from dextran sulfate and poly-L-arginine, since these polymers are biocompatible and have

been previously used to create degradable microcapsules successfully (De Koker et al., 2010, Santos et al., 2012).

Protein G can be easily grafted to PEG via the use of the biotin/streptavidin or biotin/avidin complex, providing that both protein G and PEG are biotinylated. The interaction between biotin and streptavidin is believed to be one of the strongest non-covalent interactions in biology (González et al., 1997). Furthermore, streptavidin has a more neutral isoelectric point (5-6) compared to avidin (10.5), rendering the protein less susceptible to non-specific adsorptions (Darzynkiewicz et al., 2009, Wilson et al., 2000). Since one of the functions of the proposed microcapsules is to reduce non-specific protein adsorption, it was decided that the streptavidin/biotin complexation was a reliable means of tethering protein G to PEG chains. The biotinylation process allows one to functionalise proteins with biotin. This must be performed in order to take advantage of the streptavidin/biotin linking mechanism.

6.1.4 Functionalising proteins with biotin - Biotinylation

Referring back to the structure of biotin, it has a pentanoic acid branch with its characteristic carboxylic acid group. This group can be easily derivatised to make reagents that can label protein. The so-called Biotinylation of proteins is often achieved through the use of NHS ester derivatives. The NHS- biotin derivative provides a good leaving group and is therefore easily substituted for an amine group on an immunoglobulin molecule.

Most commercially available antibodies are shipped in ascites fluid since a higher concentration of antibody is found in ascites fluid compared to cell culture supernatant. The disadvantage of this is that ascites fluid is comprised of many other proteins. Ordinarily this would not be a problem for common experiments such as ELISA and other immunoassays, however for biotinylation, this is not ideal since the NHS ester group on the biotinylation reagent reacts with any chemical or biomolecule with an amine group, giving these proteins potential to bind to the streptavidin surface of the microcapsules. Ultimately this will contaminate the surface and may reduce the binding affinity of the microcapsules to the collagen type IV antigen. Using this linking technique, the study aims to fabricate antibody-functionalised microcapsules for specific protein adsorption. Their performance will be tested on a micro-patterned platform.

To further illustrate the specific adsorption of the functionalised microcapsules, micro-patterned substrates were used. These patterns are relatively easy to synthesise and come in a wide range of shapes and sizes, ranging from tens to hundreds of microns across. Micro-patterns offer great flexibility in creating defined areas for interrogation. There have been a number of reports of microcapsule adsorption onto micro-patterns (Antipina et al., 2009, Nolte and Fery, 2004). These studies rely solely on either the physical entrapment of microcapsules on embossed patterns or electrostatic interactions between microcapsules and patterned polyelectrolytes.

Micropatterning of proteins on a planar substrate is achieved through the use of protein resistant polymers. In essence, these polymers are printed onto the substrate, creating a

negative of the desired micropattern. The substrate, usually glass or ultra-thin gold-coated glass, is then incubated in a protein solution, allowing the protein to be adsorbed onto the unprotected areas, resulting in a micropatterned protein surface (Gautrot et al., 2010). The most commonly used protein resistant polymer is polyethylene glycol (PEG). These micropatterned substates would be excellent candidates for testing the biofuctionalised microcapsules since it provide a distinct visual representation of the specificity of the microcapsules.

This study aims to create a micro-patterned protein substrate using a technique involving micro-contact printing and controlled atom-transfer radical-polymerisation (ATRP) as previously described (Gautrot et al., 2010). The biofunctionalised microcapsules will then be introduced to the various protein micro-patterns, whereby retention will be quantified using fluorescence microscopy. Zeta potential and surface plasmon resonance (SPR) was performed on the layer-by-layer assembly to verify the construction of the microcapsules. SEM was performed to monitor the surface morphology of the microcapsules.

6.2 Materials

Materials for microcapsules. Calcium chloride dihydrate ($CaCl_2.2H_2O$), sodium carbonate (Na_2CO_3), Ethylenediaminetetraacetic acid disodium salt dihydrate ($C_{10}H_{14}N_2Na_2O_8.2H_2O$), dextran sulfate sodium salt (Mol. Wt. ~40kDa), Poly-L-Arginine Hydrochloride (Mol. Wt. 15-70kDa), Streptavidin (from Streptomyces Avidinii), Protein G' (from Streptococcus Sp), Monoclonal Anti-Collagen Type IV antibody (produced in mouse), Monoclonal Anti-Fibronectin antibody (produced in

mouse), and Mix-n-Stain™ CF™ 555 Antibody Labeling Kit were purchased from Sigma-Aldrich Co. Poly-L-Lysine grafted with polyethylene glycol and polyethylene glycol-biotin(50%) (PLL(20 kDa)-PEG(2 kDa)/PEG-biotin (50%) (3.4 kDa)) was purchased from SuSoS AG. EZ-Link^{TM}. Sulfo-N-Hydroxysulfosuccinimide-6-aminocaproic acid-6-aminocaproic acid-Biotin (Sulfo-NHS-LC-LC-Biotin) was purchased from Thermo Fisher Scientific, Inc.

Materials for Micro-patterning. Collagen from human placenta (Bornstein and Traub type IV), Bovine serum albumin (BSA), Fibronectin from human plasma, oligo(ethylene glycol methyl ether methacrylate) (OEGMA, mol wt. 300 Da), CuCl, $CuBr_2$, 2,2'-dipyridyl (bpy) were purchased from Sigma-Aldrich Co. Fibronectin antibody (anti-human), rabbit polyclonal, was purchased from Abcam . Alexa Fluor® 594 Donkey Anti-Rabbit IgG (H+L) Antibody was purchased from Invitrogen. Antibodies were used at recommended dilutions. ω-Mercaptoundecyl Bromoisobutyrate was synthesised according to the literature (Jones et al., 2002).

6.3 Method

6.3.1 Fabrication of microcapsules

Microcapsules were fabricated using the LbL technique. Briefly, calcium carbonate cores (4-6μm) were formed by mixing equal volumes of 0.33M $CaCl_2$ with 0.33M Na_2CO_3. The mixture was incubated for 5 minutes to allow the formation of the cores. After washing with deionised water (18.2 MΩ·cm), dextran sulfate was adsorbed to the surface of the cores by immersing them in a 1 mg/ml solution of the polymer dissolved in

deionised water. The sample was incubated on a vortex mixer for 15 minutes, after which the cores were washed 3 times by centrifuging at 1,500 rpm and redispersing the capsules in fresh deionised water. Layers of oppositely charged polymers were sequentially deposited in this manner until 2 [Dex.S/PArg] bilayers were adsorbed to the cores. The second polyarginine layer was fluorescently labelled with rhodamine B to allow the microcapsules to be detected and quantified. A final dextran sulfate layer was then adsorbed. For protein resistance, the polymer-coated cores were immersed in PLL-PEG/PLL-PEG-biotin solution (100 μg). Cores were subsequently dissolved in 0.2M EDTA for 10 minutes and excess calcium ions were washed using fresh EDTA. Finally, the capsules were washed 3 times with PBS.

6.3.2 Biofunctionalistion of microcapsules

A sulfo-NHS derivative of biotin, complete with spacer arm to allow adequate room for a streptavidin molecule to bind, was reconstituted in ultrapure Milli-Q water (18.2 MΩ·cm). Immediately after dissolution, the reagent was added to a protein G solution (reconstituted in PBS) and incubated for half an hour. The resulting biotinylated protein G was dialysed against a regularly replenished PBS solution for 48hrs to remove any unconjugated biotin. Streptavidin (100 μg) was then adsorbed onto the aforementioned PLL-PEG/ PLL-PEG-biotin (50%) terminated microcapsules before adsorption of biotinylated protein G (100 μg). Finally, 100 μg monoclonal anti-collagen type IV was specifically adsorbed to the protein G present on the microcapsules. This resulted in the formation of PEGylated microcapsules with approximately 50% of the surface of each capsule functionalised with anti-collagen type IV (Figure 63).

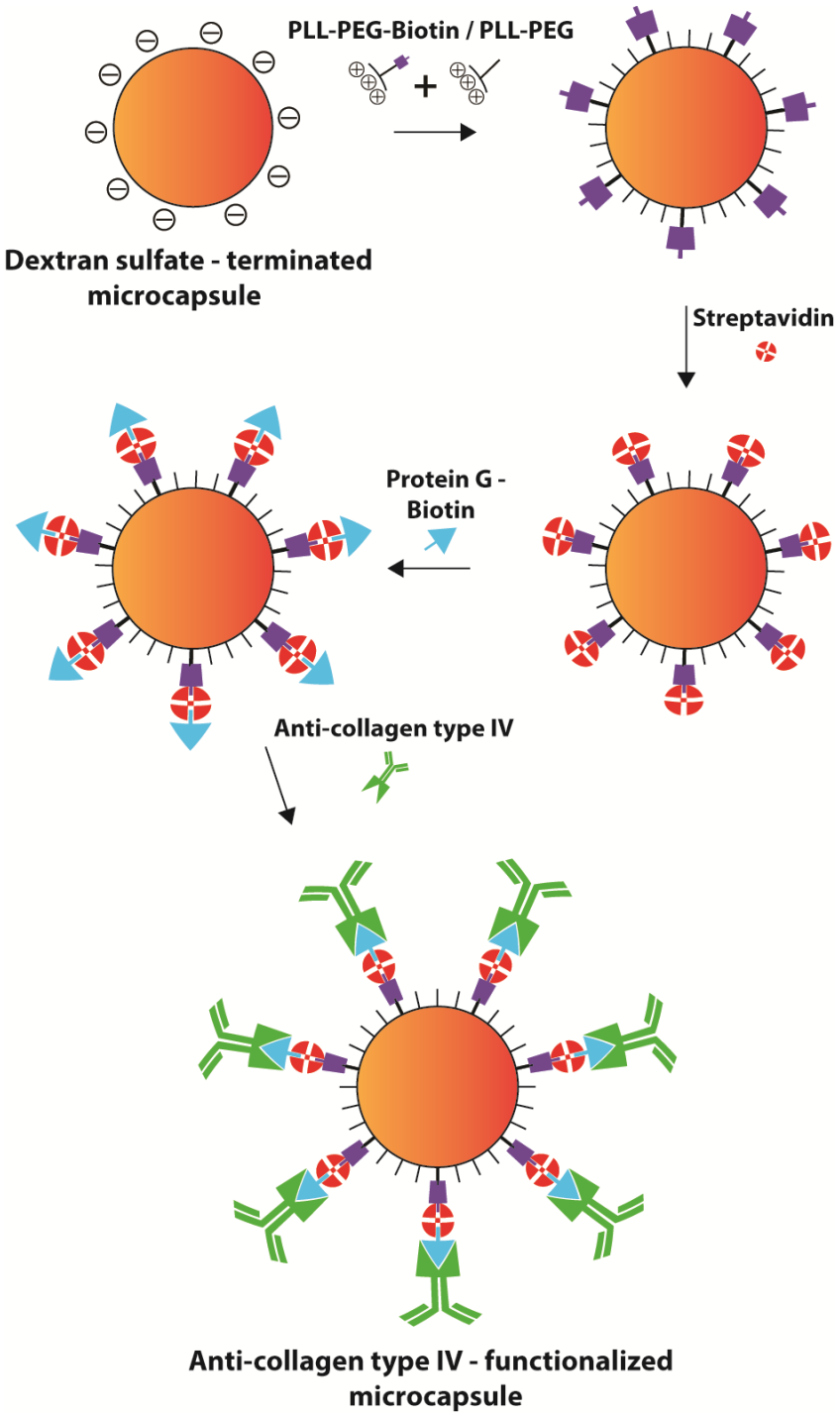

Figure 63. Reaction scheme for the synthesis of anti-collagen biofunctionalised microcapsules.

After washing off excess antibody with PBS solution, the microcapsules were stored in PBS at 4˚C. To test the versatility of the model, anti-fibronectin functionalised

microcapsules were prepared in a similar fashion. Quantities of polymer/protein required for complete adsorption were calculated by using the following estimation.

Total surface area of microcapsules in one sample is:

$$N \times 4\pi r^2,$$

where N is the total number of microcapsules per sample, which is approximately 5.0×10^7 (estimated using haemocytometry) and r is the radius of the microcapsules estimated at 3μm. Thus the estimated total surface area is 0.0057 m^2. Given that 1 m^2 can be coated by approximately 1 mg, 0.0057 mg of polymer is required to coat the surface. Hence the mass of 0.1 mg of polymer was assumed to be sufficient.

6.3.3 Micro-patterning of protein

Preparation of the substrate with gold circular islands surrounded by protein resistant poly(oligo(ethylene glycol methyl ether methacrylate)) (POEGMA) brushes was achieved using a protocol as described in a previous study (Gautrot et al., 2010). The procedure is illustrated in Figure 64.

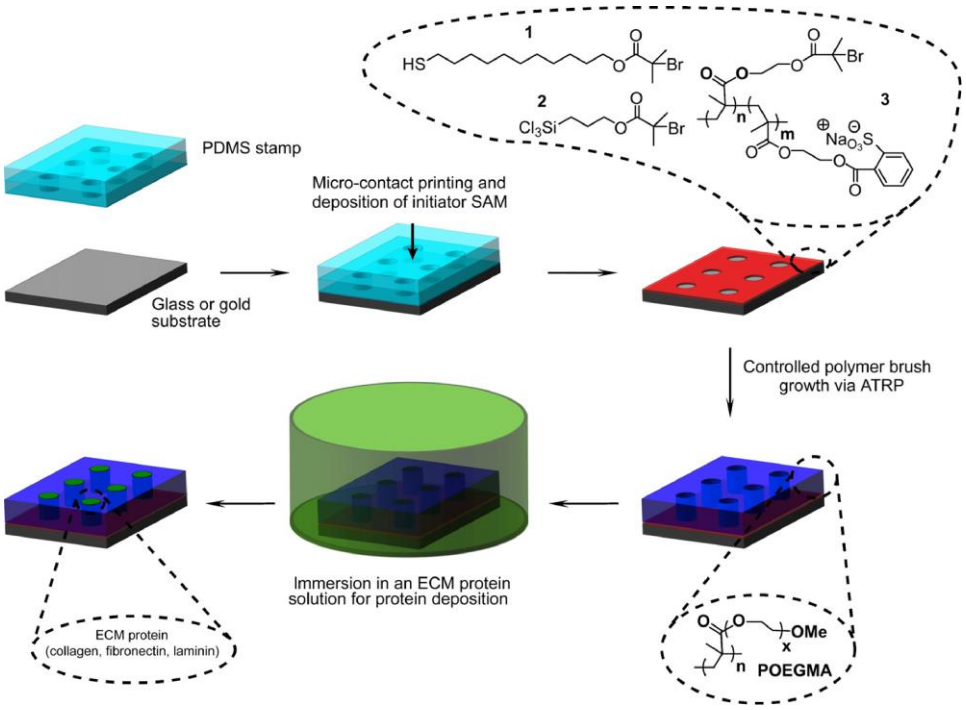

Figure 64. Protocol for micro-patterning of Protein using ATRP. Adapted from (Gautrot et el., 2010).

Briefly, a PDMS stamp to print negatives of the micro-pattern was copiously inked with ω-Mercaptoundecyl Bromoisobutyrate initiator. After 10 seconds, excess initiator was washed off with ethanol and the stamp was dried under a nitrogen stream. The stamp was then gently placed on the gold coated slide to transfer the initiator to the surface. After a further 10 seconds, the stamp was removed. Multiple substrates were prepared and placed into a glass slide chamber. A POEGMA solution, previously prepared via ATRP, was added to the chamber and the slides were left to incubate under a nitrogenous environment for 1 hour. During this time, the POEGMA selectively bound to the areas coated with ω-Mercaptoundecyl Bromoisobutyrate initiator, resulting in a pattern consisting of 400μm circular gold islands surrounded by POEGMA brushes approximately 20nm thick. The micro-patterned substrates were thoroughly washed with ethanol and dried under a nitrogen stream. The wafer was then cut into 1 cm^2 chips and

placed in wells on a 24-well plate. A collagen type IV protein solution (10 μg/ml) was applied to a 1 cm^2 micro-patterned chip in a 24-well plate and incubated for 1 hour at room temperature to allow the protein to bind to the gold islands. Excess collagen was diluted and washed off with PBS solution, resulting in a micro-patterned protein surface consisting of 400 μm collagen-coated circles. As a control, fibronectin and bovine serum albumin were micro-patterned using the same procedure.

6.3.4 Biofunctionalised microcapsule protein adsorption assay

Equal volumes of biofunctionalised microcapsule suspensions were added to each well with the protein-micro-patterned chips and left for 1 hour to allow the capsules to sink and make contact with the substrate. After 3 dilution and 3 washing steps with PBS solution, microcapsule retention was analysed using epifluorescence microscopy. Fluorescence intensity of each island was computed using Image J software and values of relative fluorescence measured in arbitrary relative fluorescence units (RFU). The fluorescence intensity was corrected by subtracting background readings to give a corrected relative fluorescence intensity (RFI) reading using the following equation:

$$RFI = FI - (A_i \times \overline{BF})$$

where FI is the total fluorescence intensity within the island, A_i is the area of the island and $\overline{BF}$ is the mean background fluorescence calculated from three readings. Control (dextran sulfate terminated), anti-collagen IV terminated, and anti-fibronectin terminated microcapsules were tested against each of the three protein substrates: collagen type IV, fibronectin and bovine serum albumin. 5 islands were randomly chosen for analysis for each scenario and the experiment was repeated 5 times for each protein. T-tests (2 tailed)

were performed on each sample to assess the significance between the experimental and each of the control groups (n=25).

6.3.5 Immuno-staining and microscopy

To prove that protein was successfully being adsorbed onto the patterned gold substrates, immuno-staining was conducted on a fibronectin-coated sample. Initially, the fibronectin was blocked using a blocking buffer (10% FBS, 0.25% gelatin). Monoclonal anti-fibronectin, diluted with blocking buffer was then applied to the substrate and left for 1 hour at room temperature, after which the sample was thoroughly washed. Finally, the substrate was incubated in Alexa Fluor® 594 Donkey Anti-Rabbit IgG secondary antibody for 1 hour at room temperature. Images were taken after thoroughly washing the micro-pattern 3 times using a pipette.

6.3.6 Zeta potential analysis

Zeta potential is commonly used to monitor the layer-by-layer polymer depositions on colloidal particles in order to ensure the successful synthesis of polyelectrolyte microcapsules (Peyratout and Dähne, 2004). In order to apply this technique to this research, one must fully understand the concept of zeta potential and how it can be measured experimentally.

Zeta potential (ζ – potential) is a parameter used to measure the average surface charge of colloidal particles suspended in a dispersion medium. It can be defined as the potential difference between the static layer of fluid adjacent to the particles and the surrounding

medium. Although it cannot be measured directly, it can be experimentally quantified using a Zeta Sizer machine, via electrophoresis. Briefly, a sample of the suspension is injected into a special cuvette with external electrodes. After loading the cuvette into the Zeta Sizer, an electric current is applied across the suspension. Naturally, particles with a positive zeta potential will migrate towards the cathode and vice versa. Furthermore, the velocity at which the particles travel is proportional to the magnitude of the charge.

This electrokinetic phenomena is measured using a Laser Doppler Anemometer. This velocity can then be inserted into an equation that corresponds to the Smoluchowski theory:

$$v_E = 4\pi\varepsilon_0\varepsilon_r \frac{\zeta}{6\pi\mu}(1 + \kappa r)$$

where μ is viscosity of the solution, r is the radius of the colloidal particles, κ is the Debye-Hückel parameter, ε_0 and ε_r are the relative dielectric constants (Sze et al., 2003).

Zeta potential analysis was performed using a Zetasizer Nano ZS system from Malvern Instruments Ltd. Calcium carbonate cores were intact during the measurements. Recordings were made after each layer was deposited on the cores. Concentrations of polymer/protein used are identical to the concentrations used in the aforementioned microcapsule fabrication methodology. All measurements were conducted in deionised water. Measurements were performed in triplicate.

6.3.7 Surface plasmon resonance (SPR) analysis

A Surface plasmon resonance (SPR) machine has the ability to detect interactions between two different molecules via optical methods. The sensor platform is made up of the sensor chip and a conductive material (usually a thin gold film approximately 50nm in thickness). Polarised light from an inclined light source hits the base of the chip. An electromagnetic component of this light is leaked through the gold chip, into the adjacent buffer/sample. This is known as an evanescent wave. At a particular angle of incident light, electrons within the gold film become excited by the evanescent wave. This stimulation of electrons results in electron charge density waves otherwise known as a surface plasmon. As a result of surface plasmon generation, the intensity of the reflective light is markedly reduced.

When a mass/substance is deposited on the film, the angle of incident light at which the surface plasmon resonance takes place changes. This is due to a change in refractive index near the surface of the sensor chip. The detector of an SPR system has the ability to monitor these angular displacements, which is measured in resonance units (RU) where 1RU = 0.0001°= 1pg.mm^{-2} of deposited material.

SPR is hugely advantageous with regard to the accuracy of binding events. Unlike many other techniques that measure quantities of adsorbed polymers/chemicals, SPR doesn't require labelling of the analyte. Labelling of analytes can lead to many inaccuracies. For example, the labelling yield of the analyte may not be 100% leading to an underestimation of the adsorbed mass. Furthermore, the labelling molecules may occupy the binding sites of the analyte leading to a lower binding affinity. SPR also enables the

user to monitor binding kinetics between a surface and an analyte allowing one to determine the binding and dissociation constants, Ka and Kd. SPR would be ideal to use for monitoring polymer and protein deposition during the layer-by-layer process and ensuring that all layers within the biofunctionalised microcapsule membrane are tethered to each other sufficiently. It will also give an indication whether there are regions terminated with just PLL-PEG since this is a vital part of the design. It's estimated that approximately 50% of the surface will be coated with only PLL-PEG and the remaining 50% of the PEG will be biotinylated and functionalised with antibody via streptavidin-biotin and protein G linkages.

SPR analysis was performed to characterise the last 5 steps of the biofunctionalised microcapsule construction, namely, dextran sulfate, PLL-PEG-biotin, streptavidin, protein G-biotin and anti-collagen type IV. This was performed to monitor the growth of each layer and ensure that each LbL assembly step was performed successfully. Measurements were taken using a Biacore X system. Gold coated chips (Ssens) were functionalised with cysteamine (5mmol in ethanol) and thoroughly washed after incubation for 24 hours. After mounting, the cysteamine chips were docked and primed with PBS buffer. A sensogram was performed for 30 minutes at 10 µL/min to equilibrate and gain a stable baseline. Once a stable baseline had been achieved, a sensogram was performed at 10µL/min using PBS. A 100 µL sample of dextran sulfate (1 mg/ml) was injected into the stream at 10 µL/min. After 10 minutes of injection, PBS was re-introduced to the sensor surface in order to wash off any non-adsorbed polymer. The system was left for at least 5 minutes or until a stable baseline was re-established. This was repeated for each consecutive layer. A concentration of 1 mg/ml of polymer/protein solution was used for each step. The Biacore X system requires the user to inject each

sample manually. Occasionally, bubbles would be unintentionally introduced into the microfluidic chamber resulting in a concomitant spike in resonance signal. This was manually removed during post-processing of the data.

6.3.8 SEM analysis of microcapsules

SEM analysis was performed using a FEI Inspect-F™ scanning electron microscope. Samples were coated in gold and were subsequently analysed using a 10kV electron beam (spot size 3.5). SEM images after each significant layer were acquired (outermost dextran sulfate, PLL-PEG-biotin, streptavidin, protein G-biotin and anti-collagen type IV).

6.4 Results

6.4.1 Micro-pattern immunostaining

The fluorescence detected after immunostaining of the patterned fibronectin confirms a high fidelity protein pattern. A high fluorescence signal can be seen within the island, indicating the presence of fibronectin, whereas no fluorescence is detected on the area surrounding the island i.e. the POEGMA brushes, as seen in Figure 65A. The sharp increase in the fluorescence intensity profile which is illustrated in Figure 65B taken along the centre of the island, further confirms this high contrast in fluorescence between the island and the brushes, consistent with the high protein resistance of POEGMA brushes (Gautrot et al., 2010).

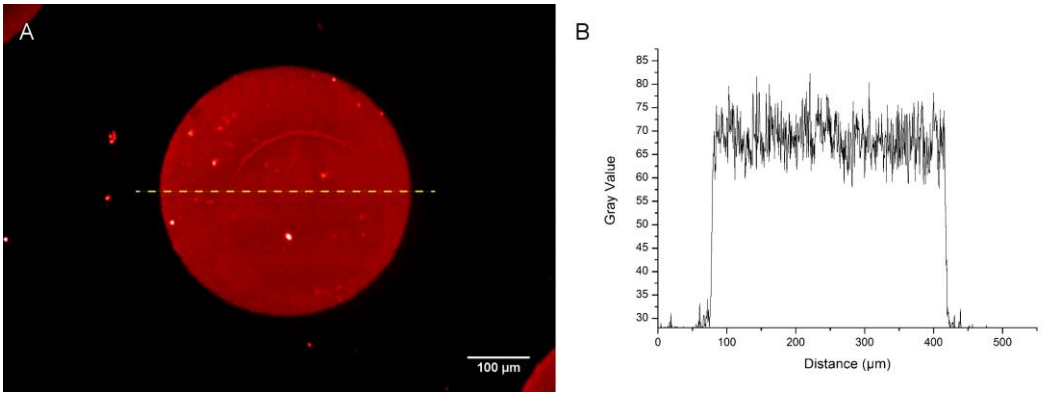

Figure 65. Immunostained fibronectin-coated island (Panel A). Fluorescence intensity profile taken from the yellow dotted line (Panel B).

6.4.2 Fluorescent tracking of antibody on modified PEG microcapsules

Figure 66 shows a collagen type IV island with adsorbed anti-collagen IV functionalised microcapsules. Fluorescence exhibited in this image is produced by CF-555 labelled anti-collagen type IV. This strong signal is indicative of successful binding of antibodies to the PEG-Streptavidin-Protein G complex. This result also shows that these microcapsules are able to be adsorbed onto collagen type IV surfaces.

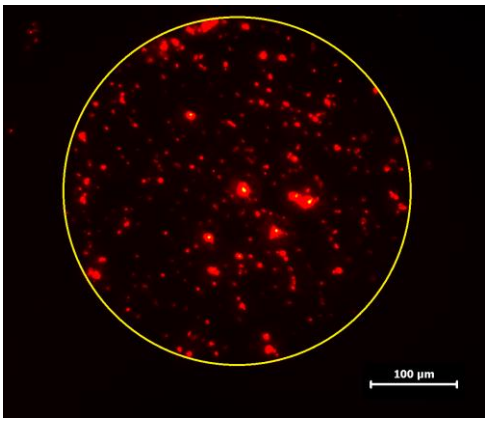

Figure 66. A single collagen type IV-coated island with adsorbed anti-collagen type IV functionalised microcapsules. This image was taken after three dilution and three washing steps. N.B. Fluorescence in this picture is produced by CF-555 labelled anti-collagen type IV. This signal is indicative of successful binding of antibody to the PEG-Streptavidin-Protein G complex.

6.4.3 Surface plasmon resonance analysis

The polyelectrolytes and proteins were sequentially injected through the microfluidic channels for 10 minutes each at 10 μL/min to allow the polyelectrolyte/protein to adsorb to the sensor surface. The channels were then flushed with PBS for at least 5 minutes at 10 μL/min (indicated as 'W' in Figure 67) to wash off excess polymer or protein. The next polymer was introduced once a stable baseline was achieved.

As expected, an increase of resonance signal was recorded after each deposition/washing cycle. Since the SPR response is related to the mass of adsorbed material, this data strongly suggests that the LbL assembly has been successfully created (Liedberg et al., 1993). A notable feature of the SPR data can be seen at the end of the graph, where the adsorbed mass increases by 236 ng/cm^2 after the deposition and washing of anti-collagen type IV. Increase in resonance units (RU) and corresponding mass adsorption for each step is shown in Table 1 (1RU = 0.1 ng/cm^2).

Table 4. SPR signal after each step of the LbL assembly.

Layer	SPR signal increase (RU)	Mass density (ng/cm^2)
Dextran sulfate	416.6	41
PLL-PEG-biotin	1559	155
Streptavidin	463.7	46
Protein G-Biotin	182.8	18
Anti-collagen type IV	2363.1	236

Values shown represent average signal/mass density recorded after washing excess polymer/protein (n=3).

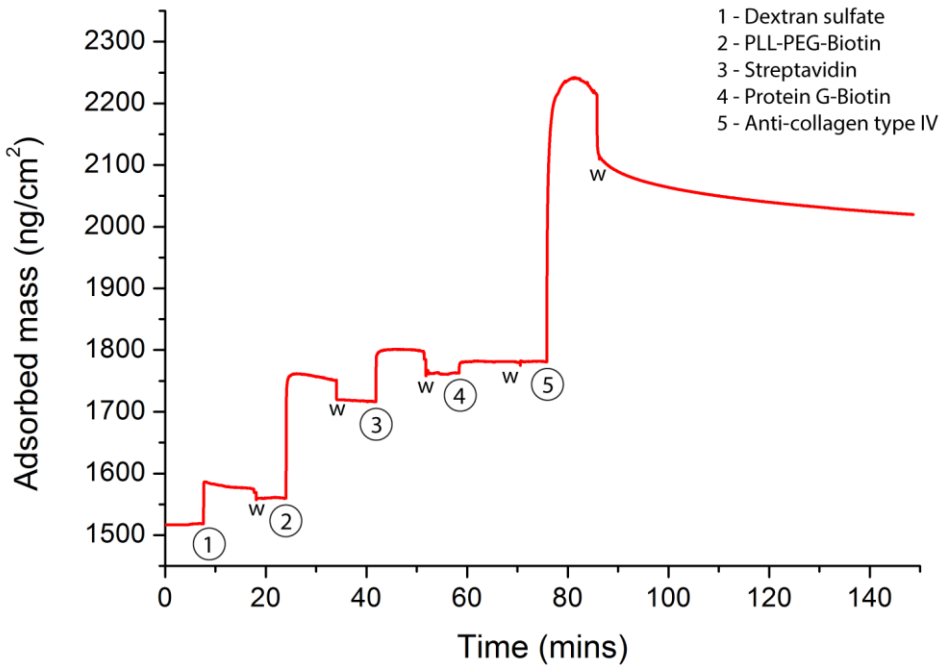

Figure 67. SPR analysis of the last 5 layers of the biofunctionalised microcapsule structure. 'W' indicates the end of the injection period and the beginning of washing for each layer.

6.4.4 SEM Analysis

SEM images reveal a significant level of aggregation once proteins were tethered to the microcapsules, as shown in Figure 68 (Panel C-E). The dextran sulfate and PLL-PEG-biotin terminated microcapsules were more well dispersed as expected (Panel A and B). Negligible differences in surface morphology were observed between the different layers (Panel F-J) with the final image, depicting the fully constructed bio-functionalised microcapsule, showing a slightly increased thickness, as shown in Panel J.

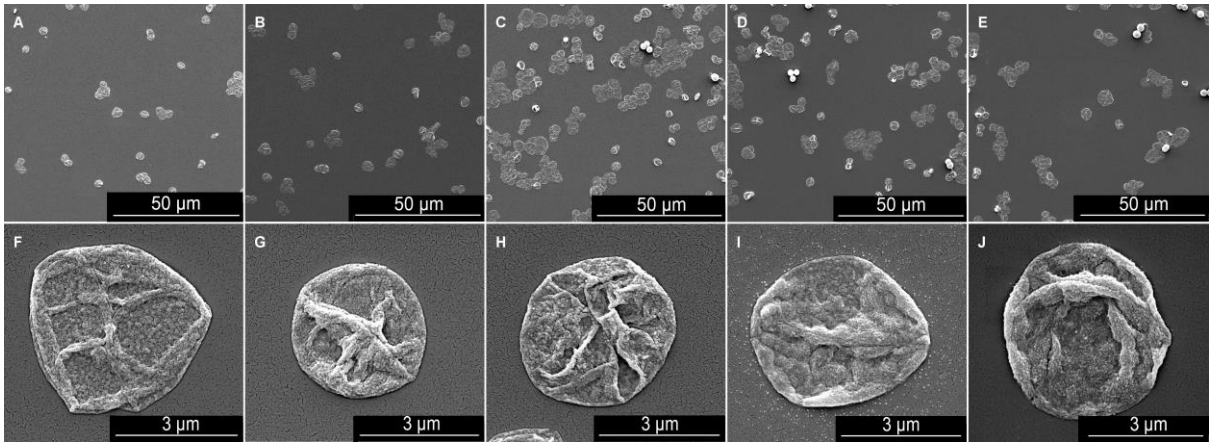

Figure 68. SEM images of a single capsule following consecutive LbL deposition: (A) outermost dextran sulfate layer, (B) PLL−PEG−biotin, (C), streptavidin, (D) protein G-biotin, and (E) monoclonal anticollagen type IV. (F−J) Zoomed in images showing single microcapsules taken from their respective samples above.

6.4.5 Zeta potential analysis

As expected, the first 5 layers of oppositely charged polyelectrolytes produced alternating zeta potentials, as shown in Figure 69. Values of -20.3mV, -21.9mV and -26.8mV were measured from the dextran sulfate layers. The zeta potential of the poly-l-arginine layers were 32.1mV and 39.4mV. As the consecutive layers are deposited, the absolute values of the zeta potentials for both anionic and cationic polymers increase, suggesting that the layers are becoming progressively more uniform. Introduction of the PEGylated layer produced a more neutral reading of -8.06mV. Further protein deposition showed minor fluctuations in zeta potential.

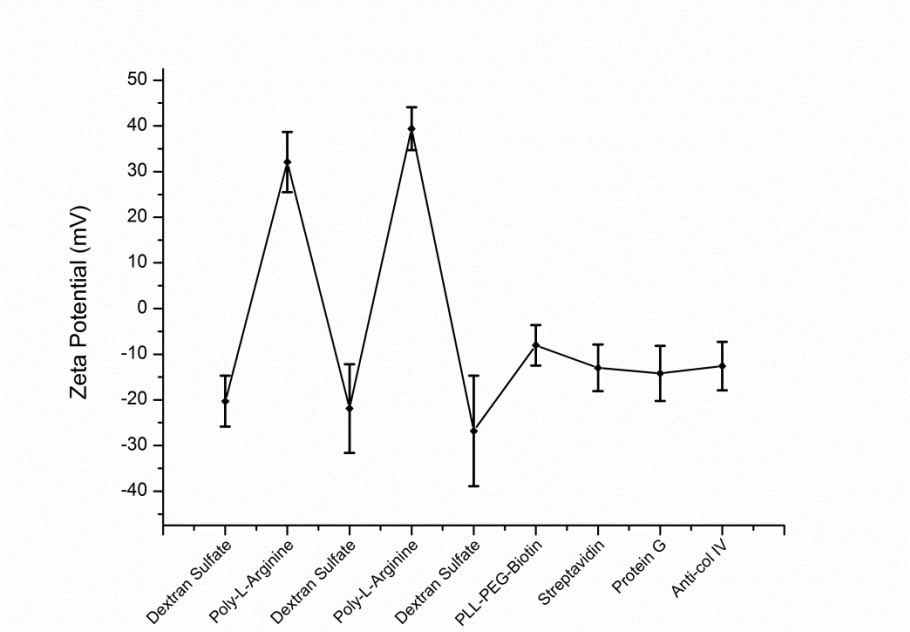

Figure 69. ζ-potential after each layer deposition. Error bars indicate the standard deviation (n = 30). All samples were measured in de-ionised water. Concentrations of polymer solutions: dextran sulfate and poly-L-arginine - 1 mg/ml, PLL-PEG-Biotin - 100 µg/ml, streptavidin – 100 µg/ml, protein G – 100 µg/ml, anti-collagen type IV – 100 µg/ml.

6.4.6 Biofunctionalised microcapsule protein adsorption assay

For control, microcapsules terminated with a dextran sulfate layer were introduced to 3 types of protein patterns. Results indicate that a high degree of non-specific binding of dextran sulfate-terminated microcapsules were present on all protein micro-patterns, as shown in Figure 70. The highest level of adsorption was noticed on the collagen type IV islands with an average RFI of 1572 RFU per island. Lower values of 232 RFU and 564 RFU were recorded from BSA and fibronectin islands respectively. When PEGylated and biofunctionalised with anti-collagen type IV, the microcapsules show preferential adsorption to the target protein, collagen type IV (652 RFU per island) and negligible binding to the control proteins (7 and 9 RFU for BSA and fibronectin respectively). Similar results can be seen when the microcapsules are functionalised with anti-fibronectin. Computed p values from the two-tailed t-tests for the anti-collagen type IV

functionalised microcapsules were 4.36×10^{-16} and 4.93×10^{-16} for collagen-BSA and collagen-fibronectin comparisons, respectively. Computed p values from t-tests performed on the anti-fibronectin functionalised microcapsules were 5.74×10^{-50} and 1.02×10^{-50} for tests between fibronectin and collagen type IV and fibronectin and BSA, respectively.

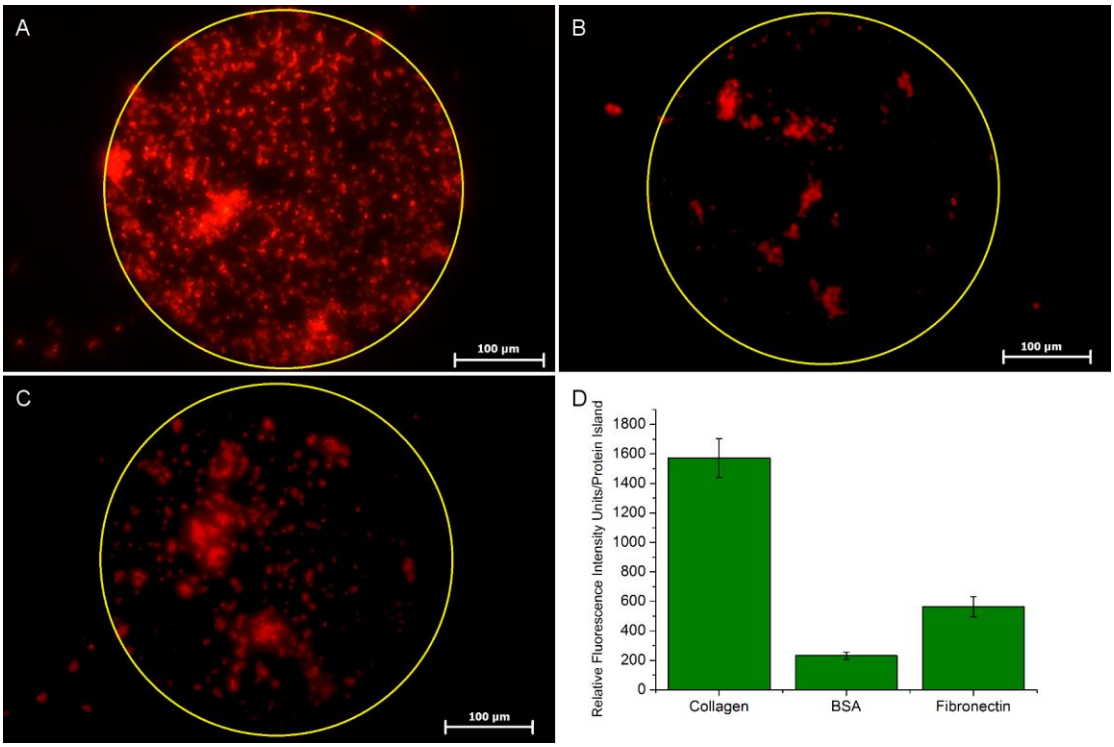

Figure 70. Typical images control microcapsules (terminated with dextran sulphate) on various protein coated islands: collagen type IV (Panel A), Bovine serum albumin (Panel B), fibronectin (Panel C). Images were taken after 3 dilution and three washing steps with PBS to remove non -adsorbed microcapsules. Panel D shows the relative fluorescence intensities recorded on each protein micropattern (n=25).

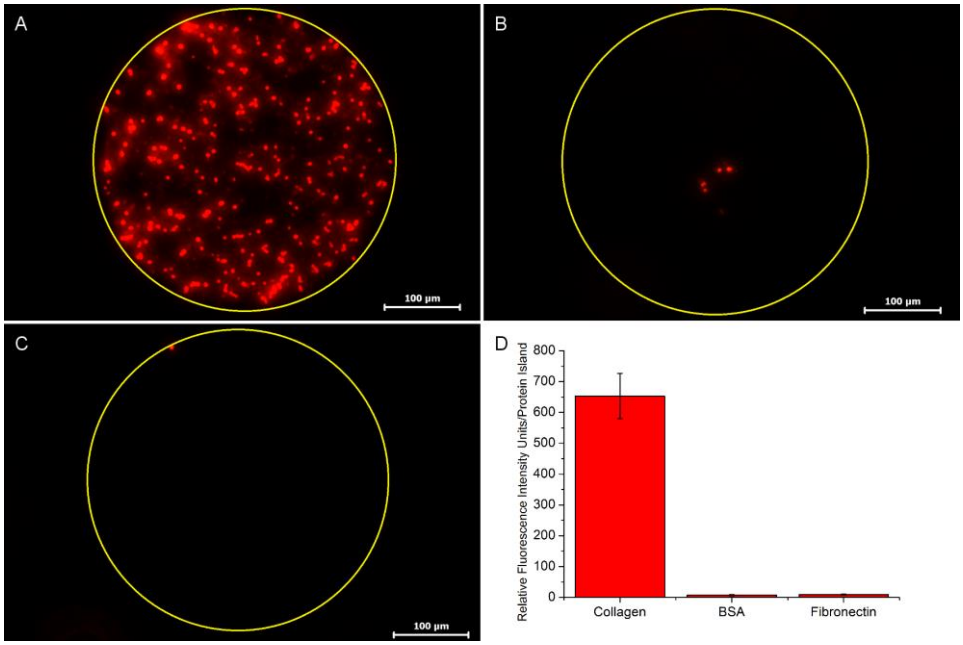

Figure 71. Typical images of Anti-collagen type IV terminated microcapsules on various protein coated islands: collagen type IV (Panel A),Bovine serum albumin (Panel B), fibronectin (Panel C). Images were taken after 3 dilution and three washing steps with PBS to remove non-adsorbed microcapsules. Panel D shows the relative fluorescence intensities recorded on each protein micropattern (n=25).

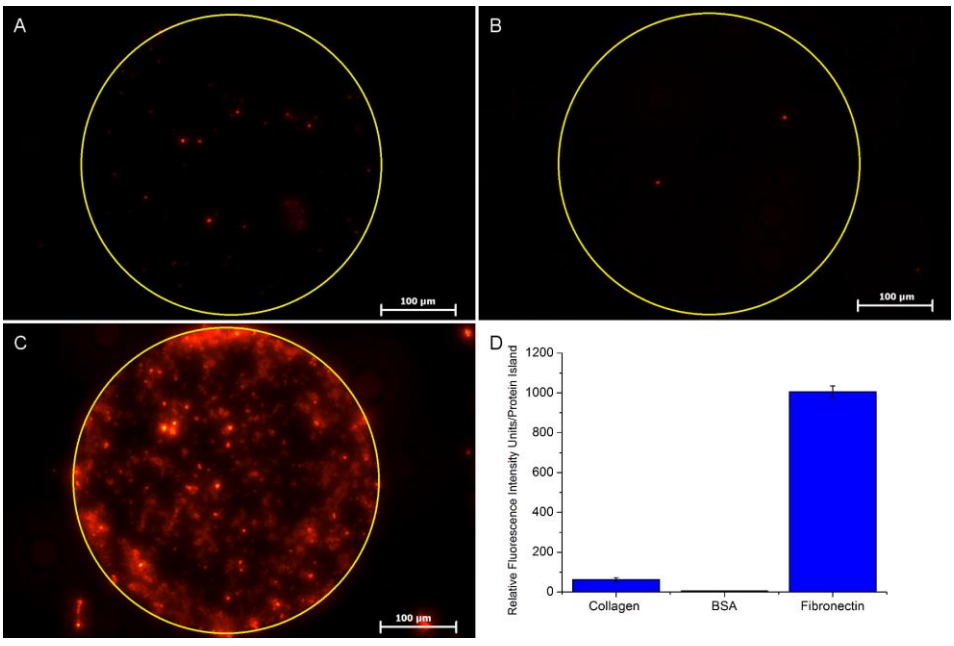

Figure 72. Typical images of Anti-fibronectin terminated microcapsules on various protein coated islands: collagen type IV (Panel A), Bovine serum albumin (Panel B), fibronectin (Panel C). Images were taken after 3 dilution and three washing steps with PBS to remove non-adsorbed microcapsules. Panel D shows the relative fluorescence intensities recorded on each protein micropattern (n=25).

6.5 Discussion

We hypothesise that by functionalising capsules with correctly orientated anti-collagen type IV, the capsules should display high binding affinity to collagen type IV surfaces, and furthermore, by incorporating a PEG layer on the periphery of the capsules, it should supress any form of unspecific binding to other proteins, giving rise to exclusive binding to the target protein. This hypothesis was tested in our study by applying these biofunctionalised microcapsules to micro-patterned substrates of collagen type IV, bovine serum albumin and fibronectin. The fluorescence recorded in Figure 66 illustrates the successful binding of CF 555-labelled anti-collagen IV onto the PEGylated/protein G-coated microcapsules, which suggests that the streptavidin-biotin complex is a viable means of conjugating protein G to the PEGylated surface of the microcapsules.

To complement this, zeta potential analysis was performed on the polymer coated calcium carbonate cores after each layer. It was necessary to keep the cores intact during analysis since the zeta potential technique is an optical technique which can only measure particles in suspension. As expected, the polyanionic and polycationic layers produced negative and positive zeta potential values, respectively. The average zeta potential of the PLL-PEG-biotin was -8.06mV. According to previously published data, this value should be approximately 0mV (Wattendorf et al., 2006, Wattendorf et al., 2008). Furthermore, the zeta potential is seldom recorded as a negative value, due to the positively charged grafted PLL. A possible reason for this could be the incomplete coverage of the underlying dextran sulfate. Regardless, the value is significantly increased from the zeta potential of the previous layer of dextran sulfate (-26.8mV), indicating that a significant quantity of PEG had been adsorbed to the surface. The remaining protein layers all

produced slightly negative zeta potential measurements, consistent with their respective isoelectric points (Aslan et al., 2007, Lindman et al., 2006). Collectively, this evidence strongly suggests that the layers were successfully tethered.

It is difficult to decipher from the SEM images whether there is a difference in the thickness or surface morphology of the microcapsules as the layers are added to the surface. Previous studies have shown a significant difference between substrates with 4 and 8 polyelectrolyte layers (Guo et al., 2009). With this in mind, one would expect to see a vast difference between the surface of capsules shown in Figure 68F and J since they are comprised of 5 and 9 layers respectively, most of which consist of large proteins. However, it is important to realise that in theory, only half of the surface is coated due to the surface being functionalised with 50% PEG and 50% PEG-biotin. This may have potentially led to the generation of a less coherent membrane. Upon observation, it appears that the surface of the microcapsules after the addition of antibody, is slightly thicker than the others samples, in particular, the dextran sulfate terminated sample Figure 68F, which only comprises of 5 polyelectrolyte layers.

The asymmetric increase in thickness between the first two polymers, as shown by the SPR data, is consistent with previous reports for polyelectrolyte mulitlayers (Ghostine et al., 2013). The level of streptavidin adsorption to the PLL-PEG-biotin was lower (46 ng/cm^2) than expected for monolayers. However, taking into consideration that only 50% of the PEG chains are biotinylated, sub-monolayers of streptavidin are expected to form. Indeed, previous reports have demonstrated that a densely packed monolayer of streptavidin has a much higher mass density of approximately 250 ng/cm^2 (Trmcic-

Cvitas et al., 2009). This result reflects the balance between binding to biotin molecules and repulsion from the protein resistant PEG side-chains. Protein G-biotin was adsorbed at a density of 18 ng/cm^2. The ratio of molecular weights between streptavidin and Protein G-biotin is 2.44. Hence the level of protein G immobilisation, being 2.5 times lower than that measured for streptavidin, implies a binding of one protein G molecule per streptavidin molecule, on average. Although streptavidin has 4 binding pockets for biotin, the 1:1 binding ratio observed could imply that other binding pockets are saturated by other biotin molecules in the PLL-PEG layer, or that the first bound protein G masks other binding pockets and prevents subsequent binding. The bound protein G is stably immobilised though, indicated by a negligible decrease after 5 min washing with buffer (<5 ng/cm^2).

A remarkable feature of the SPR graph, shown in Figure 67 is the high increase in signal corresponding to the anti-collagen type IV step. This large increase of 236 ng/cm^2 (after washing) can be explained by the high molecular weight of this antibody (170 kDa). Quartz crystal microbalance/dissipation methods have reported an IgG adsorption of approximately 700 ng/cm^2 for a similar antibody concentration to the one used in the present study (Zhou et al., 2004). Hence the adsorption that we report is in line with previous studies, the difference perhaps stemming from the sub-monolayer deposition that is achieved for protein G using PLL-PEG-biotin.

Micro-patterned substrates were chosen as they provide a surface containing many protein-coated islands with distinct boundaries. In addition to offering a clear visual representation, it allows many areas to be analysed on one sample, providing an efficient

way of collecting the data. All microcapsules were labelled by incorporating a single rhodamine B-poly-L-arginine layer within the LbL assembly. This allowed the retention to be quantified by measuring the total integrated fluorescence per protein island. Measurements were computed using Image J. This method provides an efficient way to calculate the microcapsule retention with sufficient accuracy.

To test the versatility of this model, anti-fibronectin was also tethered to the PEGylated microcapsules in a similar fashion. Analysis of the binding assay between the microcapsules functionalised with anti-collagen type IV and the collagen type IV protein pattern indicates that on all occasions, strong binding was present (Figure 71). More interestingly, these capsules refrain from adsorbing to the other proteins, suggesting that unspecific adsorption is supressed. All p values computed from the t-tests between the control and experimental groups of both types of biofunctionalised microcapsules are well below the $p \leq 0.001$ confidence threshold, indicating that the differences recorded between the groups are statistically very significant. As a reference, dextran sulfate-terminated microcapsules were tested against the 3 protein micro-patterns. As expected, unspecific adsorption was recorded in all cases, particularly with collagen type IV (Figure 70). On the other hand, fibronectin exhibited a much lower fluorescence intensity value, demonstrating a significantly lower adsorption of microcapsules to this protein. The isoelectric point of fibronectin has been reported to lie within 5.6-6.1 (Boughton and Simpson, 1984). Experiments were carried out at a $pH \approx 7.4$, therefore the protein is likely to have a negative net-charge, possibly leading to a repulsive force between itself and the microcapsules, thus explaining this decrease in microcapsule adsorption. A similar finding was made in a previous study which showed that microcapsules adsorb less readily to micro-patterned surfaces of a similar charge (Nolte and Fery, 2004). Despite

this, a 60 fold decrease in fluorescence intensity was recorded on the fibronectin patterns with biofuctionalised PEG microcapsules, suggesting that PEG is supressing this unspecific binding to a high degree. When comparing the collagen-coated islands shown in Figure 70 and Figure 71, it is clear that despite being functionalised to specifically adhere to collagen type IV, a reduction in microcapsule adsorption was noticed when compared to the control microcapsules, terminated with dextran sulfate (58.5% reduction). This could be attributed to the presence of PEG in the biofunctionalised microcapsules. Regardless, there is a significant difference when comparing the data from the target protein and the control proteins.

Anti-fibronectin microcapsules exclusively adhered to fibronectin micro-patterns, with minimal unspecific adsorption recorded on the control samples, as depicted in Figure 72. A limitation of this model is that the antibodies used may be prone to cross-reactivity with other proteins that possess similar antigen sequences (Arevalo et al., 1993). Another limitation of the current study is on the circulation time of these capsules *in-vivo*. We plan to carry out *ex-vivo* studies followed by *in-vivo* studies in the near future to address this issue.

It is believed that this biofunctionalisation protocol may be applied to both pre-loaded microcapsules (She et al., 2010b) and encapsulated drug particles (Pargaonkar et al., 2005), to provide site-specific controlled drug release. A study using microcapsules constructed of ten BSA protein layers, has shown that the microcapsules are still permeable to molecules of a lower molecular weight (Tong et al., 2008). The microcapsules used in this study comprise of 6 polymer layers and 3 protein layers and

hence should therefore provide an adequate release profile for low molecular weight drug molecules. The biofunctionalisation process is also unlikely to have an impact on the encapsulation efficiency due to the increase in sealing of microcapsules as more polymer/protein layers are applied (De Temmerman et al., 2011).

6.6 Conclusion

Polyelectrolyte microcapsules that incorporate a protein-resistant polymer (PEG), with approximately 50% of the surface functionalized with antibodies, have been successfully manufactured. By applying the microcapsules to various protein micropatterns, one has demonstrated that these microcapsules specifically and exclusively bind to their complementary target area. Furthermore, the model that has been developed for this study is versatile since similar results were noticed when a different antibody was used. This study allows for further research involving in vitro and in vivo experiments to analyze whether microcapsules can be used as targeted drug carriers.

7. Ex-vivo site-specific targeting of polyelectrolyte microcapsules

7.1 Introduction

The previous chapter clearly demonstrates that, with appropriate functionalisation, exclusive binding of polyelectrolytes can be achieved. Admittedly, the testing environment was artificial in nature, with the use of well-defined protein patterns. These capsules must be tested under more clinically relevant scenarios. *Ex-vivo* experiments allow the researcher to conduct experiments on tissues that have been removed from the body of an organism. This offers a more reliable and accurate model for experimental analysis, without the risk and ethical complications associated with *in-vivo* studies. This will provide an insight into how the specially designed biofunctionalised microcapsules will interact with the irregularities associated with biological tissues. The following pilot-study shall aim to accomplish this by means of epifluorescence microscopy of *ex-vivo* tissues.

Referring back to the arterial endothelial injury discussed in chapter one, we require a blood vessel that exhibits patches of endothelial denudation, where the basement membrane is exposed, as found in arteries that have undergone angioplasty procedures. *Ex-vivo* testing provides a platform by which one can test the effectiveness of the microcapsules within a biological setting, without encountering the risks associated with

in-vivo clinical trials. Various *ex-vivo* tests have been conducted using polyelectrolyte microcapsules.

A number of studies have reported techniques of achieving this type of wound *ex-vivo* with varying degrees of success. *Ex-vivo* wounds are typically inflicted while the vessel is either intact or open. Some studies have reported success simply by surgically scratching the luminal side on an open vessel with a scalpel blade (Darsaut et al., 2007). Another study achieved endothelial denudation by inserting a wire with a diameter of 70 microns which is slightly bigger than the mouse tail artery used (Bailey et al., 2007). The wire was passed in a retrograde proximal direction for a distance of up to 10mm and then was removed. Although successful endothelial denudation was achieved, the study does not comment on the integrity of the type IV collagen after the wire treatment.

Another study, that predates this one by more than 20 years, used an entirely different technique to achieve endothelial denudation. 30 years ago, a technique was established by which endothelial denudation was achieved without applying direct mechanical force to the endothelium (Guyton et al., 1984). The researchers had succeeded in removing the endothelium using a micro-bubble technique. Briefly, a passage of nitrogen bubbles was introduced into the lumen of an intact carotid artery. 2000 bubbles were declared sufficient for complete endothelial denudation. This method is significantly less mechanically invasive than the wire technique used in the aforementioned study. Indeed, it was reported that the basement membrane was not damaged after the technique was applied. The bubbles were generated by a pressurised tilting chamber and catheter. This method would be more favourable than physical scraping of the endothelium since it is

less mechanically invasive and less likely to damage the underlying basement membrane. Due to limited resources, this is not a viable means of endothelial denudation in the present study. Current research into the use of microcapsules in an *ex-vivo* scenario is scarce. The methodology of this study must address the important aspect of visualising the microcapsules once they have adhered to the sample. The best way to visualise what has adhered to the luminal surface is to make a longitudinal cut and open up the vessel to expose the endothelium. This involves a lot of delicate manipulation, and therefore can only be applied to larger blood vessels. For this reason, aortic sections shall be used in this study.

A limitation of this technique is that it is not fully reproducible and requires the technician to apply the same force to the sample each time the experiment is completed, which is virtually impossible. Injury to smaller blood vessels, such as the mouse femoral artery have been well-established by inserting an angioplasty guidewire into the lumen and physically shearing the endothelium, stripping the cells from the basement membrane (Roque et al., 2000). However, these vessels are simply too small (outer diameter approximately 250 μm) and delicate to handle and mount using conventional forceps. A number of trials were conducted on aortic samples that had been opened longitudinally in order to determine whether the reproducibility was sufficient enough. The main concern faced with this wound infliction technique is whether the wound would extend into the basement membrane and thus damage the collagen type IV, rendering the microcapsules dysfunctional. In order to assess whether the collagen was intact after the injury was inflicted, immunostaining was performed using an anti-collagen type IV primary antibody.

7.2 Materials

C57BL/6 mice (2-4 months old) were acquired from the James Black Centre at King's College London. Collagen type IV-functionalised microcapsules were prepared as described in chapter 6 (see chapter 6 for individual materials). Polyclonal Anti-Collagen IV antibody, produced in rabbit (cat. no. ab6586) was purchased from Abcam®. Monoclonal Anti-VE Cadherin antibody produced in rat was purchased from Abcam® (cat. no.ab91064). Alexa Fluor® 488 Goat Anti-Rat IgG (H+L) Antibody (cat. no. A-11006), Alexa Fluor® 594 Goat Anti-Rabbit IgG (H+L) Antibody (cat. no. A11012) and Alexa Fluor® 488 Goat Anti-Rabbit IgG (H+L) Antibody (cat. no. A11008) was purchased from Thermo Fisher Scientific Inc.VE-cadherin Antibody was (cat. no. sc-6458), Normal swine serum (diluted by 1:20 with PBS) (cat. no sc-2486). and Anti collagen IV antibody produced in rabbit (cat. no. sc-70246), goat anti-rabbit IgG-HRP (cat. no. sc-2030) was purchased from Santa Cruz Biotechnology Inc.

7.3 Method

Ex-vivo sample preparation

Mouse aortas were harvested from mice at Kings College London with help from experienced technicians. The aorta was carefully detached from the mouse body and all branches were severed. Excess fat surrounding the vessel was removed using forceps. This was to ensure that the samples would remain as flat as possible once mounted onto glass slides. At this stage, some samples were injured by squeezing the blood vessel gently to attempt to kill the endothelial cells and allow them to detach and be washed away.

Forceps clamp

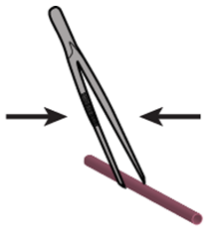

Figure 73. Schematic diagram depicting the forceps injury method, where the forceps were gently squeezed.

Before the longitudinal incision was made to open the vessel, a section (roughly around 2mm) of the aorta was compressed using forceps. The mechanical compression would serve to physically disrupt the endothelial cell membrane and cause cell death.

The aorta was then cut into sections (about 4mm in length) to provide multiple samples. Half of the samples were then cut open longitudinally and pinned down onto silicone rubber mounts with the endothelium facing upwards as illustrated by the schematic shown in Figure 74. The other half were put into Eppendorf tubes and washed inside the tube. For these samples, all procedures would take place inside the tubes. This was to determine whether results could also be obtained using a less time consuming method.

The remaining uninjured samples were then injured using the following techniques:

Needle scratch

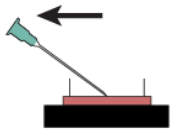

Figure 74. Schematic diagram depicting the needle scratch method.

A needle was gently scraped against the endothelial surface in a direction parallel to the long axis of the needle. It was hoped that this will provide a distinct region where the endothelial cells would be scraped off of the basement membrane.

Scalpel scrape

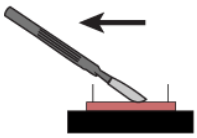

Figure 75. Schematic diagram depicting the scalpel scrape method.

A scalpel was scraped gingerly in a direction perpendicular to the long axis of the scalpel with the intention of removing a larger area of endothelium.

Once the samples were injured, they were washed thoroughly with PBS to remove any detached endothelial cells from the surface. Samples were subsequently fixed with formaldehyde for 15 minutes to preserve the sample during the adsorption assay. Previously prepared anti-collagen type IV biofunctionalised microcapsules (with a single PLL-FITC layer incorporated in the lbl structure) were then incubated onto the surface of the *ex-vivo* sections for 12 hours in a cold room at 4°C to preserve the integrity of the samples. Non-adsorbed microcapsules were subsequently washed by administering 3 dilution and 3 washing cycles, as described in section 6.3.4.

Endothelial cell verification

In order to differentiate between smooth muscle cells and endothelial cells, cell wall junctions were immunostained by using an appropriate anti-Vascular endothelial (VE) cadherin antibody. VE cadherins are calcium dependent cell adhesion proteins with many functional roles. Primarily, they serve as an intermolecular glue and therefore are located at the cell-cell junctions (Dejana et al., 1999). To highlight these junctions, samples were incubated with anti- vascular endothelial cadherin (CD144) antibody at a concentration of 1:200 PBS. After thoroughly washing, the *ex-vivo* sample was ready for secondary antibody labelling in order to detect the cell wall junction under fluorescence. Alexa Fluor 488-conjugated donkey anti-goat antibody was diluted from stock by a factor of 1:500, as indicated by the datasheet, and was applied to the sample and left for 45 minutes at room temperature. In order to determine the validity of the injury model and determine whether the collagen type IV was intact, anti-collagen type IV antibody, produced in rabbit, was incubated for 1 hour at room temperature at a dilution factor of 1:50. After thorough washing, a donkey anti-rabbit secondary antibody (conjugated with

Alexa Fluor 594 was incubated for 45 minutes at a dilution of 1:1000. Cell nuclei were stained with DAPI by incubating in DAPI solution for 5 minutes.

Immunohistochemistry verification of anti-collagen type IV antibody activity

In order to work out the optimal working dilution for the antibody, and to determine whether the antibody is able to bind successfully to the antigen present on the *ex-vivo* samples, cross sections of a mouse liver were prepared using a Microm HM 560 microtome-cryostat. Instead of using a conventional microtome, it was decided that a cryostat machine would be used instead since the traditional technique requires antigen retrieval treatment prior to the incubation of antibodies. Furthermore, the frozen sections can be kept at -20°C for long term storage.

The sample was fixed onto the specimen platform with embedding compound and the entire frozen liver sample was covered in embedding compound and placed on the freezing plate. Once frozen, the specimen was transferred to the specimen holder. The knife temperature was set to -21°C and the specimen temperature was set to -23°C. Colder temperatures were avoided to prevent the occurrence of cracks within the sample. 8µm thick cross sections were cut by rotating the handle and each section was transferred to a glass slide. After leaving the samples to air-dry for 20 minutes, they were stored at -20°C.

N.B. Prior to all primary antibody incubations, samples were blocked with goat normal serum at a recommended dilution (1:20). Furthermore, All dilutions were performed with

PBS. Dilution of the primary antibody with normal serum was considered, however, after previous testing, PBS was shown to deliver results which yielded minimal background signal.

Cross sections of an aorta from mice liver samples were then stained using immunofluorescence and immunohistochemistry techniques to determine whether the anti-collagen type IV has the ability to bind to collagen type IV in an *ex-vivo* environment (e.g. the basement membrane of the blood vessels in each cross section). Samples were allowed to dry for 5 minutes before fixing with ice-cold acetone for 8 minutes. The samples were thoroughly washed with PBS to remove the acetone. Immunofluorescence was performed as described in section 6.3.5, using polyclonal Anti-Collagen IV antibody, produced in rabbit primary antibody with Alexa Fluor® 488 Goat Anti-Rabbit IgG secondary antibody. The commonly implemented antigen retrieval step was not needed since the method of fixation with acetone increases tissue porosity and doesn't produce cross-links which would otherwise prevent the antibodies from interacting with the antigen (Pileri et al., 1997).

Immunohistochemistry was performed using a HRP-DAB kit. This technique differs from immunofluorescence in the sense that the secondary antibody is now conjugated with Horse radish peroxidase enzyme instead of a fluorophore. A substrate, cleavable by the HRP (DAB) is then applied to the sample, and areas, where the HRP has been tethered are stained brown due to the change in colour produced by the cleaved DAB.

Method: The frozen section was taken out of the freezer and left to dry for 5 minutes, before fixation via methanol. After 10 minutes of incubation, the methanol was thoroughly washed with PBS. The sample was then treated with 3% H_2o_2 for 15 minutes to destroy any endogenous enzymes that may cleave the DAB which would otherwise produce false staining. The sample was then blocked with normal swine serum for 45 minutes and subsequently incubated in primary antibody, which had been diluted in normal swine serum. After 24 hours at 4°C, the sample was washed 3 times, leaving the slides submerged in PBS for 5 minutes each time. The secondary antibody, conjugated with HRP was then diluted to the recommended dilution (1:50) and applied to the glass slides. After 1 hour of incubation at room temperature, excess secondary antibody was removed in a similar fashion to the primary antibody wash step. Finally, the DAB was applied to the sample and left for 2 minutes to allow the HRP to cleave the substrate and generate the stain. Excess DAB was washed off with PBS. Finally, counterstaining of the nucleus was achieved by hematoxylin treatment for 5 minutes. The excess dye was washed away with water and xylene before mounting.

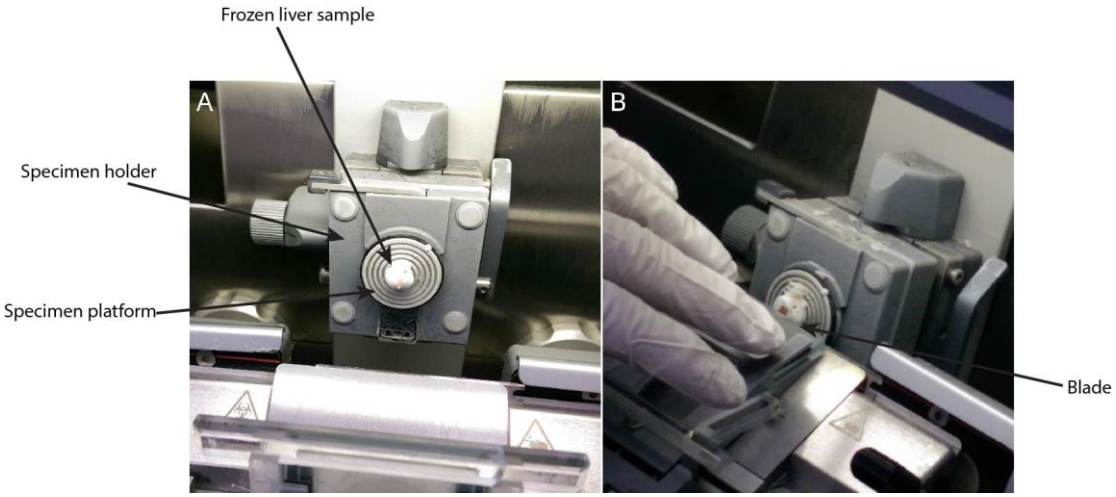

Figure 76. Photographs showing the frozen liver sample on the specimen platform (Panel A) and the specimen being sectioned (Panel B).

7.4 Results

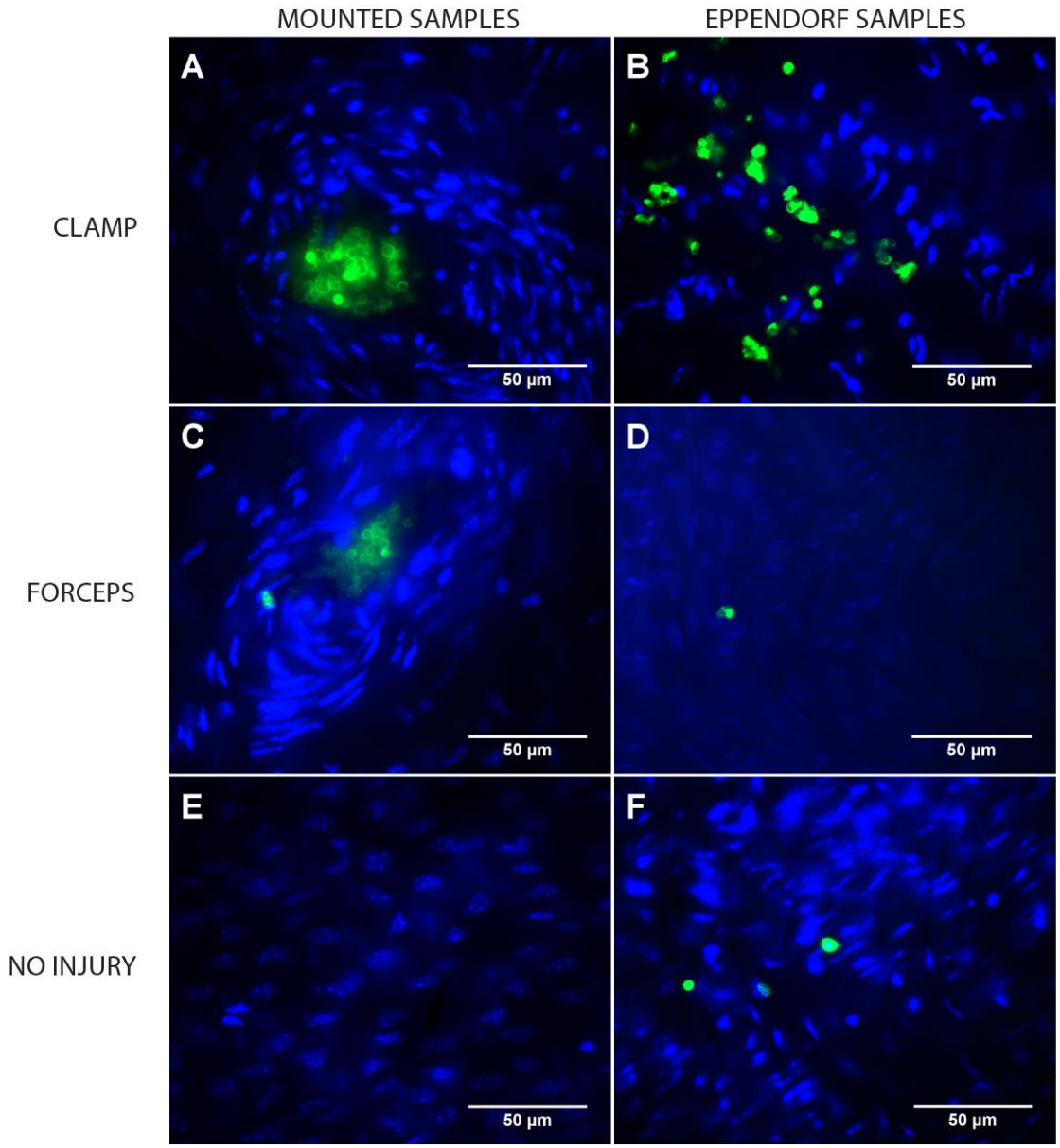

Figure 77. Fluorescent micrographs showing the retained microcapsules on the mouse aorta samples using different injury and incubation methods. Anti-collagen IV functionalised microcapsules are labelled with FITC (green fluorescence) and cell nuclei are labelled with DAPI (blue fluorescence).

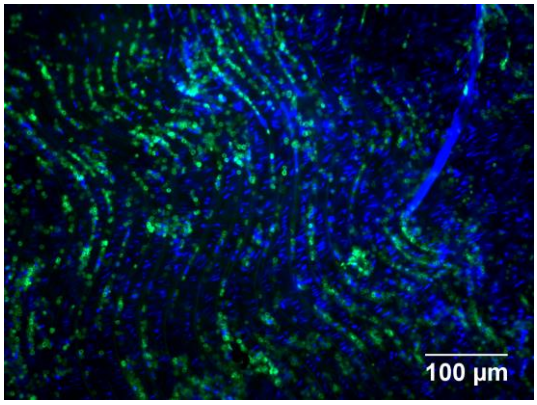

Figure 78. Control capsules (dextran sulfate-terminated) retained on an *ex-vivo* mouse aorta sample. Image shows a large degree of capsule adsorption (FITC labelled) due to the absence of PEG. Cell nuclei was stained with DAPI.

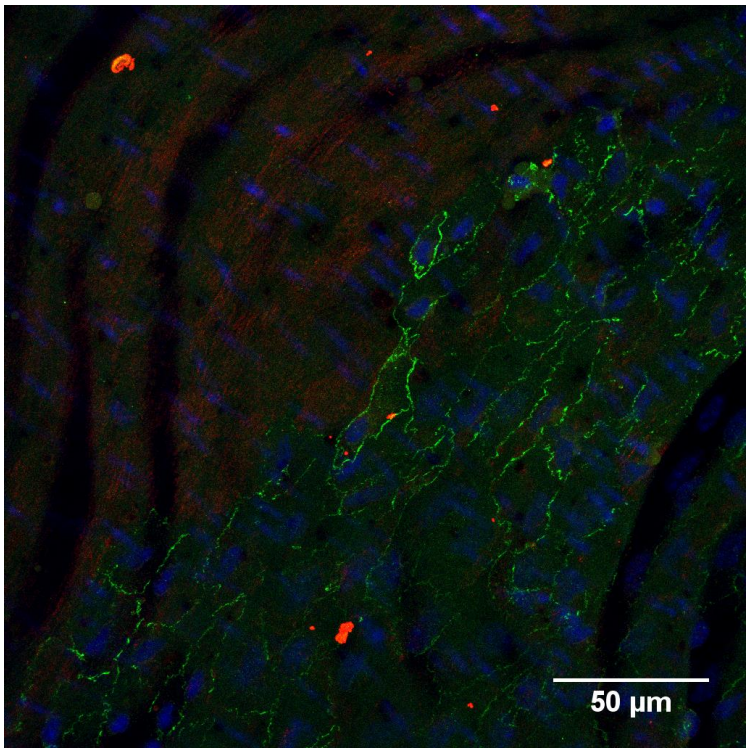

Figure 79. Confocal image of sample injured by scalpel scrape method. Collagen type IV was immunostained with Alexa Fluor 594-conjugated antibody (red fluorescence). Nuclei were stained with DAPI (blue). Endothelial cell-cell junctions were stained with anti-VE cadherin and a complementary FITC-labelled secondary antibody (green).

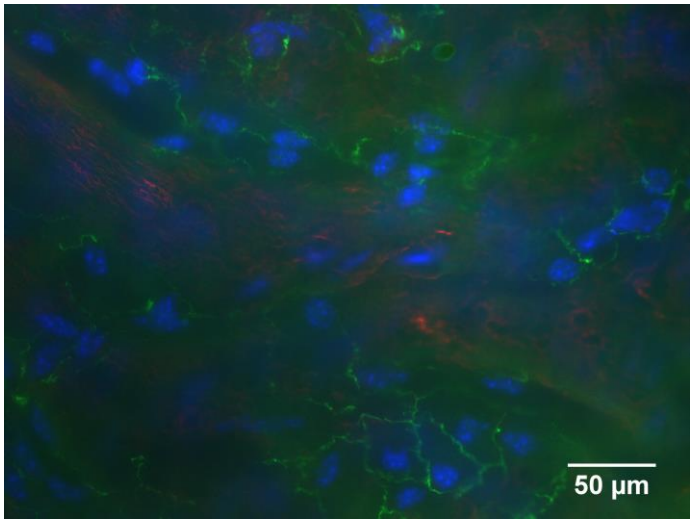

Figure 80. Epifluorescence image of sample injured by needle scratch method. Collagen type IV was immunostained with Fluor 594 conjugated antibody (red fluorescence). Nuclei were stained with DAPI (blue). Endothelial cell-cell junctions were stained with anti-VE cadherin and a complementary FITC-labelled secondary antibody (green).

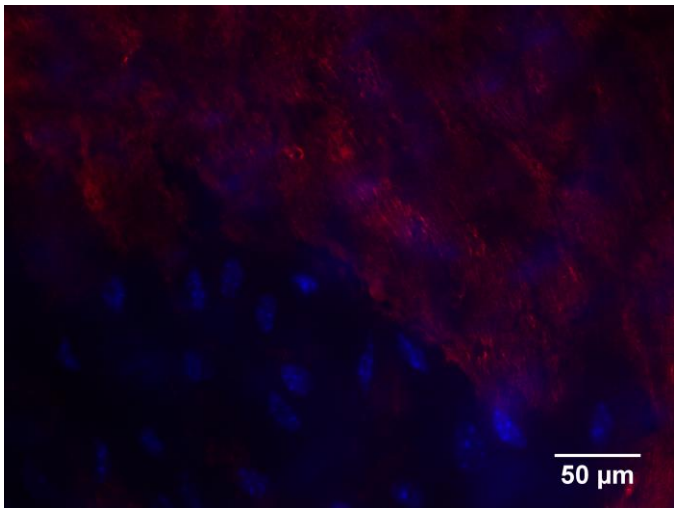

Figure 81. Epifluorescence image of sample injured by scalpel scrape method. Collagen type IV was immunostained with Alexa Fluor 594-conjugated antibody (red fluorescence). Nuclei were stained with DAPI (blue).

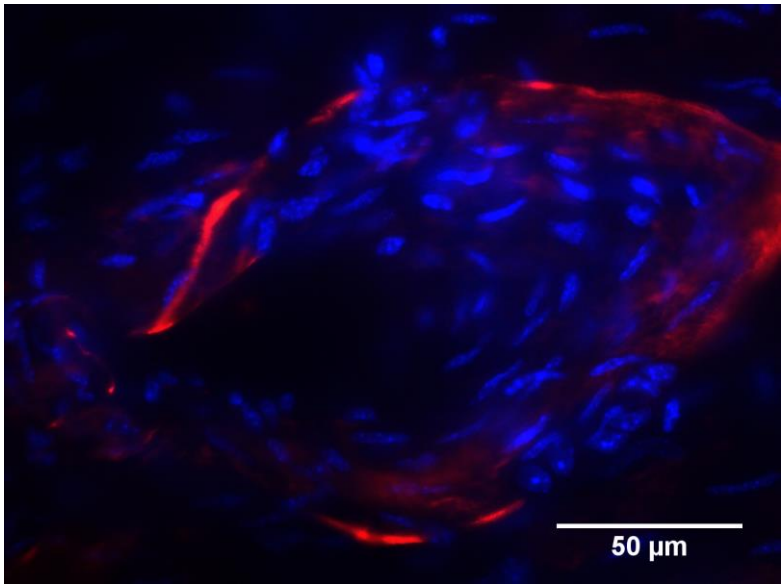

Figure 82. Epifluoresence image of an arteriole branch entrance. Sample was immunostained for collagen type IV (red). Cell Nuclei was stained with DAPI (blue).

7.5 Discussion

At first glance, the figures indicate that regions where the endothelium has been denuded are laden with biofunctionalised microcapsules, indicating that the microcapsules have successfully been adsorbed to the damage site. However, closer examination reveals that this is not the case. It is important to realise that the aorta is a branched vessel. For planar mounting of this vessel, the branches need to be severed. This leaves behind an orifice, which is noticeable, even to the naked eye. In reality, the region which is devoid of cells and covered with microcapsules, is one of these orifices as shown in Figure 77A and Figure 77C. It appears that the microcapsules have become physically entrapped and aggregated in this gap. More positively, the microcapsules refrain from adhering to the intact endothelial cells, indicating that the PEG is still exhibiting non-fouling properties, despite being functionalised indirectly with anti-collagen type IV. Further confirmation of the non-fouling properties can be seen from the incubation of the control capsules on the *ex-vivo* aorta specimens. These dextran sulfate-terminated capsules are non-

PEGylated and non-functionalised. Figure 78 clearly indicates that upon incubation for 24 hrs, followed by washing with PBS solution, many capsules remain adsorbed to the endothelium. This conclusively highlights the potency of the PEG functionalisation.

It is highly likely, that due to the nature of the injury methods used, the collagen type IV-rich basement membrane was likely to have been damaged during infliction. In order to test the integrity of the collagen type IV after injury, immunofluorescent staining was performed. As seen in Figure 81 there is a weak red signal, corresponding to the Alexa Fluor® 594 Goat Anti-Rabbit IgG secondary antibody. These signals were achieved using a relatively long exposure time of 2 seconds. It is likely that these were background signals from non-specifically adsorbed secondary antibody. This signal is also believed to have arisen due to the autofluorescence of vessel elastin, a protein which is found in abundance at this anatomical region. This uncertainty warranted an investigation into the reactivity of the rabbit anti-mouse collagen type IV primary antibody with the *ex-vivo* specimens. Intact mouse collagen type IV, believed to be present on a cross section of a proximal region of a mouse aorta was immunostained in a similar fashion.

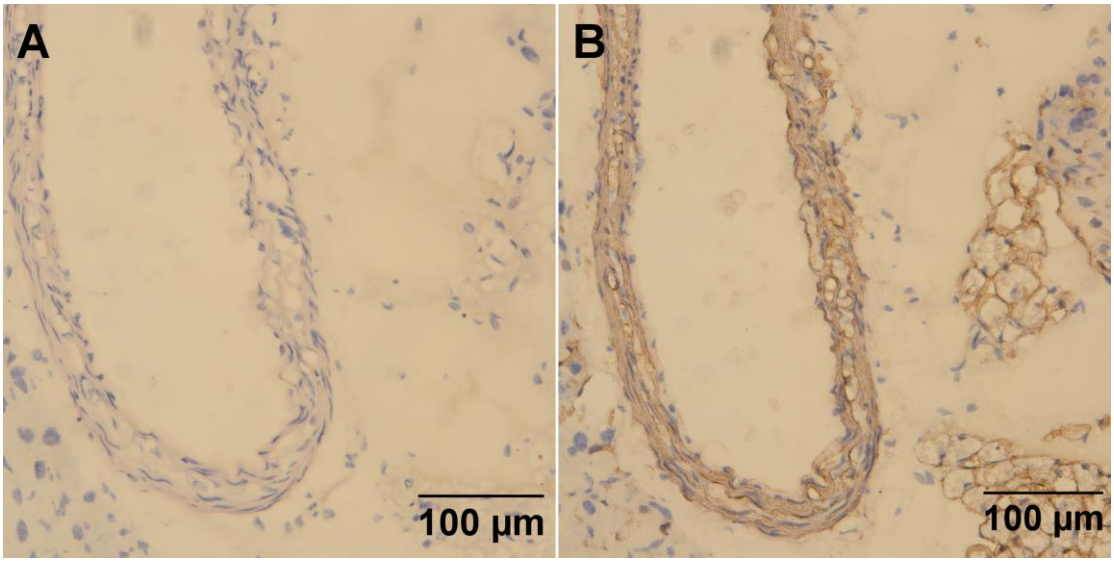

Figure 83. IHC analysis of cross section of a mouse aorta. Panel A shows the control sample without primary anti-collagen type IV and panel B shows a mouse aorta immunostained with anti-collagen type IV from Abcam (new sample).

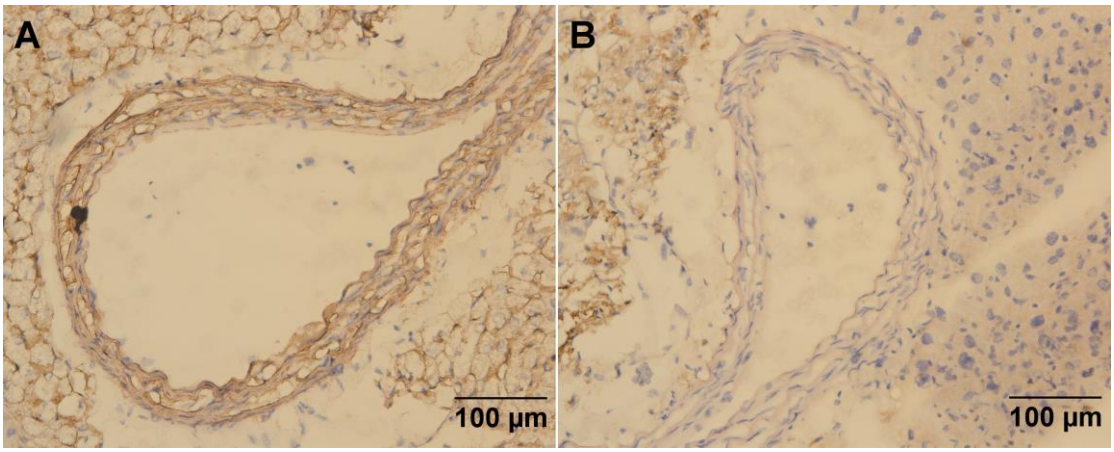

Figure 84. IHC analysis of cross section of a mouse aorta. Panel A shows the new abcam antibody and panel B shows a mouse aorta immunostained with anti-collagen type IV from Santa Cruz.

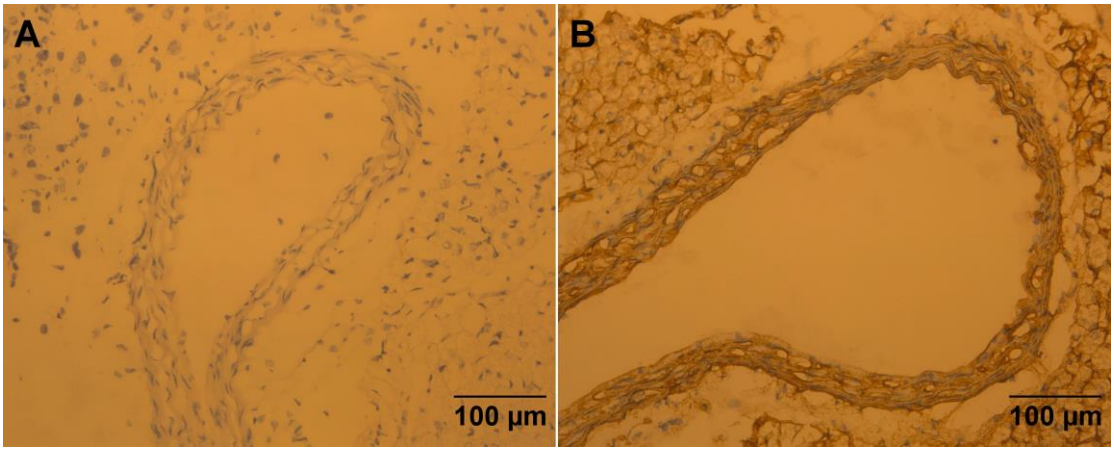

Figure 85. IHC analysis of cross section of a mouse arota Panel A shows the control sample without primary anti-collagen type IV and panel B shows a mouse aorta immunostained with fresh Abcam anti-collagen type IV.

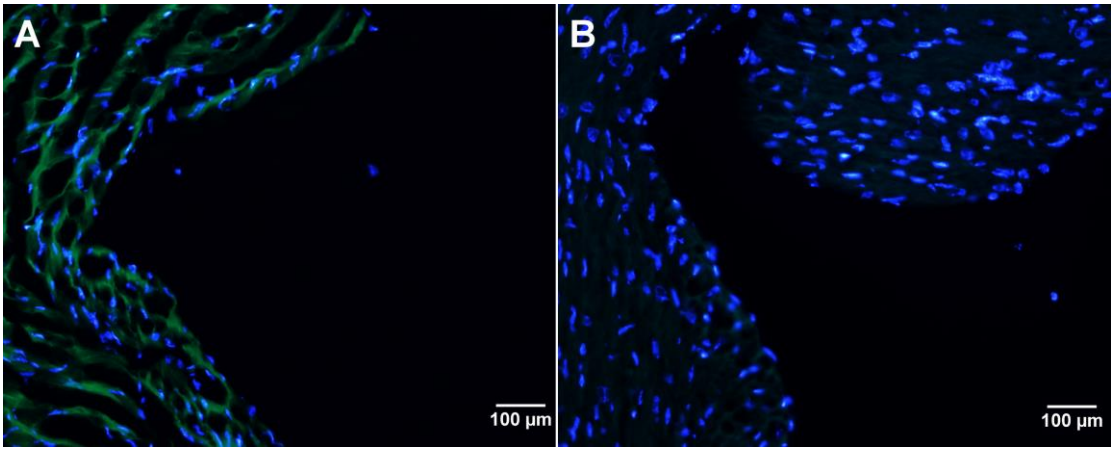

Figure 86. Epifluorescence analysis of cross section of a mouse aorta. Panel A shows the control sample without primary anti-collagen type IV and panel B shows a mouse aorta immunostained with fresh anti-collagen type IV from Abcam.

Results, as shown in Figure 86B indicate that no significant staining was present on all samples tested (n=6). Control samples (where no primary antibody was used) look virtually identical to samples that underwent full immunostaining, with one noticeable difference being a higher intensity of fluorescence on the control samples. It is important to realise that the images taken in Figure 86, are long exposure images of the green channel (1.7s). Despite this long exposure, the signals are still weak, further confirming that this is indeed a background signal, or potentially autofluorescence from elastin. The laser scanning confocal microscopy image shown in Figure 79 provides precise focus on the intimal region of the *ex-vivo* sample. This particular image shows the site of damage via the needle technique. The positive green staining at the cell-cell junctions corresponds to the Alexa Fluor® 488 Goat Anti-Rat IgG secondary antibody, which in turn, corresponds to the endothelial cell marker, anti-CD144 antibody, thus confirming the identity of these cells as endothelial cells.

Interestingly, immunohistochemistry anaylsis, performed on a mouse liver cross section containing three blood vessels, showed, significant background staining. It is important to realise that this background staining is different from the background staining noticed in the immunofluorescence images. Firstly, this technique is not prone to autofluoresence, so a pigment will only be present where secondary antibody, and consequently primary antibody has been tethered. Secondly, the intensity of the pigmented sections outside the blood vessel wall is relatively high. It was found that the intensity decreased with more washing cycles, however, the stain was never completely eliminated. This shows a significant degree of unspecific adsorption. In addition to the background staining, the entire blood vessel wall had been stained as oppose to exclusively staining the collagen type IV basement membrane. It may be the case that the antibody is cross reacting with other proteins on the sample. This is unlikely, since the samples were previously blocked with normal serum, in theory, eliminating cross-reactivity between non-target antigens and the antibody. To see if a more convincing result could be achieved, the experiment was repeated with a different anti-col IV antibody (Santa Cruz). Results indicated that no staining was present on the blood vessel wall and a weak background signal was present on all samples (n=6).

The immunostaining results of the cross section offers some evidence to suggest that the anti-collagen type IV antibody purchased from Abcam was able to adsorb to intact collagen type IV, but not exclusively. Taking this into consideration, it can be concluded that the anti-collagen type IV was unable to bind to the exposed collagen type IV of the basement membrane due to the fact that the collagen type IV was no longer intact. The shear force inflicted on the surface of the *ex-vivo* samples is likely to have mechanically damaged the collagen type IV, denaturing the antigen of the protein. This highlights the

main weakness of the antibody-functionalised microcapsules. That is, the system relies on the presence of an intact, non-denatured target protein.

A major limitation of this work, is the absence of a reliable and repeatable method of achieving endothelial denudation, while simultaneously protecting the underlying collagen type IV-rich basement membrane from mechanical damage. By applying the angioplasty guidewire technique and using a different sized diameter wire, this may have been feasible. This is not well-established and due to resource limitations, a larger angioplasty guidewire could not be acquired for this procedure.

Another potential method for endothelial denudation would be to freeze-thaw the luminal surface of an longitudinally opened aorta. Also known, as cryotherapy, this technique has been investigated as a potential method for tumor control. More recently, this method has been commercialised, highlighting the efficacy of this technique (Li et al., 2010). In essence, the subzero temperatures induce the formation of both intra and extracellular ice crystals, causing the cell membrane and organelles to rupture mechanically, ultimately leading to necrotic death (Mazur, 1963). In particular, when gradual freezing is applied to cells, the formation of extracellular ice leads to an increase in potential difference across the cell membrane. This causes water to be expelled from the cells leading to cell dehydration and ultimately cell death (Mazur et al., 1972). There has also been evidence that freezing can cause apoptosis (gene associated cell death) near the ice/cell interface (Baust and Gage, 2005).

A more recent study focused on the specific analysis of the mechanism by which ice crystals form intracellularly on human umbilical vein endothelial cells (Yang et al., 2009). In order to control the freezing and thawing rate, the cells were seeded on a coverslip and placed on a cryostage (freezing platform). The freezing of the cells were recorded via a CMOS high speed camera coupled to a microscope. In all cases, intracellular ice formation was initiated at the cell membrane closest to the nucleus. This is believed to occur due to the presence of a perpendicularly orientated area of water molecules adjacent to the phosphate lipid bilayer. This well-organised layer ultimately requires less energy for crystal nucleation, hence this region will always be the site of intracellular ice formation. After this initial ice crystal is formed, the ice dendrite then propagates into the nucleus itself, where the entire nucleus is frozen thereafter. Further freezing and thawing results in the rupture of these membrane and other membrane-bound organelles. Extracellular ice formation was reported to occur at -2.5°C, whereas intracellular ice formation initiates at -17.6°C. This study offers a vast amount of information regarding the mechanism behind endothelial cell cryotherapy, however, it only considers a monolayer of cells in an *in-vivo* environment rather than a three dimensional *ex-vivo* sample. It is unclear whether the underlying basement membrane will survive this treatment. It is a well-known fact that proteins are able to withstand a freeze/thaw cycle. However multiple freeze/thaw samples are known to denature proteins due to the changes in pH associated with proteins stored in phosphate buffers. The effects of this pH change can be suppressed by limiting the number of freeze/thaw cycles and increasing the freezing and thawing rate (Pikal-Cleland et al., 2000). One must also consider the thickness of the sample and the influence of the sub-zero temperatures on the underlying smooth muscle cells of the *ex-vivo* specimen. Should intracellular ice crystals form within the intimal region, smooth muscles cells will undoubtedly share the

same fate as the endothelial cells, hence the basement membrane will not be stably anchored to the specimen, leading to an undesirable injury model. Furthermore, the sample will have to be inverted before placed onto the cryostage to expose the endothelium to the cold surface. The freezing and thawing of the entire surface could lead to rupture of the sample. A more ideal solution would be to use a cryoprobe, similar to that used in the medical industry to concentrate the treatment to a small area.

7.6 Conclusion

In conclusion, the biodegradable microcapsules developed in chapter 6 did not function as expected in an *ex-vivo* environment. It would be wrong, however, to suggest that this result arose from a problem with the microcapsules themselves. The IHC and immunofluorescence analysis of *ex-vivo* cross sections indicated that the antibody, which was used to functionalise the microcapsules were cross-reacting with nearby tissues, rendering the functionalisation of these capsules purposeless. Furthermore, due to the lack of a repeatable damage model, it was impossible to test the microcapsules under controlled conditions. It is yet to be seen whether these biofunctionalised microcapsules would work in an *in-vivo* environment by adhering to the collagen type IV-rich basement membrane exposed due to angioplasty injury. More experimentation with different antibodies and a reliable injury model is required to provide a deeper insight into this matter. Regardless, a significant advancement has been made with respect to the exclusive protein targeting of polyelectrolyte microcapsules, as shown in chapter 6.

8. Summary

The initial work presented in this thesis has shown that self-degradable microcapsules can be successfully fabricated by encapsulating enzymes within layer-by-layer assembled polyelectrolyte microcapsules. More specifically, only one of the layer-by-layer constituents are required to be degradable by the encapsulated enzyme in order to produce noticeable capsule degradation and subsequent release of contents. The rate of release of the encapsulated contents can be controlled by increasing/decreasing the number of polyelectrolyte layers used. Furthermore, the rate of release can be altered by switching between biodegradable and non-biodegradable polyelectrolytes. 12 layer microcapsules are less affected by the relatively low concentration of proteinase within the capsules, with a release of less than 10% (at t = 24hrs) of the encapsulated proteinase recorded; hence both of these parameters must be set with precision in order to accurately control the rate of release.

Chapter 4 has successfully demonstrated that microcapsules can be functionalised to enhance cell binding using inexpensive biomaterials. This was achieved by functionalising basic PSS/PAH microcapsules with WGA. An average of 6 WGA-terminated microcapsules was recorded per endothelial cell with intact glycocalyces, showing a significant level of retention. The mechanism behind the interaction is unclear and further analysis of these microcapsules in an *in-vitro* environment is required. In addition, the site-specific targeting pilot tests conducted have shown that simple techniques can be used to target specific proteins. Furthermore, modifications can be made to polyelectrolyte microcapsules to increase or reduce binding to cells *in-vitro.*

However, these studies do not offer a definitive method for true specific binding to target proteins which includes the suppression to other proteins and cell membrane surfaces.

A system whereby microcapsules can be functionalised to specifically and exclusively bind to a streptavidin substrate has been developed, as shown in chapter 5. By preventing unspecific adsorptions via PEGylation and functionalising the capsules with biotin, the goal of producing a targeted microcapsule delivery technique has been accomplished. Results show at least a 9-fold increase in capsule retention when in contact with streptavidin, compared to control proteins. Furthermore, the capsules remain fully functional after 2 weeks, indicating good stability required for long-term use e.g. long-term therapy.

We have successfully manufactured microcapsules which incorporate a protein resistant polymer (PEG), with approximately 50% of the surface functionalised with antibodies, as demonstrated in chapter 6. By applying the microcapsules to various protein micro-patterns, we have demonstrated that these microcapsules specifically and exclusively bind to their complementary target area, with a 600 fold increase in microcapsule retention compared to control proteins. Furthermore, the model that has been developed for this study is versatile since similar results were noticed when a different antibody was used. This study allows for further research involving *in-vitro* and *in-vivo* experiments to analyse whether microcapsules can be used as a targeted drug-carriers.

8.1 Future work

In order to control the rate of release of proteinase from the self-degradable microcapsules fabricated in chapter 3, the experiments could be carried out at different temperatures. This would give a greater insight into the function of these capsules and would determine whether temperature plays a significant role in the rate of degradation and the subsequent release of contents. Indeed, the optimal working temperature range for proteinase is between 30°C and 40°C (Borodina et al., 2007). The all experiments were halted after a period of 24 hours since the rate of release remained relatively constant at this point in time. Furthermore, prolonging the experiments are likely to lead to an increase in proteinase adsorption to the Eppendorf tubes, thus resulting in false UV spectrophotometer readings. Glass tubes are known to have better non-fouling properties than polypropylene, hence by substituting the propylene tubes for glass tubes, proteinase release can be monitored over a longer period of time without proteinase-tube adsorption affecting the results.

With regard to site-specific delivery, PEG-biotin may be incorporated into microcapsules which are targeted towards more complex structures such as cell membranes. By functionalising PEG-biotinylated microcapsules with specific ligands that recognise a unique type of cell, one could potentially target specific cells, including cancer cells, thus providing a promising solution to cancer treatment.

References

2000. Water soluble multi-biotin-containing compounds. Google Patents.

2011a, Inflation of Balloon Inside a Coronary Artery, viewed 20/12/12, http://med.stanford.edu/stanfordhospital/images/greystone/heartCenter/images/ei_2253.gif

2011b, Tetramer of Avidin Binding the Biotin Ligands, viewed 12/10/2013, http://proteopedia.org/wiki/index.php/Molecular_Playground/Biotin_binding_avidin

ALBERTS, B., JOHNSON, A., LEWIS, J., WALTER, P., RAFF, M. & ROBERTS, K. 2002. *Molecular Biology of the Cell 4th Edition: International Student Edition*, Routledge.

ANAND, G., SHARMA, S., DUTTA, A. K., KUMAR, S. K. & BELFORT, G. 2010. Conformational transitions of adsorbed proteins on surfaces of varying polarity. *Langmuir,* 26**,** 10803-11.

ANGELATOS, A. S., RADT, B. & CARUSO, F. 2005. Light-responsive polyelectrolyte/gold nanoparticle microcapsules. *Journal of Physical Chemistry B,* 109**,** 3071-3076.

ANTIPINA, M. N., KIRYUKHIN, M. V., CHONG, K., LOW, H. Y. & SUKHORUKOV, G. B. 2009. Patterned microcontainers as novel functional elements for mu TAS and LOC. *Lab on a Chip,* 9**,** 1472-1475.

AREVALO, J. H., TAUSSIG, M. J. & WILSON, I. A. 1993. Molecular basis of crossreactivity and the limits of antibody–antigen complementarity. *Nature,* 365**,** 859-863.

ASLAN, F. M., YU, Y., VAJDA, S., MOHR, S. C. & CANTOR, C. R. 2007. Engineering a novel, stable dimeric streptavidin with lower isoelectric point. *Journal of Biotechnology,* 128**,** 213-225.

AUMAILLEY, M., BATTAGLIA, C., MAYER, U., REINHARDT, D., NISCHT, R., TIMPL, R. & FOX, J. W. 1993. Nidogen Mediates the Formation of Ternary Complexes of Basement-Membrane Components. *Kidney International,* 43**,** 7-12.

AZARMI, S., ROA, W. H. & LÖBENBERG, R. 2008. Targeted delivery of nanoparticles for the treatment of lung diseases. *Advanced Drug Delivery Reviews,* 60**,** 863-875.

AZZAM, T., ELIYAHU, H., SHAPIRA, L., LINIAL, M., BARENHOLZ, Y. & DOMB, A. J. 2002. Polysaccharide-oligoamine based conjugates for gene delivery. *Journal of medicinal chemistry,* 45**,** 1817-1824.

BAE, Y. M., OH, B. K., LEE, W., LEE, W. H. & CHOI, J. W. 2005. Study on orientation of immunoglobulin G on protein G layer. *Biosens Bioelectron,* 21**,** 103-10.

BAI, K. & WANG, W. 2012. Spatio-temporal development of the endothelial glycocalyx layer and its mechanical property in vitro. *Journal of The Royal Society Interface,* 9**,** 2290-2298.

BAILEY, S. R., MITRA, S., FLAVAHAN, S., BERGDALL, V. K. & FLAVAHAN, N. A. 2007. In vivo endothelial denudation disrupts smooth muscle caveolae and differentially impairs agonist-induced constriction in small arteries. *J Cardiovasc Pharmacol,* 49**,** 183-90.

BARENHOLZ, Y. 2001. Liposome application: problems and prospects. *Current Opinion in Colloid & Interface Science,* 6**,** 66-77.

BARKER, A. L., KONOPATSKAYA, O., NEAL, C. R., MACPHERSON, J. V., WHATMORE, J. L., WINLOVE, C. P., UNWIN, P. R. & SHORE, A. C. 2004. Observation and characterisation of the glycocalyx of viable human endothelial cells using confocal laser scanning microscopy. *Physical chemistry chemical physics,* 6**,** 1006-1011.

BARRETT, A. J., RAWLINGS, N. D. & WOESSNER, J. F. 2012. *Handbook of Proteolytic Enzymes,* Elsevier Science.

BAUST, J. G. & GAGE, A. A. 2005. The molecular basis of cryosurgery. *Bju International,* 95**,** 1187-1191.

BENHABBOUR, S. R., SHEARDOWN, H. & ADRONOV, A. 2008. Protein Resistance of PEG-Functionalized Dendronized Surfaces: Effect of PEG Molecular Weight and Dendron Generation. *Macromolecules,* 41**,** 4817-4823.

BORODINA, T., MARKVICHEVA, E., KUNIZHEV, S., MOEHWALD, H., SUKHORUKOV, G. B. & KREFT, O. 2007. Controlled release of DNA from self-degrading microcapsules. *Macromolecular Rapid Communications,* 28**,** 1894-1899.

BOUGHTON, B. J. 1985. Fibronectin assays and their clinical application: a review. *Cell Biochem Funct,* 3**,** 79-90.

BOUGHTON, B. J. & SIMPSON, A. 1982. Plasma fibronectin in acute leukaemia. *British journal of haematology,* 51**,** 487-91.

BOUGHTON, B. J., SIMPSON, A. & WHARTON, C. 1984. Conformational changes and loss of opsonic function in frozen or heat-treated plasma fibronectin. *Vox Sanguinis,* 46**,** 254-9.

BOUGHTON, B. J. & SIMPSON, A. W. 1984. The biochemical and functional heterogeneity of circulating human plasma fibronectin. *Biochem Biophys Res Commun,* 119**,** 1174-80.

CARREGAL-ROMERO, S., GUARDIA, P., YU, X., HARTMANN, R., PELLEGRINO, T. & PARAK, W. J. 2015. Magnetically triggered release of molecular cargo from iron oxide nanoparticle loaded microcapsules. *Nanoscale,* 7**,** 570-576.

CARUSO, F., TRAU, D., MÖHWALD, H. & RENNEBERG, R. 2000. Enzyme Encapsulation in Layer-by-Layer Engineered Polymer Multilayer Capsules. *Langmuir,* 16**,** 1485-1488.

CHAN, J. M., ZHANG, L., TONG, R., GHOSH, D., GAO, W., LIAO, G., YUET, K. P., GRAY, D., RHEE, J. W., CHENG, J., GOLOMB, G., LIBBY, P., LANGER, R. & FAROKHZAD, O. C. 2010. Spatiotemporal controlled delivery of nanoparticles to injured vasculature. *Proceedings of the National Academy of Sciences,* 107**,** 2213-2218.

CHANNON, K. M. 2002. The Endothelium and the Pathogenesis of Atherosclerosis. *Medicine,* 30**,** 54-58.

CHRISTOV, C. & KARABENCHEVA-CHRISTOVA, T. 2012. *Structural and Mechanistic Enzymology:: Bringing Together Experiments and Computing*, Elsevier Science.

CORTEZ, C., TOMASKOVIC-CROOK, E., JOHNSTON, A. P. R., RADT, B., CODY, S. H., SCOTT, A. M., NICE, E. C., HEATH, J. K. & CARUSO, F. 2006. Targeting and uptake of multilayered particles to colorectal cancer cells. *Advanced Materials,* 18**,** 1998-+.

CRUZ-CHU, EDUARDO R., MALAFEEV, A., PAJARSKAS, T., PIVKIN, IGOR V. & KOUMOUTSAKOS, P. 2014. Structure and Response to Flow of the Glycocalyx Layer. *Biophysical Journal,* 106**,** 232-243.

DARSAUT, T., BOUZEGHRANE, F., SALAZKIN, I., LEROUGE, S., SOULEZ, G., GEVRY, G. & RAYMOND, J. 2007. The effects of stenting and endothelial denudation on aneurysm and branch occlusion in experimental aneurysm models. *Journal of Vascular Surgery,* 45**,** 1228-1235.

DARZYNKIEWICZ, Z., ROBINSON, J. P. & ROEDERER, M. 2009. *Essential Cytometry Methods,* Elsevier Science.

DE GEEST, B. G., DE KOKER, S., SUKHORUKOV, G. B., KREFT, O., PARAK, W. J., SKIRTACH, A. G., DEMEESTER, J., DE SMEDT, S. C. & HENNINK, W. E. 2009a. Polyelectrolyte microcapsules for biomedical applications. *Soft Matter,* 5**,** 282-291.

DE GEEST, B. G., DE KOKER, S., SUKHORUKOV, G. B., KREFT, O., PARAK, W. J., SKIRTACH, A. G., DEMEESTER, J., DE SMEDT, S. C. & HENNINK, W. E. 2009b. Polyelectrolyte microcapsules for biomedical applications. *Soft Matter,* 5**,** 282.

DE GEEST, B. G., SANDERS, N. N., SUKHORUKOV, G. B., DEMEESTER, J. & DE SMEDT, S. C. 2007. Release mechanisms for polyelectrolyte capsules. *Chemical Society reviews,* 36**,** 636-49.

DE GEEST, B. G., VANDENBROUCKE, R. E., GUENTHER, A. M., SUKHORUKOV, G. B., HENNINK, W. E., SANDERS, N. N., DEMEESTER, J. & DE SMEDT, S. C. 2006. Intracellularly degradable polyelectrolyte microcapsules. *Advanced Materials,* 18**,** 1005-+.

DE KOKER, S., NAESSENS, T., DE GEEST, B. G., BOGAERT, P., DEMEESTER, J., DE SMEDT, S. & GROOTEN, J. 2010. Biodegradable polyelectrolyte microcapsules: antigen delivery tools with Th17 skewing activity after pulmonary delivery. *Journal of Immunology,* 184**,** 203-11.

DE TEMMERMAN, M. L., DEMEESTER, J., DE VOS, F. & DE SMEDT, S. C. 2011. Encapsulation Performance of Layer-by-Layer Microcapsules for Proteins. *Biomacromolecules,* 12**,** 1283-9.

DE GEEST, B. G., VANDENBROUCKE, R. E., GUENTHER, A. M., SUKHORUKOV, G. B., HENNINK, W. E., SANDERS, N. N., DEMEESTER, J. & DE SMEDT, S. C. 2006. Intracellularly Degradable Polyelectrolyte Microcapsules. *Advanced Materials,* 18**,** 1005-1009.

DE KOKER, S., DE GEEST, B. G., CUVELIER, C., FERDINANDE, L., DECKERS, W., HENNINK, W. E., DE SMEDT, S. C. & MERTENS, N. 2007. In vivo Cellular Uptake, Degradation, and Biocompatibility of Polyelectrolyte Microcapsules. *Advanced Functional Materials,* 17**,** 3754-3763.

DECHER, G. & SCHLENOFF, J. B. 2012. *Multilayer Thin Films: Sequential Assembly of Nanocomposite Materials,* Wiley.

DEJANA, E., BAZZONI, G. & LAMPUGNANI, M. G. 1999. Vascular endothelial (VE)-cadherin: only an intercellular glue? *Experimental cell research,* 252**,** 13-19.

DISPINAR, T., COLARD, C. A. L. & DU PREZ, F. E. 2013. Polyurea microcapsules with a photocleavable shell: UV-triggered release. *Polymer Chemistry,* 4**,** 763-772.

FARB, A., SANGIORGI, G., CARTER, A. J., WALLEY, V. M., EDWARDS, W. D., SCHWARTZ, R. S. & VIRMANI, R. 1999. Pathology of acute and chronic coronary stenting in humans. *Circulation,* 99**,** 44-52.

FARRELL, D., LIMAYE, S. Y. & SUBRAMANIAN, S. 2008. Silicon nanosponge particles. Google Patents.

FRIEDMAN, L., HIGGIN, J. J., MOULDER, G., BARSTEAD, R., RAINES, R. T. & KIMBLE, J. 2000. Prolyl 4-hydroxylase is required for viability and morphogenesis in Caenorhabditis elegans. *Proceedings of the National Academy of Sciences of the United States of America,* 97**,** 4736-4741.

GABIZON, A. A. 2001. Stealth Liposomes and Tumor Targeting: One Step Further in the Quest for the Magic Bullet. *Clinical Cancer Research,* 7**,** 223-225.

GAO, C., LEPORATTI, S., DONATH, E. & MÖHWALD, H. 2000. Surface texture of poly (styrenesulfonate sodium salt) and poly (diallyldimethylammonium chloride) micron-sized multilayer capsules: a scanning force and confocal microscopy study. *The Journal of Physical Chemistry B,* 104**,** 7144-7149.

GAUTROT, J. E., TRAPPMANN, B., OCEGUERA-YANEZ, F., CONNELLY, J., HE, X. M., WATT, F. M. & HUCK, W. T. S. 2010. Exploiting the superior protein resistance of polymer brushes to control single cell adhesion and polarisation at the micron scale. *Biomaterials,* 31**,** 5030-5041.

GE, S., KOJIO, K., TAKAHARA, A. & KAJIYAMA, T. 1998. Bovine serum albumin adsorption onto immobilized organotrichlorosilane surface: influence of the phase separation on protein adsorption patterns. *Journal of Biomaterials Science, Polymer Edition,* 9**,** 131-150.

GHOSTINE, R. A., MARKARIAN, M. Z. & SCHLENOFF, J. B. 2013. Asymmetric Growth in Polyelectrolyte Multilayers. *Journal of the American Chemical Society,* 135**,** 7636-7646.

GONZÁLEZ, M., BAGATOLLI, L. A., ECHABE, I., ARRONDO, J. L. R., ARGARAÑA, C. E., CANTOR, C. R. & FIDELIO, G. D. 1997. Interaction of Biotin with Streptavidin: THERMOSTABILITY AND CONFORMATIONAL CHANGES UPON BINDING. *Journal of Biological Chemistry,* 272**,** 11288-11294.

GRIMSLEY, G. R. & PACE, C. N. 2004. Spectrophotometric determination of protein concentration. *Current protocols in protein science***,** 3.1. 1-3.1. 9.

GUO, Y., GENG, W. & SUN, J. 2009. Layer-by-layer deposition of polyelectrolyte-polyelectrolyte complexes for multilayer film fabrication. *Langmuir,* 25**,** 1004-10.

GUYTON, J. R., DAO, D. T. & LINDSAY, K. L. 1984. Endothelial denudation and myointimal thickening in the rat carotid artery induced by the passage of bubbles. *Exp Mol Pathol,* 40**,** 340-8.

HALBLEIB, J. M. & NELSON, W. J. 2006. Cadherins in development: cell adhesion, sorting, and tissue morphogenesis. *Genes & development,* 20**,** 3199-3214.

HARNEK, J., ZOUCAS, E., CARLEMALM, E. & CWIKIEL, W. 1999. Differences in endothelial injury after balloon angioplasty, insertion of balloon-expanded stents or release of self-expanding stents: An electron microscopic experimental study. *Cardiovascular and interventional radiology,* 22**,** 56-61.

HAUTANEN, A., GAILIT, J., MANN, D. M. & RUOSLAHTI, E. 1989. Effects of modifications of the RGD sequence and its context on recognition by the fibronectin receptor. *Journal of Biological Chemistry,* 264**,** 1437-42.

HAYNIE, D. T., PALATH, N., LIU, Y., LI, B. & PARGAONKAR, N. 2005. Biomimetic Nanostructured Materials: Inherent Reversible Stabilization of Polypeptide Microcapsules. *Langmuir,* 21**,** 1136-1138.

HEUBERGER, M., DROBEK, T. & SPENCER, N. D. 2005a. Interaction forces and morphology of a protein-resistant poly(ethylene glycol) layer. *Biophys J,* 88**,** 495-504.

HEUBERGER, R., SUKHORUKOV, G., VOROS, J., TEXTOR, M. & MOHWALD, H. 2005b. Biofunctional polyelectrolyte multilayers and microcapsules: Control of non-specific and bio-specific protein adsorption. *Advanced Functional Materials,* 15**,** 357-366.

HORLITZ, M., SIGWART, U. & NIEBAUER, J. 2002. Fighting restenosis after coronary angioplasty: contemporary and future treatment options. *International Journal of Cardiology,* 83**,** 199-205.

HUDSON, B. G., REEDERS, S. T. & TRYGGVASON, K. 1993. Type-Iv Collagen - Structure, Gene Organization, and Role in Human-Diseases - Molecular-Basis of Goodpasture and Alport Syndromes and Diffuse Leiomyomatosis. *Journal of Biological Chemistry,* 268**,** 26033-26036.

IHRCKE, N. S., WRENSHALL, L. E., LINDMAN, B. J. & PLATT, J. L. 1993. Role of heparan sulfate in immune system-blood vessel interactions. *Immunology today,* 14**,** 500-505.

JANEWAY, C. 2001. *Immunobiology Five,* Garland Pub.

JOHANSSON, S., SVINENG, G., WENNERBERG, K., ARMULIK, A. & LOHIKANGAS, L. 1997. Fibronectin-integrin interactions. *Front Biosci,* 2**,** d126-46.

JONES, D. M., BROWN, A. A. & HUCK, W. T. S. 2002. Surface-initiated polymerizations in aqueous media: Effect of initiator density. *Langmuir,* 18**,** 1265-1269.

JULIANO, R. L., ALAM, R., DIXIT, V. & KANG, H. M. 2009. Cell-targeting and cell-penetrating peptides for delivery of therapeutic and imaging agents. *Wiley Interdisciplinary Reviews: Nanomedicine and Nanobiotechnology,* 1**,** 324-335.

JUNUTULA, J. R., RAAB, H., CLARK, S., BHAKTA, S., LEIPOLD, D. D., WEIR, S., CHEN, Y., SIMPSON, M., TSAI, S. P., DENNIS, M. S., LU, Y., MENG, Y. G., NG, C., YANG, J., LEE, C. C., DUENAS, E., GORRELL, J., KATTA, V., KIM, A., MCDORMAN, K., FLAGELLA, K., VENOOK, R., ROSS, S., SPENCER, S. D., LEE WONG, W., LOWMAN, H. B., VANDLEN, R., SLIWKOWSKI, M. X., SCHELLER, R. H., POLAKIS, P. & MALLET, W. 2008. Site-specific conjugation of a cytotoxic drug to an antibody improves the therapeutic index. *Nat Biotech,* 26**,** 925-932.

KALASIN, S. & SANTORE, M. M. 2009. Non-specific adhesion on biomaterial surfaces driven by small amounts of protein adsorption. *Colloids Surf B Biointerfaces,* 73**,** 229-36.

KALLURI, R. 2003. Basement membranes: structure, assembly and role in tumour angiogenesis. *Nat Rev Cancer,* 3**,** 422-433.

KARLSSON, M., EKEROTH, J., ELWING, H. & CARLSSON, U. 2005. Reduction of irreversible protein adsorption on solid surfaces by protein engineering for increased stability. *Journal of Biological Chemistry,* 280**,** 25558-25564.

KARSTEN, U., PAPSDORF, G., ROLOFF, G., STOLLEY, P., ABEL, H., WALTHER, I. & WEISS, H. 1985. Monoclonal anti-cytokeratin antibody from a hybridoma

clone generated by electrofusion. *European Journal of Cancer and Clinical Oncology,* 21**,** 733-740.

KAYITMAZER, A. B., SEEMAN, D., MINSKY, B. B., DUBIN, P. L. & XU, Y. S. 2013. Protein-polyelectrolyte interactions. *Soft Matter,* 9**,** 2553-2583.

KELLY, C., JEFFERIES, C. & CRYAN, S.-A. 2011. Targeted Liposomal Drug Delivery to Monocytes and Macrophages. *Journal of Drug Delivery,* 2011**,** 11.

KERDJOUDJ, H., BERTHELEMY, N., RINCKENBACH, S., KEARNEY-SCHWARTZ, A., MONTAGNE, K., SCHAAF, P., LACOLLEY, P., STOLTZ, J.-F., VOEGEL, J.-C. & MENU, P. 2008. Small Vessel Replacement by Human Umbilical Arteries With Polyelectrolyte Film-Treated Arteries: In Vivo Behavior. *Journal of the American College of Cardiology,* 52**,** 1589-1597.

KIVELA, A. & HARTIKAINEN, J. 2006. Restenosis related to percutaneous coronary intervention has been solved? *Annals of Medicine,* 38**,** 173-187.

KÖHLER, K., SHCHUKIN, D. G., SUKHORUKOV, G. B. & MÖHWALD, H. 2004. Drastic Morphological Modification of Polyelectrolyte Microcapsules Induced by High Temperature. *Macromolecules,* 37**,** 9546-9550.

KOLÁŘOVÁ, H., AMBRŮZOVÁ, B., ŠVIHÁLKOVÁ ŠINDLEROVÁ, L., KLINKE, A. & KUBALA, L. 2014. Modulation of Endothelial Glycocalyx Structure under Inflammatory Conditions. *Mediators of Inflammation,* 2014.

KOLIAKOS, G. G., KOUZIKOLIAKOS, K., FURCHT, L. T., REGER, L. A. & TSILIBARY, E. C. 1989. The Binding of Heparin to Type-Iv Collagen - Domain Specificity with Identification of Peptide Sequences from the Alpha-1(Iv) and Alpha-2(Iv) Which Preferentially Bind Heparin. *Journal of Biological Chemistry,* 264**,** 2313-2323.

KOUTSOUKOS, P., NORDE, W. & LYKLEMA, J. 1983. Protein adsorption on hematite (α-Fe< sub> 2</sub> O< sub> 3</sub>) surfaces. *Journal of Colloid and Interface Science,* 95**,** 385-397.

KREFT, O., JAVIER, A. M., SUKHORUKOV, G. B. & PARAK, W. J. 2007. Polymer microcapsules as mobile local pH-sensors. *Journal of Materials Chemistry,* 17**,** 4471-4476.

KUNKEL, E. J. & LEY, K. 1996. Distinct Phenotype of E-Selectin–Deficient Mice E-Selectin Is Required for Slow Leukocyte Rolling In Vivo. *Circulation Research,* 79**,** 1196-1204.

KURKI, P., KARJALAINEN, J., HAUTANEN, A. & VIRTANEN, I. 1989. Desmin antibodies in acute infectious myopericarditis. *APMIS,* 97**,** 527-32.

LAUNES, J. & HAUTANEN, A. 1988. Nephropathia epidemica encephalitis. *Acta Neurol Scand,* 78**,** 234-5.

LEINONEN, A. 1999. *Human type IV collagen: characterization of primary structures of alpha3(IV) and alpha4(IV) chains, structure of COL4A5 gene, and expression of recombinant alpha3(IV) chain,* Oulun yliopisto.

LEPORATTI, S., GAO, C., VOIGT, A., DONATH, E. & MOHWALD, H. 2001. Shrinking of ultrathin polyelectrolyte multilayer capsules upon annealing: A confocal laser scanning microscopy and scanning force microscopy study. *European Physical Journal E,* 5**,** 13-20.

LI, Y., WANG, F. & WANG, H. 2010. Cell death along single microfluidic channel after freeze-thaw treatments. *Biomicrofluidics,* 4**,** 014111.

LIEDBERG, B., LUNDSTROM, I. & STENBERG, E. 1993. Principles of Biosensing with an Extended Coupling Matrix and Surface-Plasmon Resonance. *Sensors and Actuators B-Chemical,* 11**,** 63-72.

LINDMAN, S., XUE, W. F., SZCZEPANKIEWICZ, O., BAUER, M. C., NILSSON, H. & LINSE, S. 2006. Salting the Charged Surface: pH and Salt Dependence of Protein G B1 Stability. *Biophys J,* 90**,** 2911-21.

LIU, W., WANG, X., BAI, K., LIN, M., SUKHORUKOV, G. & WANG, W. 2014. *Microcapsules functionalized with neuraminidase can enter vascular endothelial cells in vitro*.

LOUGHNEY, J. W., LANCASTER, C., HA, S. & RUSTANDI, R. R. 2014. Residual bovine serum albumin (BSA) quantitation in vaccines using automated Capillary Western technology. *Analytical biochemistry*.

LOWE, H. C., CHESTERMAN, C. N. & KHACHIGIAN, L. M. 2001. Does thrombus contribute to in-stent restenosis in the porcine coronary stent model? *Thromb Haemost,* 85**,** 1117-8.

LV, H., ZHANG, S., WANG, B., CUI, S. & YAN, J. 2006. Toxicity of cationic lipids and cationic polymers in gene delivery. *Journal of Controlled Release,* 114**,** 100-109.

LVOV, Y., ARIGA, K., ICHINOSE, I. & KUNITAKE, T. 1995. Assembly of Multicomponent Protein Films by Means of Electrostatic Layer-by-Layer Adsorption. *Journal of the American Chemical Society,* 117**,** 6117-6123.

MANISH, G. & VIMUKTA, S. 2011. Targeted drug delivery system: A Review. *Research Journal of Chemical Sciences*_____*Vol,* 1**,** 2.

MANJU, S. & SREENIVASAN, K. 2011. Hollow microcapsules built by layer by layer assembly for the encapsulation and sustained release of curcumin. *Colloids and Surfaces B-Biointerfaces,* 82**,** 588-593.

MAZUR, P. 1963. Kinetics of water loss from cells at subzero temperatures and the likelihood of intracellular freezing. *The Journal of General Physiology,* 47**,** 347-369.

MAZUR, P., LEIBO, S. & CHU, E. 1972. A two-factor hypothesis of freezing injury: evidence from Chinese hamster tissue-culture cells. *Experimental cell research,* 71**,** 345-355.

MEDINA, O. P., ZHU, Y. & KAIREMO, K. 2004. Targeted liposomal drug delivery in cancer. *Curr Pharm Des,* 10**,** 2981-9.

MERMUT, O., LEFEBVRE, J., GRAY, D. G. & BARRETT, C. J. 2003. Structural and Mechanical Properties of Polyelectrolyte Multilayer Films Studied by AFM. *Macromolecules,* 36**,** 8819-8824.

MICHEL, M., TONIAZZO, V., RUCH, D. & BALL, V. 2012. Deposition Mechanisms in Layer-by-Layer or Step-by-Step Deposition Methods: From Elastic and Impermeable Films to Soft Membranes with Ion Exchange Properties. *ISRN Materials Science,* 2012**,** 13.

MÜLLER, M., VÖRÖS, J., CSUCS, G., WALTER, E., DANUSER, G., MERKLE, H., SPENCER, N. & TEXTOR, M. 2003. Surface modification of PLGA microspheres. *Journal of Biomedical Materials Research Part A,* 66**,** 55-61.

NAGATA, Y. & BURGER, M. M. 1972. Wheat germ agglutinin isolation and crystallization. *Journal of Biological Chemistry,* 247**,** 2248-2250.

NOLTE, M. & FERY, A. 2004. Coupling of individual polyelectrolyte capsules onto patterned substrates. *Langmuir,* 20**,** 2995-2998.

PAHAKIS, M. Y., KOSKY, J. R., DULL, R. O. & TARBELL, J. M. 2007. The role of endothelial glycocalyx components in mechanotransduction of fluid shear stress. *Biochemical and Biophysical Research Communications,* 355**,** 228-233.

PALAMÀ, I. E., LEPORATTI, S., LUCA, E. D., RENZO, N. D., MAFFIA, M., GAMBACORTI-PASSERINI, C., RINALDI, R., GIGLI, G., CINGOLANI, R. & COLUCCIA, A. M. 2010. Imatinib-loaded polyelectrolyte microcapsules for sustained targeting of BCR-ABL+ leukemia stem cells. *Nanomedicine,* 5**,** 419-431.

PARGAONKAR, N., LVOV, Y. M., LI, N., STEENEKAMP, J. H. & DE VILLIERS, M. M. 2005. Controlled release of dexamethasone from microcapsules produced by polyelectrolyte layer-by-layer nanoassembly. *Pharm Res,* 22**,** 826-35.

PASTORINO, L., EROKHINA, S., SOUMETZ, F. C., BIANCHINI, P., KONOVALOV, O., DIASPRO, A., RUGGIERO, C. & EROKHIN, V. 2011. Collagen containing microcapsules: smart containers for disease controlled therapy. *J Colloid Interface Sci,* 357**,** 56-62.

PATEL, E. & OSWAL, R. 2012. Nanosponge and micro sponges: a novel drug delivery system. *Int J Research Pharmacy Chemistry,* 2**,** 237-44.

PATEL, H. 1991. Serum opsonins and liposomes: Their interaction and opsonophagocytosis. *Critical reviews in therapeutic drug carrier systems,* 9**,** 39-90.

PETERS, B. P., EBISU, S., GOLDSTEIN, I. J. & FLASHNER, M. 1979. Interaction of wheat germ agglutinin with sialic acid. *Biochemistry,* 18**,** 5505-5511.

PEYRATOUT, C. S. & DÄHNE, L. 2004. Tailor-Made Polyelectrolyte Microcapsules: From Multilayers to Smart Containers. *Angewandte Chemie International Edition,* 43**,** 3762-3783.

PHIPPS, R. P. 2000. Atherosclerosis: the emerging role of inflammation and the CD40-CD40 ligand system. *Proc Natl Acad Sci U S A,* 97**,** 6930-2.

PIERSCHBACHER, M. D. & RUOSLAHTI, E. 1987. Influence of stereochemistry of the sequence Arg-Gly-Asp-Xaa on binding specificity in cell adhesion. *Journal of Biological Chemistry,* 262**,** 17294-8.

PIKAL-CLELAND, K. A., RODRIGUEZ-HORNEDO, N., AMIDON, G. L. & CARPENTER, J. F. 2000. Protein denaturation during freezing and thawing in phosphate buffer systems: monomeric and tetrameric beta-galactosidase. *Archives of Biochemistry and Biophysics,* 384**,** 398-406.

PILERI, S. A., RONCADOR, G., CECCARELLI, C., PICCIOLI, M., BRISKOMATIS, A., SABATTINI, E., ASCANI, S., SANTINI, D., PICCALUGA, P. P. & LEONE, O. 1997. Antigen retrieval techniques in immunohistochemistry: comparison of different methods. *The Journal of pathology,* 183**,** 116-123.

POTIER, P., DREVET, P., GOUNOT, A.-M. & HIPKISS, A. R. 1990. Temperature-dependent changes in proteolytic activities and protein composition in the psychrotrophic bacterium Arthrobacter globiformis S155. *Journal of general microbiology,* 136**,** 283-291.

PRESCOTT, M. F., SAWYER, W. K., VON LINDEN-REED, J., JEUNE, M., CHOU, M., CAPLAN, S. L. & JENG, A. Y. 1999. Effect of matrix metalloproteinase inhibition on progression of atherosclerosis and aneurysm in LDL receptor-deficient mice overexpressing MMP-3, MMP-12, and MMP-13 and on restenosis in rats after balloon injury. *Annals of the New York Academy of Sciences,* 878**,** 179-90.

QIAN, J., XU, B., CHEN, J. L., YANG, Y. J., QIAO, S. B., LI, J. J., QIN, X. W., YAO, M., LIU, H. B., WU, Y. J., YUAN, J. Q., CHEN, J., YOU, S. J., DAI, J. & GAO, R. L. 2009. Persistent Inhibition of Neointimal Hyperplasia after Firebird2

Sirolimus-Eluting Stent Implantation Long-Term (Up to 3 Years) Clinical Follow-Up a Single Center Experience. *Cardiology,* 114**,** 1-1.

RADT, B., SMITH, T. A. & CARUSO, F. 2004. Optically addressable nanostructured capsules. *Advanced Materials,* 16**,** 2184-+.

RAGNETTI, M. & OBERTHÜR, R. C. 1986. Conformation of a chain polyelectrolyte in solution with low molecular weight salt: small angle neutron scattering measurements. *Colloid and Polymer Science,* 264**,** 32-45.

ROQUE, M., FALLON, J. T., BADIMON, J. J., ZHANG, W. X., TAUBMAN, M. B. & REIS, E. D. 2000. Mouse model of femoral artery denudation injury associated with the rapid accumulation of adhesion molecules on the luminal surface and recruitment of neutrophils. *Arterioscler Thromb Vasc Biol,* 20**,** 335-42.

RUOSLAHTI, E. 1991. Integrins. *Journal of Clinical Investigation,* 87**,** 1.

RUOSLAHTI, E. 1996. RGD and other recognition sequences for integrins. *Annu Rev Cell Dev Biol,* 12**,** 697-715.

SAH, H., TODDYWALA, R. & CHIEN, Y. W. 1995. Continuous Release of Proteins from Biodegradable Microcapsules and in-Vivo Evaluation of Their Potential as a Vaccine Adjuvant. *Journal of Controlled Release,* 35**,** 137-144.

SAHA, K., BENDER, F. & GIZELI, E. 2003. Comparative study of IgG binding to proteins G and A: nonequilibrium kinetic and binding constant determination with the acoustic waveguide device. *Analytical Chemistry,* 75**,** 835-42.

SALMON, A. H., FERGUSON, J. K., BURFORD, J. L., GEVORGYAN, H., NAKANO, D., HARPER, S. J., BATES, D. O. & PETI-PETERDI, J. 2012. Loss of the endothelial glycocalyx links albuminuria and vascular dysfunction. *Journal of the American Society of Nephrology,* 23**,** 1339-1350.

SANTOS, J. L., NOURI, A., FERNANDES, T., RODRIGUES, J. & TOMAS, H. 2012. Gene delivery using biodegradable polyelectrolyte microcapsules prepared through the layer-by-layer technique. *Biotechnol Prog,* 28**,** 1088-94.

SATO, K., YOSHIDA, K., TAKAHASHI, S. & ANZAI, J.-I. 2011. pH- and sugar-sensitive layer-by-layer films and microcapsules for drug delivery. *Advanced Drug Delivery Reviews,* 63**,** 809-821.

SAURER, E. M., FLESSNER, R. M., BUCK, M. E. & LYNN, D. M. 2011. Fabrication of Covalently Crosslinked and Amine-Reactive Microcapsules by Reactive Layer-by-Layer Assembly of Azlactone-Containing Polymer Multilayers on Sacrificial Microparticle Templates. *Journal of Materials Chemistry,* 21**,** 1736-1745.

SCHAEFFER, H., BREITFELLER, J. & KROHN, D. 1982. Lectin-mediated attachment of liposomes to cornea: influence on transcorneal drug flux. *Investigative Ophthalmology & Visual Science,* 23**,** 530-533.

SCHWEFEL, D., MAIERHOFER, C., BECK, J. G., SEEBERGER, S., DIEDERICHS, K., MÖLLER, H. M., WELTE, W. & WITTMANN, V. 2010. Structural basis of multivalent binding to wheat germ agglutinin. *Journal of the American Chemical Society,* 132**,** 8704-8719.

SHAH, G. 1998. Why do we still use serum in the production of biopharmaceuticals? *Developments in biological standardization,* 99**,** 17-22.

SHE, Z., ANTIPINA, M. N., LI, J. & SUKHORUKOV, G. B. 2010a. Mechanism of Protein Release from Polyelectrolyte Multilayer Microcapsules. *Biomacromolecules,* 11**,** 1241-1247.

SHE, Z., ANTIPINA, M. N., LI, J. & SUKHORUKOV, G. B. 2010b. Mechanism of protein release from polyelectrolyte multilayer microcapsules. *Biomacromolecules,* 11**,** 1241-7.

SHRINGIRISHI, M., PRAJAPATI, S. K., MAHOR, A., ALOK, S., YADAV, P. & VERMA, A. Nanosponges: a potential nanocarrier for novel drug delivery-a review.

SINGH, R. & LILLARD JR, J. W. 2009. Nanoparticle-based targeted drug delivery. *Experimental and Molecular Pathology,* 86**,** 215-223.

SKIRTACH, A. G., DEJUGNAT, C., BRAUN, D., SUSHA, A. S., ROGACH, A. L., PARAK, W. J., MOHWALD, H. & SUKHORUKOV, G. B. 2005. The role of metal nanoparticles in remote release of encapsulated materials. *Nano Letters,* 5**,** 1371-1377.

SKIRTACH, A. G., KARAGEORGIEV, P., DE GEEST, B. G., PAZOS-PEREZ, N., BRAUN, D. & SUKHORUKOV, G. B. 2008. Nanorods as Wavelength-Selective Absorption Centers in the Visible and Near-Infrared Regions of the Electromagnetic Spectrum. *Advanced Materials,* 20**,** 506-510.

SKOOG, D., WEST, D., HOLLER, F. & CROUCH, S. 2013. *Fundamentals of Analytical Chemistry*, Cengage Learning.

SKOOG, D. A., WEST, D. M. & HOLLER, F. J. 2000. *Analytical Chemistry: An Introduction*, Saunders College Pub.

SMITH, R. N., MCCORMICK, M., BARRETT, C. J., REVEN, L. & SPIESS, H. W. 2004. NMR Studies of PAH/PSS Polyelectrolyte Multilayers Adsorbed onto Silica. *Macromolecules,* 37**,** 4830-4838.

SOCHYNSKY, R. A., BOUGHTON, B. J., BURNS, J., SYKES, B. C. & MCGEE, J. O. 1980. The effect of human fibronectin on platelet-collagen adhesion. *Thromb Res,* 18**,** 521-33.

SONG, W., HE, Q., MOHWALD, H., YANG, Y. & LI, J. 2009a. Smart polyelectrolyte microcapsules as carriers for water-soluble small molecular drug. *J Control Release,* 139**,** 160-6.

SONG, W., HE, Q., MÖHWALD, H., YANG, Y. & LI, J. 2009b. Smart polyelectrolyte microcapsules as carriers for water-soluble small molecular drug. *Journal of Controlled Release,* 139**,** 160-166.

STUBER, W., KNOLLE, J. & BREIPOHL, G. 1989. Synthesis of peptide amides by Fmoc-solid-phase peptide synthesis and acid labile anchor groups. *International journal of peptide and protein research,* 34**,** 215-21.

SUKHORUKOV, G. B., BRUMEN, M., DONATH, E. & MOHWALD, H. 1999. Hollow polyelectrolyte shells: Exclusion of polymers and donnan equilibrium. *Journal of Physical Chemistry B,* 103**,** 6434-6440.

SUKHORUKOV, G. B., ROGACH, A. L., GARSTKA, M., SPRINGER, S., PARAK, W. J., MUÑOZ-JAVIER, A., KREFT, O., SKIRTACH, A. G., SUSHA, A. S., RAMAYE, Y., PALANKAR, R. & WINTERHALTER, M. 2007. Multifunctionalized Polymer Microcapsules: Novel Tools for Biological and Pharmacological Applications. *Small,* 3**,** 944-955.

SUKHORUKOV, G. B., ROGACH, A. L., ZEBLI, B., LIEDL, T., SKIRTACH, A. G., KÖHLER, K., ANTIPOV, A. A., GAPONIK, N., SUSHA, A. S., WINTERHALTER, M. & PARAK, W. J. 2005. Nanoengineered Polymer Capsules: Tools for Detection, Controlled Delivery, and Site-Specific Manipulation. *Small,* 1**,** 194-200.

SUKHORUKOV, G. B., VOLODKIN, D. V., GUNTHER, A. M., PETROV, A. I., SHENOY, D. B. & MOHWALD, H. 2004. Porous calcium carbonate microparticles as templates for encapsulation of bioactive compounds. *Journal of Materials Chemistry,* 14**,** 2073-2081.

SZE, A., ERICKSON, D., REN, L. & LI, D. 2003. Zeta-potential measurement using the Smoluchowski equation and the slope of the current–time relationship in electroosmotic flow. *Journal of Colloid and Interface Science,* 261**,** 402-410.

TARONE, G., HIRSCH, E., BRANCACCIO, M., DE ACETIS, M., BARBERIS, L., BALZAC, F., RETTA, S. F., BOTTA, C., ALTRUDA, F. & SILENGO, L. 2000. Integrin function and regulation in development. *Int J Dev Biol,* 44**,** 725-31.

THOMPSON, E. G., 2008, Atherosclerosis, viewed 04/06/12, http://edu.westpenncardio.com/ItemPopup.aspx?HWID=tp10638&SEC=tp10638-sec

TONG, H., MA, W., WANG, L., WAN, P., HU, J. & CAO, L. 2004. Control over the crystal phase, shape, size and aggregation of calcium carbonate via a l-aspartic acid inducing process. *Biomaterials,* 25**,** 3923-3929.

TONG, W. J., GAO, C. Y. & MOEHWALD, H. 2008. pH-responsive protein microcapsules fabricated via glutaraldehyde mediated covalent layer-by-layer assembly. *Colloid and Polymer Science,* 286**,** 1103-1109.

TOUBLAN, F. J., BOPPART, S. & SUSLICK, K. S. 2006. Tumor targeting by surface-modified protein microspheres. *Journal of the American Chemical Society,* 128**,** 3472-3.

TRMCIC-CVITAS, J., HASAN, E., RAMSTEDT, M., LI, X., COOPER, M. A., ABELL, C., HUCK, W. T. S. & GAUTROT, J. E. 2009. Biofunctionalized

Protein Resistant Oligo(ethylene glycol)-Derived Polymer Brushes as Selective Immobilization and Sensing Platforms. *Biomacromolecules,* 10**,** 2885-2894.

TROTTA, F., ZANETTI, M. & CAVALLI, R. 2012. Cyclodextrin-based nanosponges as drug carriers. *Beilstein journal of organic chemistry,* 8**,** 2091-2099.

TSILIBARY, E. C., KOLIAKOS, G. G., CHARONIS, A. S., VOGEL, A. M., REGER, L. A. & FURCHT, L. T. 1988. Heparin Type-Iv Collagen Interactions - Equilibrium Binding and Inhibition of Type-Iv Collagen Self-Assembly. *Journal of Biological Chemistry,* 263**,** 19112-19118.

VENKATRAMAN, S. S., HUANG, Y. Y., BOEY, F. Y. C., LAHTI, E. M., UMASHANKAR, P. R., MOHANTY, M., ARUMUGAM, S., KHANOLKAR, L. & VAISHNAV, S. 2010. In vitro and in vivo performance of a dual drug-eluting stent (DDES). *Biomaterials,* 31**,** 4382-4391.

VERGARO, V., SCARLINO, F., BELLOMO, C., RINALDI, R., VERGARA, D., MAFFIA, M., BALDASSARRE, F., GIANNELLI, G., ZHANG, X., LVOV, Y. M. & LEPORATTI, S. 2011. Drug-loaded polyelectrolyte microcapsules for sustained targeting of cancer cells. *Advanced Drug Delivery Reviews,* 63**,** 847-864.

VILASECA, P., DAWSON, K. A. & FRANZESE, G. 2012. Understanding surface-adsorption of proteins: the Vroman effect. *arXiv preprint arXiv:1202.3796*.

WANG, C., YE, W., ZHENG, Y., LIU, X. & TONG, Z. 2007a. Fabrication of drug-loaded biodegradable microcapsules for controlled release by combination of solvent evaporation and layer-by-layer self-assembly. *Int J Pharm,* 338**,** 165-73.

WANG, C., YE, W., ZHENG, Y., LIU, X. & TONG, Z. 2007b. Fabrication of drug-loaded biodegradable microcapsules for controlled release by combination of

solvent evaporation and layer-by-layer self-assembly. *International Journal of Pharmaceutics,* 338**,** 165-173.

WANG, S., LI, X., PARRA, M., VERDIN, E., BASSEL-DUBY, R. & OLSON, E. N. 2008. Control of endothelial cell proliferation and migration by VEGF signaling to histone deacetylase 7. *Proc Natl Acad Sci U S A,* 105**,** 7738-43.

WATTENDORF, U., KOCH, M. C., WALTER, E., VOROS, J., TEXTOR, M. & MERKLE, H. P. 2006. Phagocytosis of poly(L-lysine)-graft-poly(ethylene glycol) coated microspheres by antigen presenting cells: Impact of grafting ratio and poly(ethylene glycol) chain length on cellular recognition. *Biointerphases,* 1**,** 123-33.

WATTENDORF, U., KREFT, O., TEXTOR, M., SUKHORUKOV, G. B. & MERKLE, H. P. 2008. Stable stealth function for hollow polyelectrolyte microcapsules through a poly(ethylene glycol) grafted polyelectrolyte adlayer. *Biomacromolecules,* 9**,** 100-108.

WEINBAUM, S., TARBELL, J. M. & DAMIANO, E. R. 2007. The structure and function of the endothelial glycocalyx layer. *Annu. Rev. Biomed. Eng.,* 9**,** 121-167.

WIETHOFF, C. M., SMITH, J. G., KOE, G. S. & MIDDAUGH, C. R. 2001. The Potential Role of Proteoglycans in Cationic Lipid-mediated Gene Delivery: STUDIES OF THE INTERACTION OF CATIONIC LIPID-DNA COMPLEXES WITH MODEL GLYCOSAMINOGLYCANS. *Journal of Biological Chemistry,* 276**,** 32806-32813.

WILSON, L., MATSUDAIRA, P. T., DARZYNKIEWICZ, Z., ROBINSON, J. P. & CRISSMAN, H. A. 2000. *Cytometry*, Elsevier Science.

XIONG, J.-P., STEHLE, T., ZHANG, R., JOACHIMIAK, A., FRECH, M., GOODMAN, S. L. & ARNAOUT, M. A. 2002. Crystal structure of the extracellular segment of integrin αVβ3 in complex with an Arg-Gly-Asp ligand. *Science,* 296**,** 151-155.

YADAV, G. V. & PANCHORY, H. P. 2013. Nanosponges - A Boon the the targeted drug delivery system. *Journal of Drug Delivery and Therapeutics,* 3.

YANG, G., ZHANG, A. & XU, L. X. 2009. Experimental study of intracellular ice growth in human umbilical vein endothelial cells. *Cryobiology,* 58**,** 96-102.

YANG, J.-C., ZHAO, C., HSIEH, I. F., SUBRAMANIAN, S., LIU, L., CHENG, G., LI, L., CHENG, S. Z. D. & ZHENG, J. 2012a. Strong resistance of poly (ethylene glycol) based L-tyrosine polyurethanes to protein adsorption and cell adhesion. *Polymer International,* 61**,** 616-621.

YANG, J. C., ZHAO, C., HSIEH, I. F., SUBRAMANIAN, S., LIU, L. Y., CHENG, G., LI, L. Y., CHENG, S. Z. D. & ZHENG, J. 2012b. Strong resistance of poly (ethylene glycol) based L-tyrosine polyurethanes to protein adsorption and cell adhesion. *Polymer International,* 61**,** 616-621.

YEUNG, T., GILBERT, G. E., SHI, J., SILVIUS, J., KAPUS, A. & GRINSTEIN, S. 2008. Membrane phosphatidylserine regulates surface charge and protein localization. *Science,* 319**,** 210-213.

YI, Q. & SUKHORUKOV, G. B. 2013. Photolysis Triggered Sealing of Multilayer Capsules to Entrap Small Molecules. *Acs Applied Materials & Interfaces,* 5**,** 6723-6731.

ZHAO, Q. H. & LI, B. Y. 2008. pH-controlled drug loading and release from biodegradable microcapsules. *Nanomedicine-Nanotechnology Biology and Medicine,* 4**,** 302-310.

ZHOU, C., FRIEDT, J. M., ANGELOVA, A., CHOI, K. H., LAUREYN, W., FREDERIX, F., FRANCIS, L. A., CAMPITELLI, A., ENGELBORGHS, Y. & BORGHS, G. 2004. Human immunoglobulin adsorption investigated by means of quartz crystal microbalance dissipation, atomic force microscopy, surface acoustic wave, and surface plasmon resonance techniques. *Langmuir,* 20**,** 5870-5878.